INSIGHT INTO THE BIOENERGETICS OF CLEAR CELL RENAL CELL CARCINOMA (CCRCC)

LIM HWEE YING
(BSc, NUS)

A THESIS SUBMITTED

FOR THE DEGREE OF MASTER OF SCIENCE
DEPARTMENT OF BIOCHEMISTRY
NATIONAL UNIVERSITY OF SINGAPORE

2014

DECLARATION

I hereby declare that this thesis is my original work and it has been written by me in its entirety. I have duly acknowledged all the sources of information which have been used in the thesis.

This thesis has also not been submitted for any degree in any university previously.

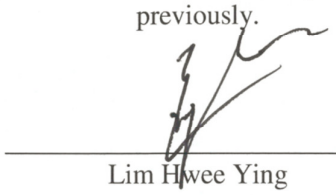

Lim Hwee Ying
12 August 2014

ACKNOWLEDGEMENTS

First of all, I am grateful to my supervisor, Professor Barry Halliwell for accepting me as his student. I would like to express my deepest gratitude to my co-supervisor, Emeritus Professor Sit Kim Ping for her guidance, support and patience throughout my career. Without her constant encouragement, I would not have pursued my Master's degree. I would like to thank my friends and colleagues, Dr. Annette Shoba Vincent, Ms. Kate Ho Qin Shi and Dr. Patrick Goo Chong Kiat for their help and encouragement all this while. I would like to acknowledge our collaborators, Professor Kesavan Esuvaranathan, Dr. Edmund Chiong and Dr. Ho Yee Tiong (Dept. of Urology, NUHS). My sincere thanks go to Dr. Deng Lih Wen (Dept. of Biochemistry, NUHS) for gifting the 786-O cells; Dr. Yeong Foong May (Dept. of Biochemistry, NUHS) and Mr. Chin Cheen Fei for their assistance rendered especially with regard to experiments pertaining to propagation of UCP2 plasmid.

I would like to take this opportunity to thank my parents for their unconditional love, support and encouragement. Special thanks to my devoted husband, Mr. Gun Yong Kait who has always been so accommodating and supportive and our dear son, Rui Heng, the origin of my happiness.

TABLE OF CONTENTS

SUMMARY

Clear cell renal cell carcinoma (ccRCC) is characterized by an increased expression of the hypoxia inducible factors (HIF) due to VHL gene mutations. Targets of HIF, namely hexokinase II, lactate dehydrogenase 5 and pyruvate dehydrogenase (PDH) kinase 1 (PDHK1) are higher than patient-matched normal tissues. PDHK1 phosphorylates and inhibits PDH whose enzymatic activity was negligible, depriving the TCA cycle of acetyl CoA. Lower expression of transcription factors (mtTFA, PGC-1α and NRF1) involved in mitochondrial biogenesis lead to the attenuated expressions and activities of the respiratory complexes, oxidative phosphorylation (OXPHOS) was therefore predicted to be compromised. However, we found that the biosynthesis of ATP, induction of mitochondrial membrane potential (MMP) and oxygen flux were measurable from the oxidation of conventional respiratory substrates in mitochondria isolated from ccRCC tumor tissues, demonstrating their "potential" for OXPHOS. Interestingly, a consistently higher basal MMP was observed in tumor which could be due to the loss of UCP2. In addition, the ability of metabolizing the glutamine-derived substrates suggested the addiction of ccRCC tumor towards glutaminolysis due to a disconnection between glycolysis and the TCA cycle. Taken together, this study revealed the OXPHOS capacity of mitochondria isolated from ccRCC despite its glycolytic phenotype and suggested plausible mechanisms supporting the higher inherent MMP.

LIST OF TABLES

LIST OF FIGURES

LIST OF ABBREVIATIONS AND SYMBOLS

Abbreviations/Symbols	Definition
·OH	hydroxyl radical
18^{F}-deoxyglucose	18F-fluoro-deoxyglucose
AA	antimycin A
ADP	adenosine diphosphate
AMP	adenosine monophosphate
AMPK	AMP-activated protein kinase
ASC	ascorbate
ATCC	American Type Culture Collection
ATP	adenosine triphosphate
BSA	bovine serum albumin
CCRCC	clear cell renal cell carcinoma
Complex I	NADH-coenzyme Q oxidoreductase
Complex II	Succinate-Q oxidoreductase
Complex III	Q-cytochrome c oxidoreductase
complex IV	cytochrome c oxidase
Complex V	ATP synthase
CS	citrate synthase
CuZnSOD	copper zinc superoxide dismutase
DCFDA	2′,7′-dichlorofluorescin diacetate
DMSO	dimethyl sulfoxide
DNA	deoxyribonucleic acid
DTNB	5,5'-dithio-bis(2-nitrobenzoic acid)
EGTA	ethylene glycol tetraacetic acid
ETC	electron transport chain
$FADH_2$	reduced flavin adenine dinucleotide
FCCP	carbonyl cyanide p-trifluoromethoxyphenylhydrazone
FH	fumarate hydratase
FLCN	folliculin
G-6-P	glucose-6-phosphate
Gln	glutamine
H2O2	hydrogen peroxide
HBSS	Hank's balanced salt solution
HGF	hepatocyte growth factor
HIFs	hypoxia inducible factors
HKII	hexokinase II
HRP	horse radish peroxidase
IMM	inner mitochondrial membrane
JC-1	5,5’,6,6’-tetrachloro 1,1, 3,3’

	tetraethylbenzimidazolcarbocyanine iodide
KGA/GLS1	kidney-type (K-type) mitochondrial glutaminase
LDH5	lactate dehydrogenase isoenzyme V
LDH-A	lactate dehydrogenase A
Mal/Glut	malate and glutamate
MCT	monocarboxylate transporters
MDH	malate dehydrogenase
MET	mesenchymal-epithelial transition
MMP	mitochondrial membrane potential
MnSOD	manganese superoxide dismutase
mtDNA	mitochondrial DNA
mTOR	mammalian target of rapamycin
mtTFA	mitochondrial transcription factor A
NAD^+	nicotinamide adenine dinucleotide
NADH	reduced nicotinamide adenine dinucleotide
NADPH	reduced nicotinamide adenine dinucleotide phosphate
NO·	nitric oxide
NP-40	Nonidet P-40
NRF	nuclear respiratory factors
$O_2^{-}\cdot$	superoxide
$ONOO^-$	peroxynitrite
OXPHOS	oxidative phosphorylation
PBS	phosphate buffered saline
PDH	pyruvate dehydrogenase
PDHK	pyruvate dehydrogenase kinase
PDP	pyruvate dehydrogenase phosphatases
PEP	phosphoenolpyruvate
PGC-1α	peroxisome proliferator-activated receptor gamma coactivator 1-alpha
PHD	prolyl hydroxylase
PK	pyruvate kinase
PMSF	phenylmethylsulfonyl fluoride
RC	respiratory chain
RNA	ribonucleic acid
ROS	reactive oxygen species
ROT	rotenone
RPMI	Roswell Park Memorial Institute
SDH	succinate dehydrogenase
SDS	sodium dodecyl sulfate
Succ	succinate
TBST	tris buffered saline with Tween 20
TCA	tricarboxylic acid
TMPD	N,N,N′,N′-tetramethyl-p-phenylenediamine

TMRM	2',7'-dichlorofluorescein diacetate, tetramethylrhodamine methyl ester
TSC	tuberous sclerosis complex
UCPs	uncoupling proteins
VDAC	voltage-dependent anion channels
VEGF	vascular endothelial growth factor
VHL	von Hippel-Lindau
WHO	World Health Organization
α-KG	α-ketoglutarate
Δp	electrochemical gradient
ΔpHm	mitochondrial pH gradient
ΔΨm	mitochondrial membrane potential

CHAPTER 1 GENERAL INTRODUCTION AND AIMS OF STUDY

1.1 The kidneys

The kidneys are bean-shaped organs located at the rear of the abdominal cavity with one on each side of the vertebral column. The main function of kidneys is to filter waste products and excess fluid out of the blood in the form of urine which is eventually diverted into the urinary bladder. In the process of producing urine, wastes such as urea and ammonium are excreted whereas glucose, amino acids and a certain volume of water were reabsorbed.

Besides their essential role in urinary system, kidneys are also responsible for regulation of electrolytes including sodium (Na^+), chloride (Cl^-), calcium (Ca^{2+}), potassium (K^+), magnesium (Mg^{2+}) and hydrogen phosphate (HPO_4^{2-}); maintenance of acid-base balance by reabsorption of bicarbonate and excretion of hydrogen ions; regulation of blood pressure via maintaining the water and salt balance; production of hormones (calcitriol and erythropoietin) and enzyme (renin). Calcitriol is the activated form of vitamin D and it is also important for the intestinal reabsorption of calcium and renal reabsorption of phosphate. Erythropoietin stimulates erythropoiesis in the bone marrow under hypoxic condition and renin, on the other hand, regulates the aldosterone level via the renin-angiotensin-aldosterone system.

1.2 Renal cell carcinoma (RCC)

Renal cell carcinoma (RCC) is a type of kidney cancer that the cancer cells form in the renal tubules in contrast to those that involve renal pelvis. RCC accounts for 3% of adult cancers and about 90% of all renal malignancies (Jemal

et al., 2010). The most recent estimation by the American Cancer Society states that 63920 new cases of kidney cancer and renal pelvis cancer are expected to occur and lead to 13860 deaths in the United States in 2014 (Siegel et al., 2014).

RCC is a heterogeneous disease with histological variants of different clinical course, gene mutation and response to therapy. According to World Health Organization (WHO) classification, RCC is categorized into different subtypes based on morphology, namely clear cell, papillary, chromophobe, granular, spindle cell, cyst-associated, translocation carcinomas and collecting-duct carcinomas (Eble J, 2004; Kovacs et al., 1997). Of these, clear cell renal cell carcinoma (ccRCC) is the most prevalent form, accounting for 75% followed by papillary 10%, chromophobe 5% and undifferentiated represent approximately 10% of cases. ccRCC is named according to the typical presentation of clear cytoplasm due to intracellular lipid accumulation as depicted in Fig. 1.2.

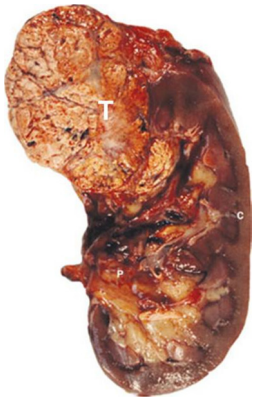

Fig. 1.2 Macroscopic appearance of clear cell RCC with the tumor area appears golden due to intracellular lipid accumulation. Abbreviations: C, renal cortex; P, renal pelvis; T, tumor. Reprinted by permission from Macmillan Publishers Ltd: Nature Reviews Urology, 8, Valera VA and Merino MJ, Misdiagnosis of clear cell renal cell carcinoma, page 324, copyright 2011. (License Number: 3446241101034).

1.2.1 Epidemiology

The incidence rates for RCC are highest in Europe and North America and lowest in Asia and Africa. RCC occurs more often in men as compared to women with ratio of 1.5:1 (Landis et al., 1999). Higher rates are also reported for urban in contrast to rural populations and black compared with white Americans (Decastro and McKiernan, 2008; McLaughlin et al., 2006; Pascual and Borque, 2008). RCC is a tumor of adults with the highest incidence reported in the fifth decade of life; about 80% of all RCC patients are between 40 to 69 year old (Pascual and Borque, 2008). However, there were patients that were diagnosed with RCC at younger age of less than 40 or 14-18 years old in rare cases (Bruder et al., 2004; Taccoen et al., 2007).

1.2.2 Etiology

The exact cause of RCC is poorly understood but there are several risk factors that are associated with the development of RCC and tobacco smoking is one of them. Outcome from a meta-analysis demonstrated that people who smoke had higher risk for renal cancer than those who never smoke (Ferlay et al., 2007). Workers in industries who were exposed to toxic substances such as cadmium, coke ovens, steel, gasoline/petroleum (Boffetta et al., 2001; Mandel et al., 1995), trichloroethylene (TCE) (Bruning et al., 2003; Lungberg BC, 2011) and pesticides (Karami et al., 2008) had an increased risk for RCC. RCC is also associated with excess body weight as shown by the meta-analysis of prospective studies by Chow *et al* (Chow et al., 1999) in which the risk was increased by 1.24 in men and 1.34 in women per 5kg/m^2 increase in body mass index. Dietary habit of fruit

and vegetable consumption was shown to have an inverse association with the incidence of RCC (29) but the correlation was not observed in two other studies (George et al., 2009; Weikert et al., 2006). In addition, alcohol intake has been shown to have an inverse association with risk of renal cell cancer (Lee et al., 2006; Setiawan et al., 2007).

1.2.3 Genetics

Most cases of RCC are sporadic; however, with the several hereditary kidney cancer syndromes come to light, genes implicated in familial renal cancers have been identified.

1.2.3.1 VHL

Most of the RCC patients harbor the mutation in their von Hippel-Lindau (*VHL*) gene. It was first found in 1993 that RCC is associated with the chromosomal loss of *VHL* gene on chromosome 3p25-26 (Latif et al., 1993). The VHL protein is a tumor suppressor which together with elongin B, elongin C and cullin 2 (Kibel et al., 1995), form a complex that targets the hypoxia inducible factors (HIFs) for ubiquitination followed by proteasomal degradation (Iliopoulos et al., 1996; Maxwell et al., 1999).

HIFs are basic helix-loop-helix transcription factors which regulate the expression for downstream genes in response to oxygen deprivation. Targets of HIFs such as vascular endothelial growth factor (VEGF), platelet-derived growth factor and glucose transporter 1 (Pfaffenroth and Linehan, 2008) are important genes implicated in angiogenesis, energy metabolism, erythropoiesis, cell proliferation and survival, pH regulation, proteolysis and apoptosis.

During normoxia, HIF-α is hydroxylated by HIF prolyl hydroxylase (PHD) at the critical proline residues which facilitate the binding site of VHL protein and subsequent proteolysis by the E3 ubiquitin ligase complex. Molecular oxygen, 2-oxoglutarate, ascorbate and Fe^{2+} are required in this process. In contrast, PHD cannot hydroxylate HIF-α under hypoxic conditions or when *VHL* gene is mutated, no binding of pVHL leads to the accumulation of HIF-α. The steps involved in HIF1α by PHD are depicted in Fig. 1.2.3.1. There is considerable amount of overlap between the genes that are transcriptionally regulated by HIF-1α and HIF-2α but the later was reported to be the crucial HIF for tumorigenesis in clear cell kidney cancer (Kondo et al., 2002).

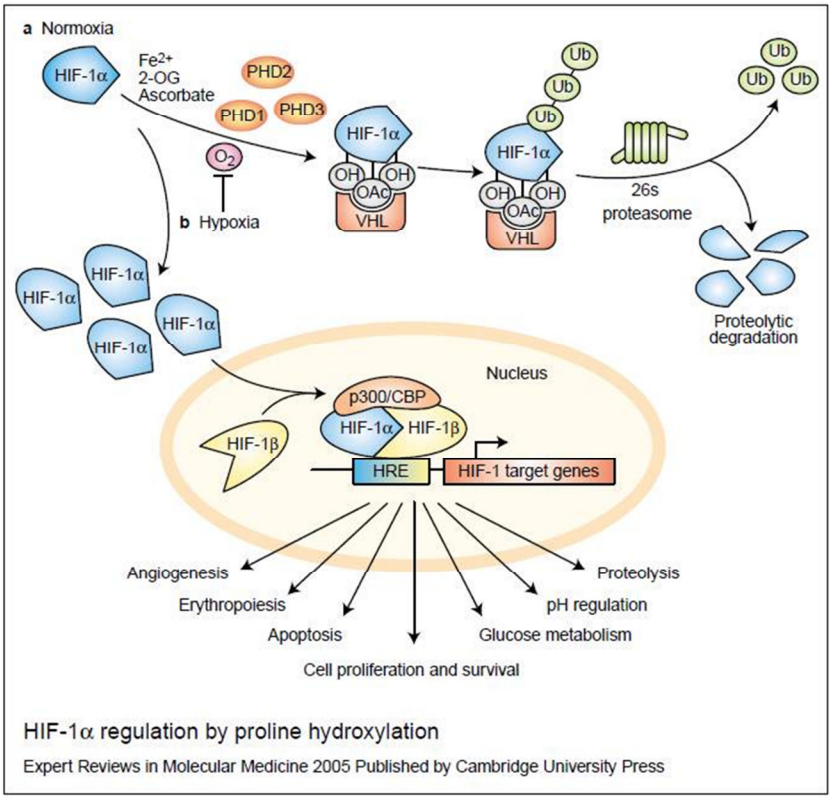

Fig. 1.2.3.1 Regulation of HIF1α by proline hydroxylation. Veronica AC and Margaret, Targeting the molecular basis for tumor hypoxia, Expect Reviews in Molecular Medicine, 7, page 5, 2005, reproduced with permission from Cambridge University Press (License Number: 34456900869341)

1.2.3.2 MET

The proto-oncogene mesenchymal-epithelial transition (*MET*) encodes a tyrosine kinase membrane receptor (Finley et al., 2011) for the binding of hepatocyte growth factor (HGF) which plays a role in mitogenesis, morphogenesis and motogenesis (Peruzzi and Bottaro, 2006). Gain-of-function mutations in the tyrosine kinase domain of MET result in consecutive activation of the receptor and multiple tumorigenic processes which have been reported in the germline of affected patients as well as in a subset of sporadic type 1 papillary kidney cancers (Schmidt et al., 1997; Schmidt et al., 1999).

1.2.3.3 TSC1-TSC2

Germline mutations in the tuberous sclerosis genes (*TSC1* and *TSC2*) are implicated with the development of pulmonary lymphangiomyomatosis, cutaneous angiofibromas and renal tumors (Faivre et al., 2006). Hamartin and tuberin, encoded by *TSC1* and *TSC2* form a heterodimer that activates Rheb (a Ras family GTPase) which in turn inhibit mammalian target of rapamycin (mTOR) activity. Lack of mTOR inhibition by TSC1-TSC results in an increased phosphorylation of 4E-BP1, p70S6 kinase, S6 ribosomal protein and thus causes higher protein synthesis.

1.2.3.4 FLCN

The loss-of-function mutations in the folliculin gene (FLCN) have been identified in patients with Birt-Hogg-Dubé syndrome (Schmidt et al., 2001) and they are at higher risk to develop benign cutaneous tumors (fibrofolliculomas) , pulmonary cysts (Birt et al., 1977) and chromophobe kidney tumors (Pavlovich et

al., 2005). Complex of folliculin with its interacting proteins 1 and 2 (FNIP1 and FNIP2) binds to ɣ-subunit of AMPK and regulates AMPK-mTOR signaling. The function of protein folliculin is not fully understood (Finley et al., 2011) but its inactivation leads to polycystic kidney degeneration and renal tumors in mouse models (Baba et al., 2006; Schmidt et al., 2001). An association between FLCN function and mTORC1 activity during renal tumorigenesis was also suggested (Baba et al., 2006; Chen et al., 2008; Hartman et al., 2009).

1.2.3.5 FH

FH encodes mitochondrial fumarate hydratase (FH) and its mutation is responsible for the development of hereditary leiomyomatosis renal cell carcinoma (HLRCC) (Tomlinson et al., 2002). Inhibition of FH leads to the accumulation of fumarate which inhibits the activity of PHD and resulting in upregulation of HIF (Isaacs et al., 2005). Glucose dependency (Sudarshan et al., 2009; Yang et al., 2010) and impaired oxidative phosphorylation (OXPHOS) (Xie et al., 2009; Yang et al., 2010) are observed in FH-deficient kidney cancer cell lines.

1.2.3.6 SDH

Germline mutations in the three succinate dehydrogenase genes (*SDHB*, *SDHC* and *SDHD*) have been associated with familial pheochromocytoma and familial paraganglioma (Baysal et al., 2000; Vanharanta et al., 2004). Similar to FH, loss of SDH and the accumulation of succinate also result in pseudohypoxia and the stabilization of HIF (Isaacs et al., 2005).

1.2.4 Current treatments

Nephrectomy, either partial or radical is the primary and most effective treatment known for localized renal cell carcinoma (Robson et al., 1969). For patients with metastatic tumor, surgical treatment is given as palliative care in addition to the standard regimens involving immunomodulatory agents and molecular-targeted therapy. Cytokine immunotherapy with interleukin-2 was shown to increase the median survival rate from 10 months to 34 months in 20% of patients with metastatic ccRCC. Tyrosine kinase inhibitors (sunitinib, sorafenib) that target the angiogenesis pathway and mTOR inhibitor (temsirolimus) which induces cell cycle arrest have been approved for the treatment of RCC. A response rate of 31% towards sunitinib observed in patients with advanced RCC assures the effectiveness of gene-targeting therapy and researchers are focusing on identifying more agents for targeted approaches including those contributing to the metabolic defect in RCC (Linehan et al., 2010; Turcotte et al., 2008).

1.3 Energy metabolism in cells

Cells require energy for their cellular activities such as cell growth, movement, transport and synthesis of macromolecules. The energy is derived from the oxidation of carbohydrate, fat or protein and is captured in the high-energy phosphate bonds of adenosine triphosphate (ATP). The energy currency, ATP can then be used for energy-requiring reactions. The two major pathways implicated in the cellular bioenergetics are glucose metabolism and lipid metabolism.

1.3.1 Glucose metabolism

Glucose is the six-carbon sugar that serves as the primary source of energy. It is converted into two molecules of three-carbon product, pyruvate by a metabolic pathway known as glycolysis. Energy released during this process is used to form adenosine triphosphate (ATP) and reduced nicotinamide adenine dinucleotide (NADH). Glycolysis comprises of ten enzyme-catalyzed reactions that take place in the cytoplasm (Fig. 1.3.1a).

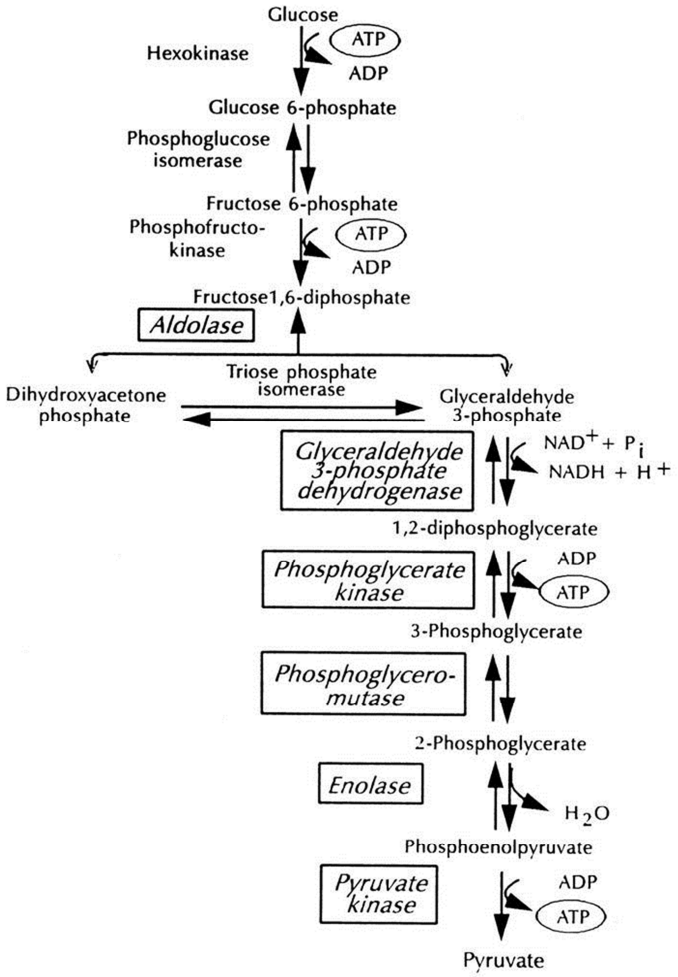

Fig. 1.3.1a Glycolysis. Reproduced from Circulation Research, 77, Xu KY *et al*, Functional coupling between glycolysis and sarcoplasmic reticulum Ca2 Transport, Figure 1, 1995, with permission from Wolters Kluwer Health (License Number: 3445740299155).

Under anaerobic conditions, pyruvate is reduced to lactate by lactate dehydrogenase A (LDH-A) in the cytoplasm and lactate is exported from the cells via monocarboxylate transporters (MCTs). In the presence of oxygen, the end product, pyruvate enters the mitochondria and is oxidized to acetyl CoA by the action of pyruvate dehydrogenase (PDH). Other than pyruvate, acetyl CoA can also be generated by the oxidation of fatty acids and ketogenic amino acids. Acetyl CoA together with oxaloacetate initiate the tricarboxylic acid (TCA) cycle and give rise to the reducing equivalents, NADH and reduced flavin adenine dinucleotide ($FADH_2$) which are ultimately channeled into electron transport chain (ETC) and ATP generation via oxidative phosphorylation (OXPHOS).

OXPHOS is carried out by the five respiratory complexes found on the inner mitochondrial membrane (IMM). NADH and $FADH_2$ from the TCA cycle are oxidized by Complex I (NADH-coenzyme Q oxidoreductase) and II (Succinate-Q oxidoreductase) respectively and the electrons-carried by them are transferred sequentially to the coenzyme Q (also known as ubiquinone), complex III (Q-cytochrome c oxidoreductase), cytochrome c and end at complex IV (cytochrome c oxidase) where oxygen is reduced to water. As the electrons pass through the chain, protons are pumped from the matrix into the intermembrane space, creating potential energy in the form of a pH gradient and an electrical potential across IMM. Protons return to the matrix via the complex V and the energy released is used to form ATP from adenosine diphosphate (ADP). The oxidative process is normally coupled to phosphorylation of ADP and therefore termed the OXPHOS and the details are depicted in Fig. 1.3.1b.

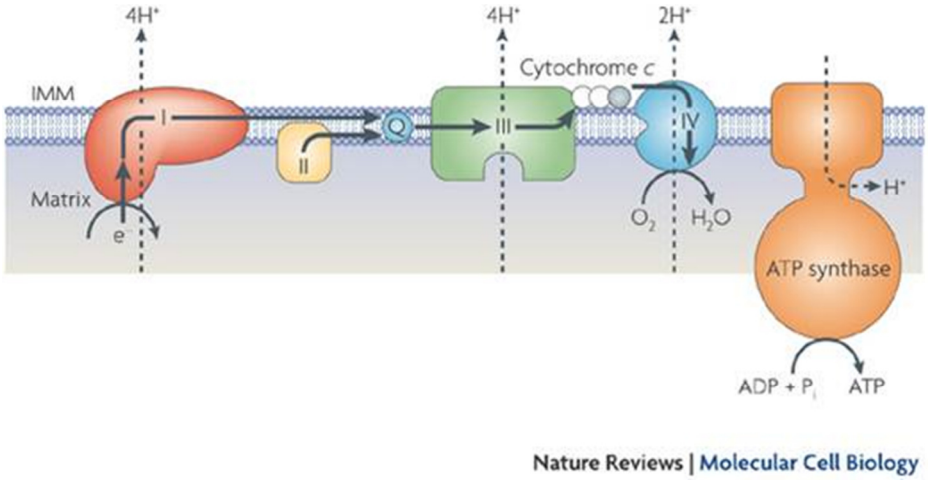

Fig. 1.3.1b Schematic diagram of the respiratory complexes that involved in the transfer the electrons and formation of ATP occur in the oxidative phosphorylation (OXPHOS). Reprinted by permission from Macmillan Publishers Ltd: Nature Reviews Molecular Cell Biology, 9, Ow, YP et al, Cytochrome c: functions beyond respiration, page 535, copyright 2008. (License Number: 3445760329775).

OXPHOS is a more efficient pathway in generating energy because only two moles of ATP per mole of glucose are produced by glycolysis as compared to 36 moles of ATP from OXPHOS in which glucose is fully oxidized to carbon dioxide and water.

1.3.2 Lipid metabolism

Lipids are important storage for energy, fundamental constituents of cell membranes and precursor of steroid hormones. The breakdown of lipids starts with the hydrolysis of lipid in the cytoplasm and give rise to glycerol and fatty acids. Glycerol can be metabolized to dihydroxyacetone phosphate, an intermediate of glycolysis or converted to glucose-6-phosphate in gluconeogenesis. Fatty acids are processed in the mitochondria, yielding acetyl-coA, NADH and $FADH_2$ via a pathway called beta-oxidation. The fatty acids are first converted to fatty acyl-CoA by the enzyme fatty acyl CoA dehydrogenase at

the expense of one ATP. It is followed by a stepwise oxidation whereby the fatty acids are degraded by two carbons at a time, generating acetyl CoA and a fatty acyl-CoA shorter by two carbons. One molecule each of NADH and $FADH_2$ formed per round of oxidation are directed towards electron transport chain whereas the acetyl-coA enters the citric acid cycle.

Total of 130 ATPs (21 from 7 NADH; 14 from $FADH_2$; 96 from acetyl CoA and minus one used in the first step) can be produced per molecule of a 16-carbon fatty acid via beta- oxidation. By comparing the molecular mass of a saturated 16-carbon fatty acid which is 256 and that of glucose which is 180, fatty acids have 2.5 times higher yield of ATP per gram which explain why lipids are better energy storage than polysaccharides.

1.4 Aims of study

This study aims to gain insights into the metabolic signature of clear cell renal cell carcinoma (ccRCC) when compared to the patient-matched normal tissue. Particulars of patients and clinical data on specimens collected were listed in Table 1. Understanding of these bioenergetic differences would provide clues toward the development of potential therapeutic strategy for ccRCC.

Chapter 2 described work that confirmed the glycolytic phenotype of ccRCC with altered protein expressions of HIFs' targets. This was accompanied with reduced protein levels of mitochondrial respiratory complexes and transcription factors responsible for mitochondrial biogenesis. These observations indicate that ccRCC depends greater on glycolysis than oxidative phosphorylation (OXPHOS) which believed to be impaired in cancer cells as suggested by Warburg.

Chapter 3 addressed the controversy of respiratory injury in cancer cells by examining the mitochondrial functions using intact mitochondria isolated from ccRCC tumor and normal tissue. Here the OXPHOS capacity from the aspects of ATP biosynthesis, oxygen consumption and mitochondrial membrane potential was examined. In addition, production of reactive oxygen species (ROS) will also be described.

As results from Chapter 4 suggested a higher basal mitochondrial membrane potential (MMP) in the ccRCC, role of uncoupling proteins (UCPs), ADP and respiratory substrates in maintaining the higher MMP was examined. 786-O cells with UCP2 overexpression were assessed for the change in their

MMP. The ability of mitochondria isolated from ccRCC tumor in utilizing glutamine and its-derived substrates for synthesizing ATP and energization of MMP will be described.

Sample #	Gender	Tumor wt. (gms)	Tumor size (cm)	Tumor type	Grade (Fuhrman)	Malignancy
1	M	493	2.5 x 1.7 x 1.5	ccRCC	3/4	No evidence of invasion
2	F	648	9.0 x 7.5 x 6.5	ccRCC	2	No evidence of malignancy
3	F	417	10 x 6 x 4	ccRCC	1	Invasion not identified
4	M	984[(a)]	13 x 11 x 9.0	ccRCC	Predominantly 2/4, with a focal area of 3/4	No evidence of malignancy
5	M	650.0	11.0 x 8.5 x 4.5	Renal cell carcinoma, clear cell type	3	Malignant
6	M	474	4.3x4X4	Clear cell (conventional) renal carcinoma	2	Malignant
7	M	686.0	9.0 x 7.5 x 7.0	Renal cell carcinoma, clear cell type	4	Malignant
8	M	678	9.3 x 8.0 x 8.0	Renal cell carcinoma, unclassified, 9.3 cm	3	Malignant
9	M	717.2	10.7 x 8.3 x 8.0	Clear cell renal cell carcinoma with focal sarcomatoid change, 10.7 cm	4	Malignant
10	M	674.0	7.2 x 6.2 x 5.0	Renal cell carcinoma, clear cell type, 7.2 cm in largest dimension	3	Malignant

11	F	647.0	13.0 x 11.0 x 4.0	Epithelioid angiomyolipoma13.0 cm	NP	Epithelioid angiomyolipoma, 13.0 cm
12	F	328.0	4.5 x 4.0 x 3.0	Clear cell renal cell carcinoma 4.5cm	3	Malignant
13	F	176.0	6.0 x 4.0 x 1.8	Clear cell renal cell carcinoma	2	Malignant
14	F	882.0	13.5 x 9.5 x 6.0	Chromophobe renal cell carcinoma with extensive tumor necrosis and calcifications	4	Malignant
15	M	826.0	10.5 x 8.0 x 7.5	Conventional Clear cell carcinoma	2	Malignant
16	M	1406	10.2 x 9.0 x 7.0	Renal cell carcinoma, clear cell type	3	Tumor focally invades the perinephric fat and is present within a major vein branch
17	NP	575.0	10.0 x 9.0 x 4.5	Conventional clear cell renal cell carcinoma	3	See below[(b)]
18	NP	370.0	9.5 x 8.5 x 7.5	Conventional renal clear cell carcinoma	3	See below[(c)]

Table 1. Particulars of patients and classification of tumors. NP: Information not provided.

[(a)] Tumor grossly encapsulated and extends beyond the confines of kidney; extensive areas of haemorrhage and necrosis

[b] Tumor extends into major vein, pT3a, hilar vascular margin with intraluminal tumor thrombus, without tumor invasion into vessel wall, Ureteric and perinephric resection margins not involved by tumor, one hilar lymph node with no evidence of malignancy (0/1). Para-aortic lymph node: One lymph node with no evidence of malignancy (0/1), Aorto-caval lymph nodes: Two lymph nodes with no evidence of malignancy (0/2).

[c] Tumor has invaded into the perirenal fat and renal sinus fat, tumor seen grossly and microscopically in the large veins, lymphovascular invasion is present, tumor does not invade the pericolic fat or bowel wall. Twenty-two pericolic lymph nodes identified with no evidence of metastatic carcinoma (0/22). Resection margins are not involved by tumor. (B) "Duodenum", wedge resection: Negative for malignancy.

CHAPTER 2 WARBURG EFFECT IN CLEAR CELL RENAL CELL CARCINOMA (CCRCC)

2.1 Introduction

2.1.1 Warburg effect

Normal differentiating cells rely mainly on oxidative phosphorylation for the production of energy required for cellular functions and processes. In contrast, cancer and proliferating cells convert glucose into lactate even in the presence of oxygen, a phenomenon known as "aerobic glycolysis" or the "Warburg effect". The high rates of glucose uptake and lactic production in cancer cells was first described by Otto Warburg in 1956 (Warburg, 1956b) and this finding facilitates the exploitation of 18^{F}-deoxyglucose positron emission tomography scanning in detecting solid tumor (Ter-Pogossian et al., 1975). Besides cancer's sweet tooth, Warburg and his colleagues found that oxygen consumption was lower in cancer cells as compared to normal tissue cells even when oxygen was ample (Koppenol et al., 2011) and the impairment in respiration was postulated to be the underlying cause (Warburg, 1956a).

Half a century has passed and majority of cancer types have been found to display the Warburg phenotype which enables the generation of building blocks from glycolytic intermediates to allow the rapid proliferation of cancer cells (Hsu and Sabatini, 2008). Many tumors are characterized by the elevated lactate and the resulted acidosis degrades the stroma that surrounds the non-neoplastic cells which eventually lead to increased invasiveness of the cancer. In addition, the Warburg effect is always associated with the enhanced expression of the

transcription factor hypoxia-inducible factor-1α (HIF-1α) that regulates more than 100 genes including those involved in glucose metabolism, angiogenesis, vasomotor regulation, cell growth and apoptosis (Chowdhury et al., 2008).

2.1.2 Hexokinase II (HKII) and lactate dehydrogenase isoenzyme V (LDH5)

Glycolytic enzymes, hexokinase II (HKII) and lactate dehydrogenase isoenzyme V (LDH5) are known to be transcriptionally regulated by HIF-1α (Koukourakis et al., 2005; Mathupala et al., 2001; Semenza et al., 1994). Hexokinase (HK) is the glycolytic enzyme that catalyzes rate-limiting step in glycolysis in which glucose is phosphorylated to glucose-6-phosphate (G6P). There are four major isozymes of hexokinase, referred as Types I, II, III and IV. Type II hexokinase (HKII) is the major isozymes that is overexpressed in cancer cells especially in those highly malignant tumor whereby there is a >100-fold elevation in its expression. Most of the HKII is bound to the outer mitochondrial membrane via the interaction with a protein called porin or VDAC (Nakashima et al., 1986). This strategic location of HKII allows preferred access to mitochondrially generated ATP (Arora and Pedersen, 1988), reduces the enzyme's sensitivity to product inhibition by glucose-6-phosphate (G-6-P) (Bustamante and Pedersen, 1977) and offers protection against proteolytic degradation (Rose and Warms, 1982).

Under hypoxic condition, pyruvate produced by glycolysis is converted into lactate by the action of lactate dehydrogenase (LDH). This reaction is accompanied by the interconversion of NADH to NAD^+ which is crucial in ensuring the regeneration of NAD^+ for glycolysis and other metabolic activities.

Five LDH isozymes have been described and structurally they are tetramers constituted by M and H protein subunits. M and H protein are encoded by the *LDHA* and *LDHB* genes respectively. M subunits catalyze the pyruvate transformation to lactate but the conversion of pyruvate to acetyl-CoA is favored in the presence of H subunits when the ability of the enzyme to catalyze the reaction is lowered. Each of the LDH isozymes has its unique subunits composition which is summarized in the Table 2. LDH5 is the most important isozyme for promoting anaerobic glycolysis; increase in its expression has been associated with the aggressiveness and metastasis of various cancer types (Koukourakis et al., 2005).

	Subunits composition
LDH1	4H
LDH2	3H1M
LDH3	2H2M
LDH4	1H3M
LDH5	4M

Table 2. Subunit compositions of lactate dehydrogenase (LDH).

2.1.3 Pyruvate dehydrogenase (PDH) and pyruvate dehydrogenase kinase (PDHK)

Under normoxic condition, pyruvate which is the end product of glycolysis is converted into acetyl-CoA via the action of pyruvate dehydrogenase complex (PDHc). The acetyl-CoA then combines with oxaloacetate to form citrate which starts the tricarboxylic acid (TCA) cycle. PDH complex is composed of three enzymes: pyruvate dehydrogenase (E1), dihydrolipoamide acyltransferase (E2) and dihydrolipoamide dehydrogenase (E3) (Reed and Hackert, 1990). Sequence of reactions catalyzed by the PDH complex is depicted in Fig. 2.1.3.

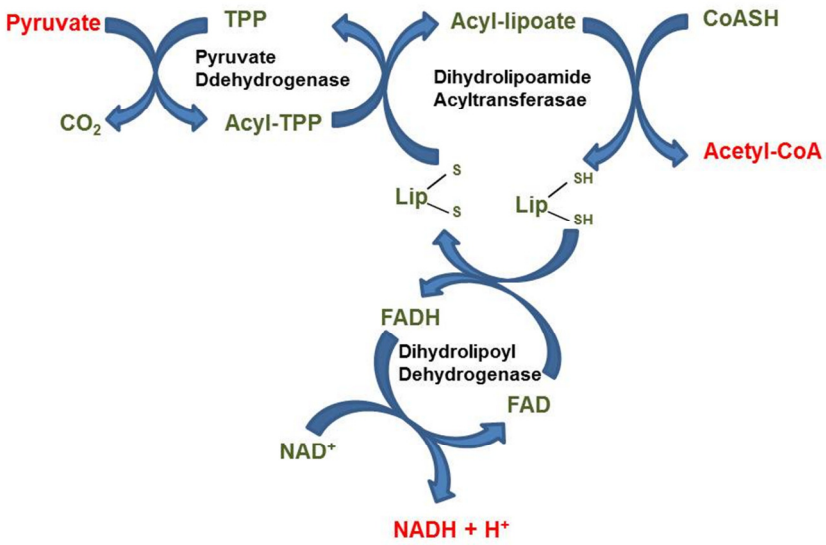

Fig. 2.1.3 Sequential reactions catalyzed by PDH complex in which pyruvate is decarboxylated to form acetyl-CoA.

In view of its central role in linking glycolysis and TCA cycle, PDH is tightly regulated by three mechanisms: inhibition by acetyl-CoA and NADH, stimulation by reduced energy in the cell and inhibition by regulatory phosphorylation of its E1 subunit at Ser232, Ser293 and Ser300 by pyruvate dehydrogenase kinase (PDHK) (Holness and Sugden, 2003; Sugden and Holness,

2003). There are four known isozymes of PDHK expressed in a tissue-specific manner in vertebrates (Roche et al., 2001) , each has a different reactivity towards the three phosphorylation sites. Among all, PDHK1 and PDHK3 have been reported to be hypoxia-inducible (Denko et al., 2003; Papandreou et al., 2006). The inhibition caused by PDHK could be reversed by the two pyruvate dehydrogenase phosphatases (PDP1 and PDP2) which dephosphorylate the E1α subunit and activate the enzyme.

2.1.4 Mitochondrial biogenesis

The elevated protein levels of hypoxia-inducible factor 1 (HIF-1) seen in most cancer cells has been shown to inhibit mitochondrial biogenesis (Zhang et al., 2007). This provides evidence to Warburg's theory that aerobic glycolysis observed in cancer cells is due to defective mitochondrial respiration. Mitochondrial biogenesis is defined as the growth and division of pre-existing mitochondria (Ventura-Clapier et al., 2008). It can be affected by environmental stimuli and cellular stress such as low temperature, exercise, oxidative stress, caloric restriction, cell division, renewal and differentiation. Mitochondrial biogenesis involves the variations in number, in size and in mass. During this process, majority of mitochondrial proteins comes from the nuclear genome whereas the mitochondrial genome encodes only 13 subunits of the electron transport chain complexes I, III, IV, V, ribosomal and transfer RNAs. Expressions of the various genes are regulated by a network of transcription factors.

Peroxisome proliferator-activated receptor gamma coactivator 1-alpha (PGC-1α) is the master regulator of mitochondrial biogenesis (Puigserver et al.,

1998). PGC-1α does not bind to DNA but it is a transcriptional co-activator that interacts and activates various transcription factors, including nuclear respiratory factors (NRF-1 and NRF-2). The NRF-1 and NRF-2 in turn promote the expression of mitochondrial transcription factor A (mtTFA) which directly drives the transcription of mtDNA (Virbasius and Scarpulla, 1994).

2.2 Results and Discussions

2.2.1 Higher protein expressions of hypoxia-inducible factor alpha subunits (HIF-1alpha and HIF-2alpha) in ccRCC tumor lysate

Deactivation of VHL gene, the most common mutation in ccRCC leads to the stabilization and increase of hypoxia inducible factors (Nyhan et al., 2011). Consistent with earlier reports, HIF-1α and HIF-2α were upregulated in 83.3% (5/6) and 87.5% (7/8) of ccRCC tumors respectively (Fig. 2.2.1a & 2.2.1b) HIF-2α expression in sample #6 was excluded as the blot was damaged at that region.

All the tumor samples that showed an augmentation in HIF-1α expression had a corresponding increase in HIF-2α expression suggesting that their protein stability are regulated in a similar manner. Indeed, the oxygen-dependent-degradation domains of the two HIF-α subunits, are highly homologous and thus explaining the identical trend between the two (Loboda et al., 2010). Although HIF-1α and HIF-2α are structurally similar in their DNA binding and dimerization domains, the difference in their transactivation domains imply that their effect on the expression of some genes may vary. Results by Hu *et al* indicate that despite of sharing some common targets, HIF-1α but not HIF-2α is involved in regulation of transcription of genes encoding enzymes involved in the glycolytic pathway (Hu et al., 2003). On the other hand, HIF-2α was suggested as a renal cancer oncogene as its overexpression is important for the development of renal carcinoma in patients with the von Hippel-Lindau syndrome (Kondo et al., 2003).

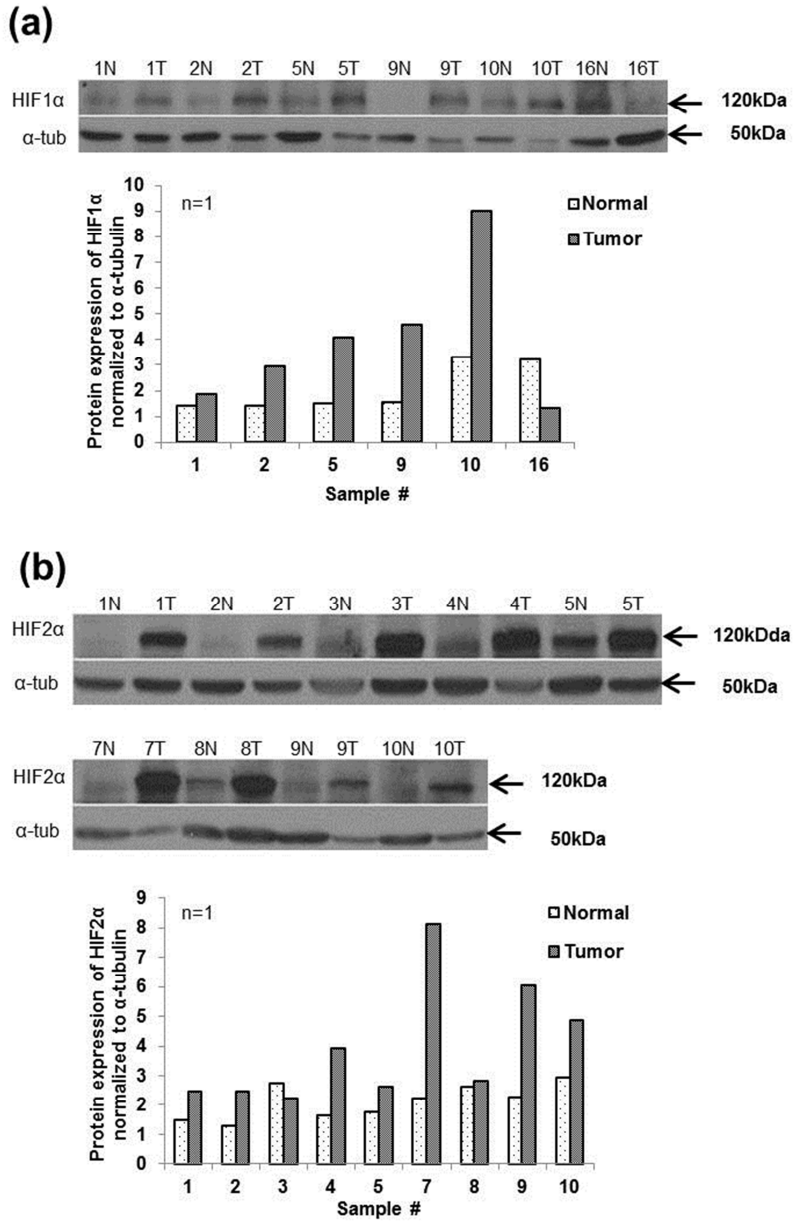

Fig. 2.2.1 Western blot analysis of hypoxia-inducible factor alpha subunits, (a) HIF1α and (b) HIF2α.

Lysates prepared from human ccRCC tumor and paired, adjacent normal tissues were probed with the respective antibodies. Of note, sample #8 was derived from an unclassified renal cell carcinoma and therefore was excluded from percentage calculation shown in the results. Intensity of bands was quantified using the ImageJ software and expressed as relative to α-tubulin. HIF1α and HIF2α were, respectively, higher in 5 out of 6 and 7 out of 8 ccRCC tumor (T) as compared to the corresponding normal tissues (N). No replicate was performed due to the limited lysate derived from the tiny piece of human tissue.

2.2.2 Increased expression of HIF-regulated glycolytic gene: Hexokinase II (HKII) and Lactate dehydrogenase isoenzyme V (LDH5) in ccRCC tumor lysate

Corroborating with the enhanced expression of HIF-1α, protein expression of HKII and LDH5 were also upregulated in sample #1, #2, #5, #9 and #10. Overall expression of HKII and LDH5 are higher in 88.9% (8/9 in Fig. 2.2.2a) and 77.8% (7/9 in Fig. 2.2.2b) of ccRCC tumor lysate as compared to their adjacent non-neoplastic tissue.

Interestingly, HKII and LDH5 expressions also correlated to those of HIF-2α indicating a possible role of HIF-2α in regulating their transcriptions although they were previously demonstrated as unique targets of HIF-1α (Hu et al., 2003). In fact, the direct association between LDH5 up-regulation and HIF-1α and HIF-2α accumulation had been reported (Koukourakis et al., 2005).

Lactic acid produced by the elevated aerobic glycolysis contributes to the acidification of intratumoral environment which facilitates tumor growth and invasion (Walenta et al., 1997; Walenta et al., 2000). Unlike cancer cells whose proliferation is not affected by low pH, normal cells grow slower (Ceccarini and Eagle, 1971). Furthermore, acidosis causes apoptosis (Park et al., 1999), increases the degradation of extracellular matrix (Rozhin et al., 1994) and retards the immune response (Lardner, 2001) in normal cells.

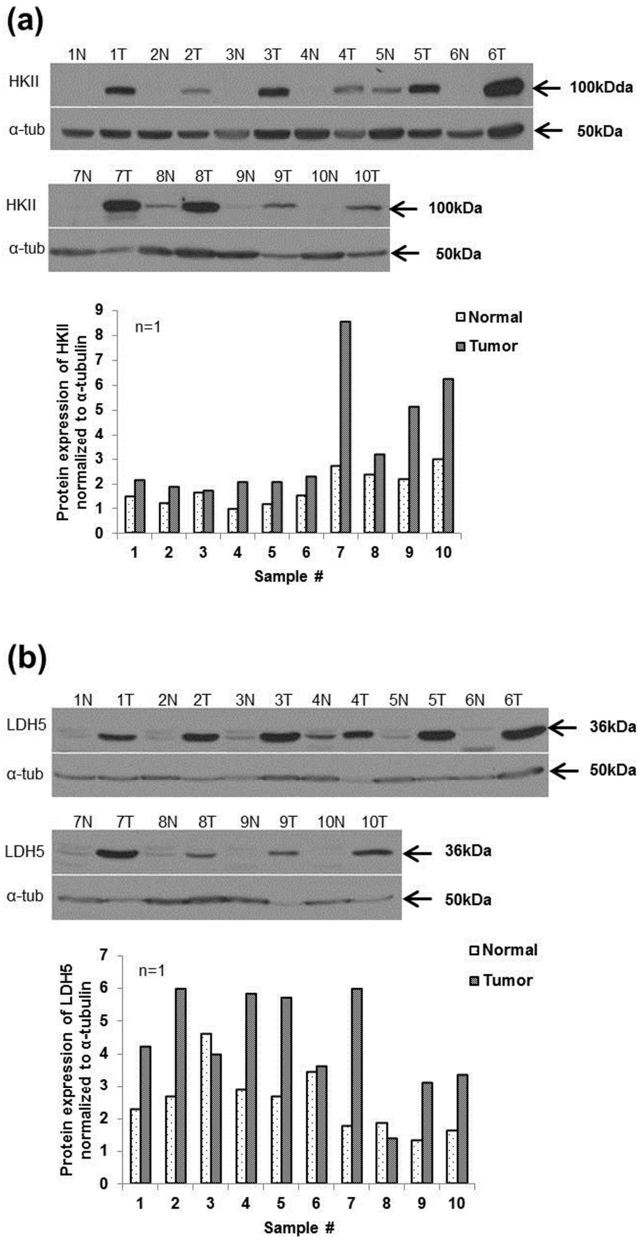

Fig. 2.2.2 Western blot analysis of enzymes which are known to be targets of HIF1α.

(a) Hexokinase II (HKII) and (b) lactate dehydrogenase isoenzyme V (LDH5) were found to be highly expressed in the ccRCC tumor lysate (T) as compared to the patient-matched normal tissue (N). Of note, sample #8 was derived from an unclassified renal cell carcinoma and therefore was excluded from percentage calculation shown in the results. Intensity of bands was quantified using the ImageJ software and expressed as relative to α-tubulin, the loading control.

2.2.3 Elevated expression of pyruvate dehydrogenase kinase (PDHK1) and reciprocal loss of pyruvate dehydrogenase (PDH) expression and activity in ccRCC tumor

Other than HKII and LDH5, pyruvate dehydrogenase kinase 1 (PDHK1) is another downstream target of HIF-1α. It was found to be higher in 66.7% (6/9) in ccRCC tumor sample (Fig. 2.2.3a). There was a correlation between the expression of HIF-1α and PDHK1 since the latter is a known target of the former (Kim et al., 2006; Papandreou et al., 2006).

PDHK1 phosphorylates and inhibits pyruvate dehydrogenase (PDH) activity. Examination on the total and active PDH activity of sample # 9 and #10 which showed higher PDHK1 expression revealed a complete loss of activity measured in mitochondria isolated from the tumor (Fig. 2.2.3b). The experiment was not performed on the other samples due to insufficient mitochondrial extract.

However, the absence of even the total PDH activity in contrast to the significant activity observed in normal mitochondria could not be explained by the inhibition of PDHK1 since phosphorylation will only attenuate the active fraction of the PDH activity. Therefore, the protein expression of PDH E1α was studied. There was minimal amount of PDH E1α present in the ccRCC tumor (Fig. 2.2.3c) which could explain why PDH activity was not detected. Synthesis of pyruvate dehydrogenase complex could be compromised due to the low level of its inducing metabolite, pyruvate (Dietrich and Henning, 1970). Of note, the PDH E1α expression was inversely related to their corresponding PDHK1 counterparts (Fig. 2.2.3a).

The loss of PDH enzymatic activity in ccRCC tumor deprives the Krebs cycle of acetyl-coA and leads to shortage of TCA metabolites and reducing equivalents for oxidative phosphorylation. This forces the cancer cells to seek for alternative fuel source which will be addressed in Chapter 4.

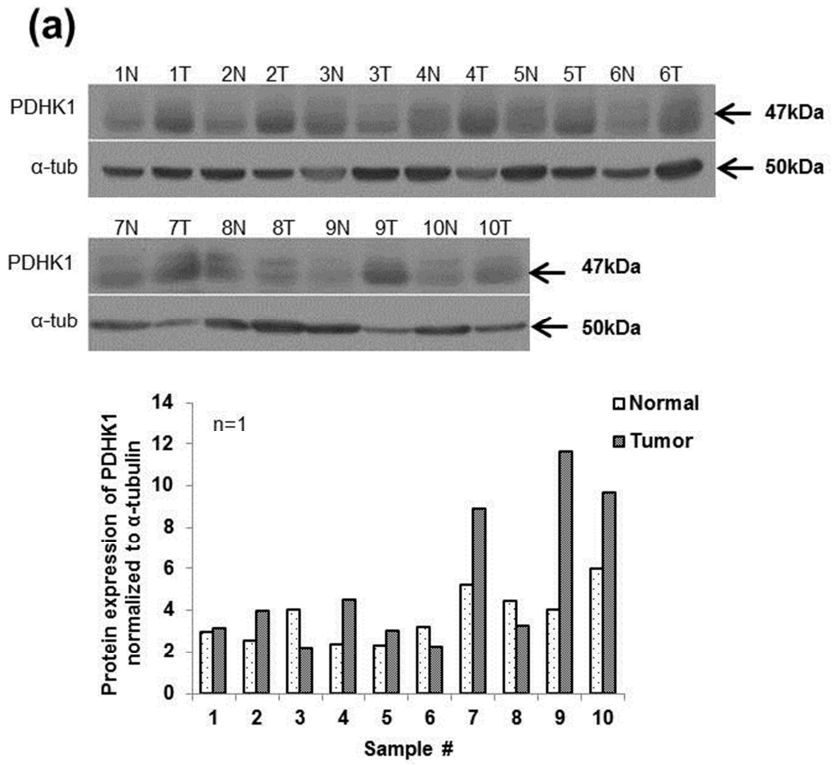

\

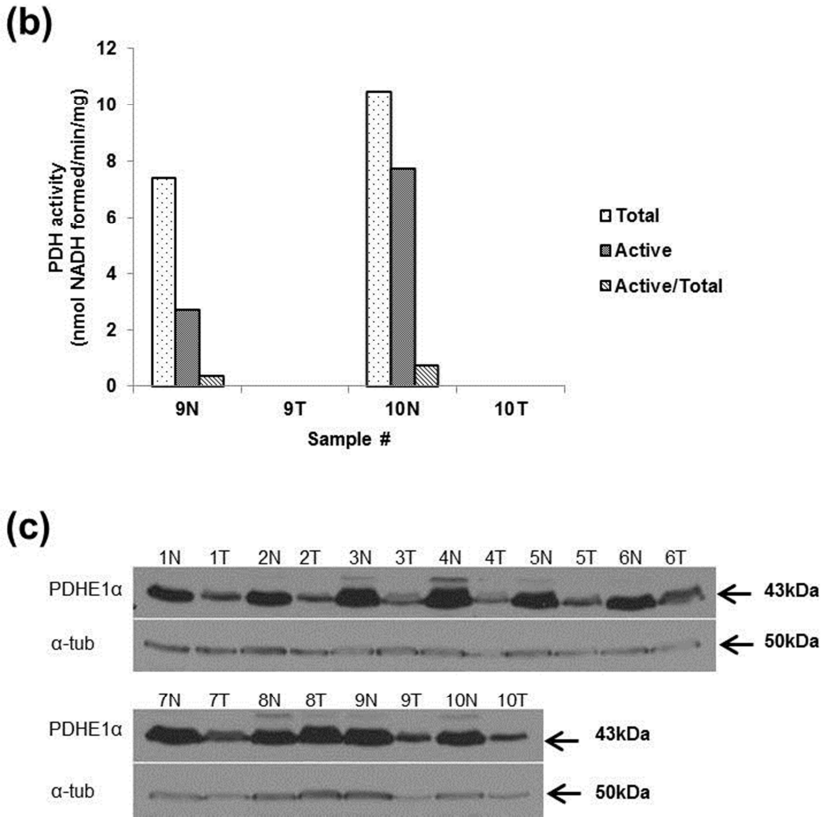

Fig. 2.2.3 Pyruvate dehydrogenase kinase (PDHK) and its relationship with pyruvate dehydrogenase complex (PDHc).

(a) Antibody against PDHK1 was used to detect the protein expression level of PDHK1 and it was found to be generally higher in the ccRCC tumor as compared to their normal counterparts.

(b) PDH enzymatic activity The total and active PDH enzyme activities were present in the mitochondrial extracts of normal (N) but absent from those of the tumor (T).

(c) Protein expression of PDH complex was probed using an antibody against its PDHE1α subunit. PDH is regulated by phosphorylation of three serine residues on the E1α subunit (Dahl et al., 1987; Yeaman et al., 1978). An inverse relationship between the protein levels of PDHK1 and PDHE1α was observed (Fig. 2.2.3a and 2.2.3c).

2.2.4 ccRCC tumor has lower protein expressions of respiratory chain (RC) complexes I to V

Warburg proposed that injury to respiration in cancer cells is responsible for their addiction towards aerobic glycolysis; therefore, the components of the respiratory chain were examined. All the respiratory chain (RC) complexes I-V (corresponding to NADH dehydrogenase, succinate dehydrogenase, ubiquinol dehydrogenase, cytochrome c oxidase and ATP synthase) were uniformly down-regulated in the ccRCC tumor lysates tested (Fig. 2.2.4). A cocktail of five antibodies corresponding to the respective subunits of RC complexes was applied in this case (as shown in Table 3). All the subunits detected are nuclear-encoded except that of MTCO1 of complex IV. Therefore, the general reduction across the subunits in tumor is not peculiar to either origin of DNA.

RC Complex	Subunit detected	Function	Encoded by
I	NDUFB8	Accessory subunit that transfers electrons from NADH to the respiratory chain.	Nuclear DNA
II	SDHB	Iron-sulfur protein (IP) subunit that transfers electrons from succinate to ubiquinone (coenzyme Q).	Nuclear DNA
III	UQCRC2	Core protein 2 is required for the assembly of the complex.	Nuclear DNA
IV	MTCO1	CO1 is the catalytic subunit of Complex IV.	Mitochondrial DNA
V	ATP5A	Subunits alpha and beta form the catalytic core in F_1-ATPase.	Nuclear DNA

Table 3. The details on subunits and functions of the five antibodies in OXPHOS cocktail.

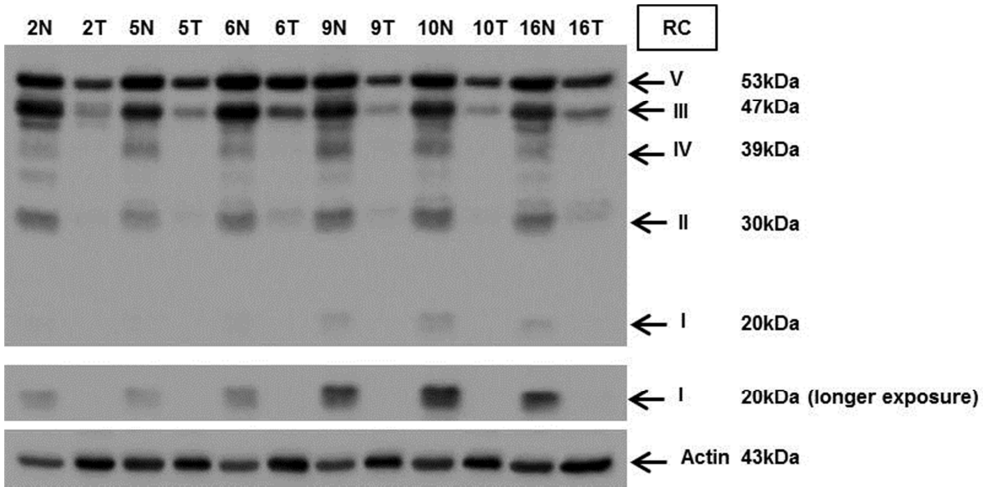

Fig. 2.2.4 Protein expressions of respiratory complexes I to V.
The cocktail employed contained antibodies to probe for the following subunits of the five respiratory complexes (RC), namely Complex I subunit NDUFB8, Complex II subunit 30kDa, Complex III subunit Core 2, Complex IV subunit I and ATP synthase subunit α. Expressions of RC I to V were uniformly reduced in tumor (T) as compared to corresponding normal (N) lysate. Bands of complex I required a longer exposure to be visible. Actin which was meant for loading control was increased in the tumor. The tumor grades of the samples are shown in Table 1.

2.2.5 Mitochondrial enzymes activities

In agreement with the protein expressions, enzymatic activities of RC Complex I (NADH dehydrogenase) and Complex V were compromised in the ccRCC tumor. There was a 3.3-fold reduction of NADH dehydrogenase activity in tumor mitochondria of sample #1 as compared to its normal counterpart (Fig. 2.2.5a). Sample #9 and #10 displayed a 6.2- and 4.7-fold reduction in the Complex V activity measured as the oligomycin-sensitive F_o-ATPase activity (Fig. 2.2.5b). This finding is supported by earlier reports demonstrating the lower protein expressions and activities of respiratory complexes in ccRCC (Meierhofer et al., 2004; Simonnet et al., 2002).

In order to determine if the down-regulated RC activities were due to the difference on the content of intact mitochondria, activity of citrate synthase (CS) was measured. CS is commonly used as a mitochondrial, quantitative marker enzyme (Holloszy et al., 1970; Hood et al., 1989; Williams et al., 1986) because its activity in a specific tissue is frequently constant when expressed per mg of mitochondrial protein. CS activity was found to be negligibly compromised in tumor of sample #9 in contrast to 33% increase in tumor of sample #10 (Fig. 2.2.5c).

Apart from citrate synthase, malate dehydrogenase is another enzyme involved in the Krebs cycle. It reversibly catalyzes the conversion from malate to oxaloacetate at the expense of NAD to form NADH. There was no significant difference in malate dehydrogenase (MDH) activity between the normal and tumor mitochondria suggested a functional TCA cycle in the tumor (Fig. 2.2.5d).

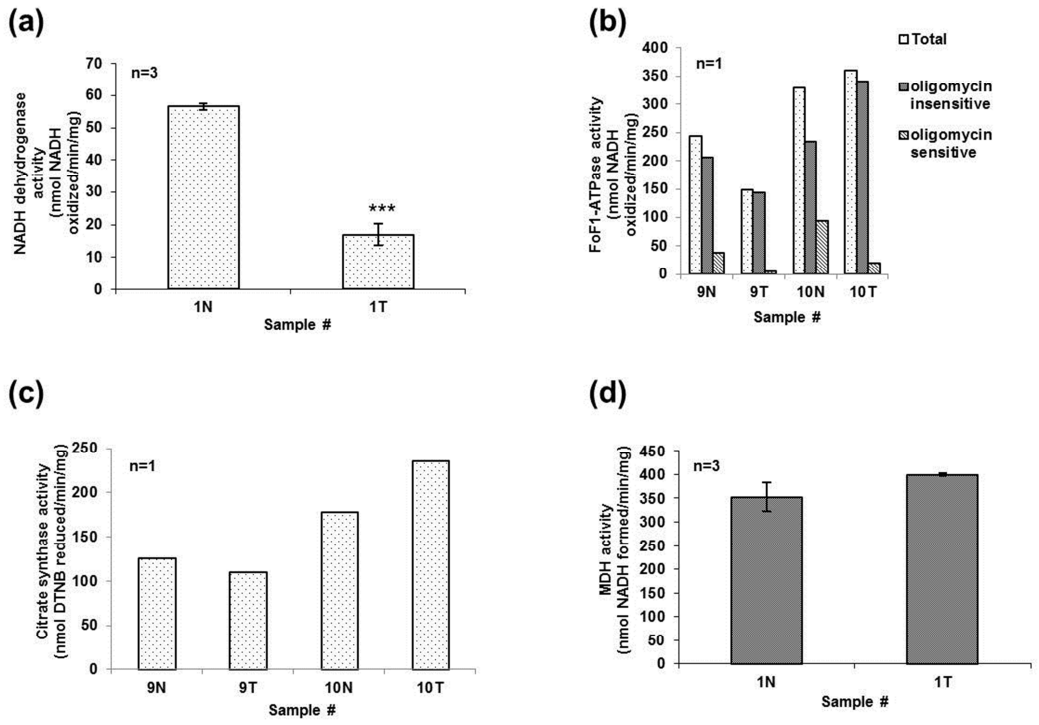

Fig. 2.2.5 Activities of mitochondrial enzymes.

(a) NADH dehydrogenase (RCI) activity Complex I activity was measured in freeze-thawed mitochondrial extracts. There was a significant difference in RCI enzymatic activity between the tumor (T) and matched normal (N) tissues with ***p<0.005 for n=3.

(b) FoF1-ATPase enzymatic activity As represented by its oligomycin sensitivity, the FoF1-ATPase activity determined in two freeze-thawed mitochondrial extracts was quite compromised in ccRCC tumor (T) as compared to matched normal (N) tissues.

(c) Citrate synthase (CS) activity CS activity was comparable between the tumor (T) and patient-matched (N) mitochondrial extracts.

(d) Malate dehydrogenase (MDH) activity There was no significant difference in MDH activity between freeze-thawed mitochondrial extracts derived of tumor (T) and normal (N) tissues where n=3.

2.2.6 Reduced expression of transcription factors: mtTFA, PGC-1α and NRF-1 in mitochondrial biogenesis

The overall decreased protein levels of respiratory complexes described above suggested a possible global decrease in mitochondrial genesis which led us to measure the associated transcription factors: mitochondrial transcription factor A (mtTFA), peroxisome proliferator-activated receptor gamma coactivator 1-alpha (PGC-1α) and the nuclear respiratory factor 1 (NRF-1). Our Western blot analyses showed lower expressions of mtTFA (Fig. 2.2.6a), and PGC-1α except for samples #6, #8 or/and #7 (Fig. 2.2.6b). In a separate blot of seven sets of tissue samples, NRF-1 was also lower in tumor tissues (Fig. 2.2.6c). Together, a deficient mitochondrial biogenesis was implicated.

Indeed, compromised mitochondrial biogenesis has been attributed to the deficiency of von Hippel-Lindau factor (VHL) since mitochondrial DNA, respiratory chain contents and mtTFA were upregulated when VHL is restored in VHL-deficient ccRCC cells (Hervouet et al., 2005). This is substantiated by the finding that HIF1α mediates the reduction of mitochondrial mass and oxygen consumption in ccRCC via inhibition of c-myc (Zhang et al., 2007).

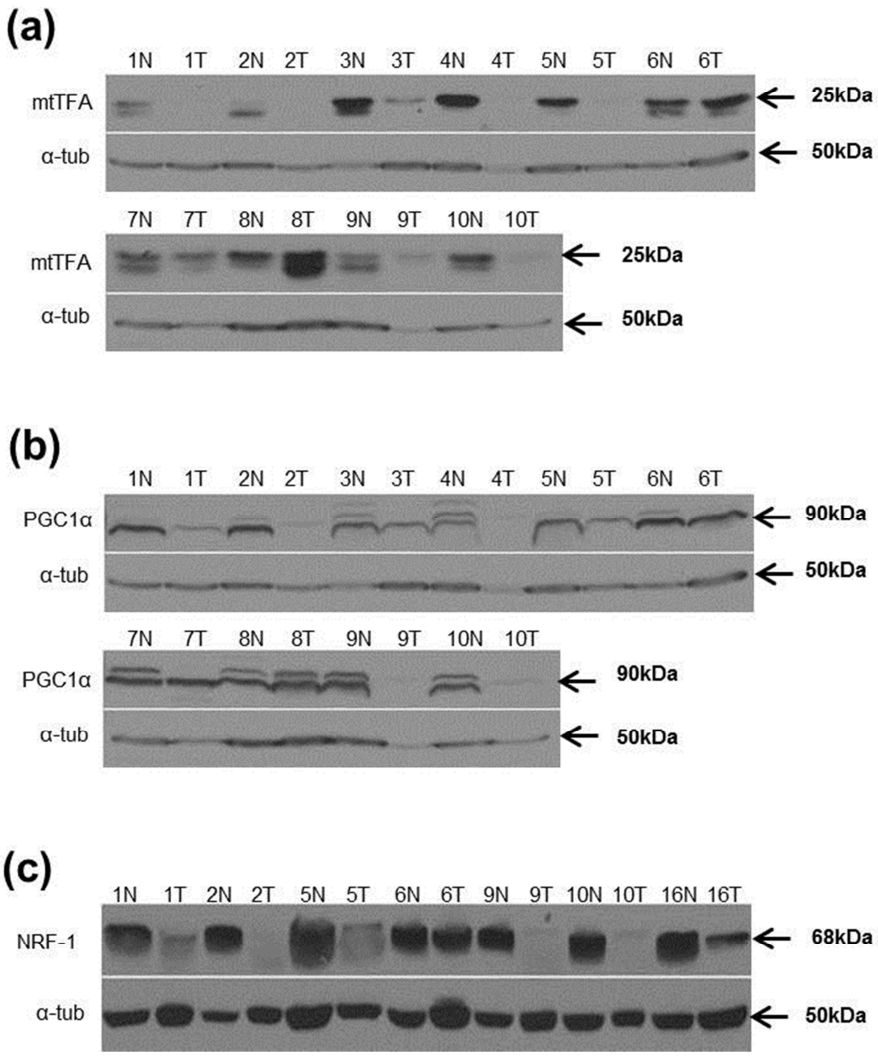

Fig. 2.2.6 Protein expression of transcription factors involved in mitochondrial biogenesis.

The three transcription factors are (a) mitochondrial transcription factor A (mtTFA), (b) peroxisome proliferator-activated receptor gamma coactivator-1-alpha (PGC-1alpha) and (c) nuclear respiratory factor (NRF-1). The protein expressions of all three were generally down-regulated, suggesting a decrease in mitochondrial biogenesis in ccRCC tumor tissues.

CHAPTER 3 OXIDATIVE PHOSPHORYLATION (OXPHOS) CAPACITY AND ROS PRODUCTION IN CLEAR CELL RENAL CELL CARCINOMA (CCRCC)

3.1 Introduction

3.1.1 Oxidative phosphorylation in tumor cells

The phenomenon of increased dependence on glycolysis due to defective mitochondrial functions were generally applied to all types of cancer after Warburg's finding with solid and ascites tumor cells was reported in 1956 (Baggetto, 1992; Pedersen, 1978; Robey et al., 2005; Rossignol et al., 2004; Stubbs et al., 2003; Warburg, 1956b). Indeed, all tumors exhibit elevated glycolysis and many are characterized by compromised oxidative metabolism (Pedersen, 1978) which is associated with lower pyruvate oxidation (Baggetto and Lehninger, 1987), truncated TCA cycle (Parlo and Coleman, 1984), change in mitochondrial ultrastructure (Hoberman, 1975; Springer, 1980), lower mitochondrial content per cell and deficiency in respiratory chain complexes (Lichtor and Dohrmann, 1987; Pedersen, 1978), Crabtree effect in which oxidative phosphorylation was inhibited by glycolysis (Melo et al., 1998; Rodriguez-Enriquez et al., 2001; Sauer, 1977; Sussman et al., 1980), increased of ATP synthase inhibitory peptide (Bravo et al., 2004; Solaini and Harris, 2005) or increased mtDNA damage by oxidative stress (Carew and Huang, 2002; Meierhofer et al., 2006; Penta et al., 2001).

However, there are contradicting results that challenge the explanations mentioned above. In AS30-D hepatoma, citrate flux in Krebs cycle was not

truncated and the activities of TCA cycle enzymes were found to be 1-30 times higher than that of normal liver mitochondria (Briscoe et al., 1994; Dietzen and Davis, 1993). Enzymatic activities of NADH cytochrome c reductase was increased by 2 to 5 fold in brain tumors despite the lower expressions of respiratory chain components (Lichtor and Dohrmann, 1987; White and Nandi, 1976). Inhibitory peptide of ATP synthase was shown to affect only the hydrolytic reaction when mitochondrial membrane potential (MMP) was low (Solaini and Harris, 2005) but not the synthetic reaction which was supported by high MMP; therefore, the mitochondrial ATP synthesis should not be decreased by the lower level of this protein. Although correlation was observed between mutation in mtDNA and ROS production accompanied with lower mitochondrial functions in oncocytic thyroid carcinomas (Bonora et al., 2006), human renal carcinoma displays low mtDNA mutations which should not be responsible for the compromised aerobic energy capacity (Meierhofer et al., 2006) in this tumor.

In fact, tumor cell lines were shown to have elevated rates of respiration (Weinhouse, 1956) in which 85-90% of the respiration rate in AS-30D and HeLa were sensitive to the ATP synthase inhibitor, oligomycin indicating their reliance on oxidative phosphorylation. The higher activities of mitochondrial malic enzyme (Mandella and Sauer, 1975) and phosphate-dependent glutaminase (Matsuno and Goto, 1992; Molina et al., 1995) in tumor cells as compared to their original tissue counterpart suggest mitochondria in cancer cells are active. Furthermore, the supply of mitochondrial ATP required for cell cycle transition from resting to active proliferating state in Ehrlich tumor cells (Muller et al., 1986)

as well as the oxidation of pyruvate and glutamine in glycolytic gliomas during low glucose condition (Griguer et al., 2005) demonstrates the existence of fully functional mitochondria in tumors. We have also shown that OXPHOS-competent mitochondria are present in ovarian cancer tissues and skin fibroblasts from human keloid as shown by studies in our lab (Lim et al., 2011; Vincent et al., 2008).

Enhancement of glycolysis accompanied by impaired mitochondria could be peculiar to certain cancer types but is definitely not a universal mechanism. Thus, the oxidative metabolism of each cancer type has to be assessed before any precise conclusion can be drawn. Apart from the heterogeneity of tumors, reduction in the protein expression and/or enzymatic activity of a particular enzyme might not necessarily be detrimental to the metabolic pathway. Therefore, a much appropriate approach is employed here to examine the OXPHOS capacity via the measurement of ATP synthesis, oxygen consumption rate and mitochondrial membrane potential in intact, isolated mitochondria from ccRCC tumor and the corresponding patient-matched normal tissue.

3.1.2 Reactive oxygen species (ROS)

Mitochondria are the major production site of reactive oxygen species (ROS) whereby electrons leak out from the electron transport chain and combine with molecular oxygen to form superoxide anion ($O_2^{-\cdot}$), a precursor of most ROS. Sites of superoxide formation are depicted in Fig. 3.1.2. The contribution of each site to the overall superoxide level is organ specific and also depends on how reduced the respiration chain is (Barja, 1999). Higher superoxide production is anticipated when the mitochondria are not synthesizing ATP and have a high mitochondrial membrane potential due to the sluggish electron transfer. Complex I is the primary superoxide generator in the brain under normal conditions (Barja, 1999; Herrero and Barja, 1998) and it is also responsible for ROS produced in pathological conditions such as in Parkinson's disease (Betarbet et al., 2002; Herrero and Barja, 1998; Kushnareva et al., 2002; Trojanowski, 2003). In contrast, superoxide produced in heart and lung mitochondria originate from Complex III (Turrens and Boveris, 1980; Turrens et al., 1982). Superoxide generated at the intermembrane space can be converted to hydrogen peroxide (H_2O_2) by the action of copper zinc superoxide dismutase (CuZnSOD) which is used to reduce cytochrome c or be released into the cytoplasm via voltage-dependent anion channels (Han et al., 2003). Superoxide formed in the matrix however is converted to hydrogen peroxide through a reaction catalyzed by manganese SOD (MnSOD).

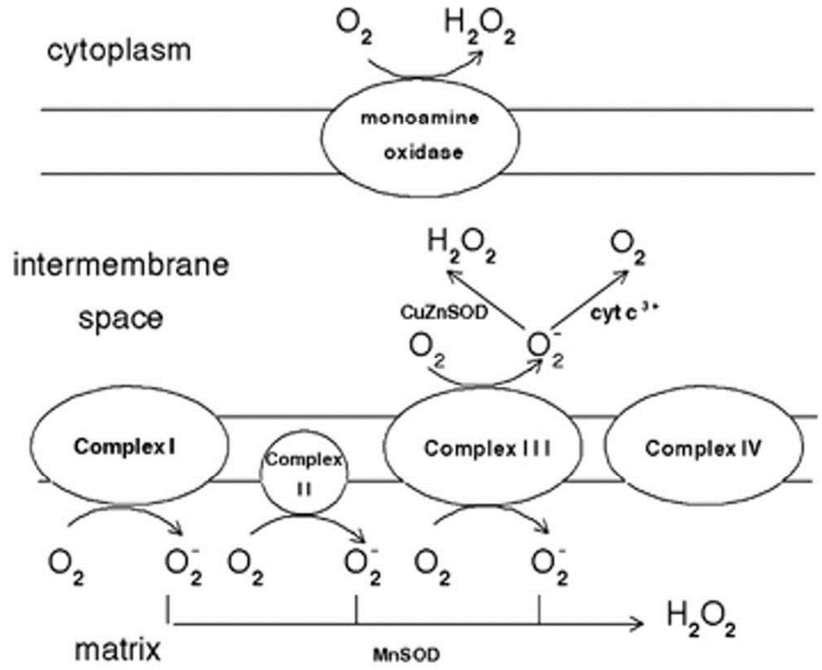

Fig. 3.1.2 Sites of superoxide production. Reproduced from Journal of Physiology, 552, Turrens JF, Mitochondrial formation of reactive oxygen species, page 336, 2003, with permission from John Wiley and Sons (License Number: 3445700946667).

The three main mammalian superoxide dismutases are SOD1, SOD2 and SOD3. SOD1 and SOD3 contain copper and zinc in their active site and SOD1 is found in the intermembrane space and cytosol whereas SOD3 is localized extracellularly. SOD2 is the manganese SOD that is exclusively distributed in the mitochondria. Hydrogen peroxide produced by dismutation of superoxide is then fully reduced to water or partially reduced and gives rise to one of the strongest oxidants, hydroxyl radical (·OH). Superoxide can also react with radicals such as nitric oxide (NO·) and produce another potent oxidant, peroxynitrite ($ONOO^-$) (Beckman and Koppenol, 1996; Radi et al., 2002). Both hydroxyl radical and peroxynitrite trigger the deleterious effect on the cells upon reacting with lipids, nucleic acids and proteins.

3.2 Results and Discussions

3.2.1 ccRCC tumor mitochondria are capable of synthesizing ATP

ATP synthesis by isolated mitochondria when fortified with exogenous ADP and respiratory substrates measures the OXPHOS capacity. It involves the oxidation of added substrates followed by the transfer of electron from NADH / $FADH_2$ to oxygen by a series of complexes which coupled to the phosphorylation of ADP to form ATP.

The rate of ATP biosynthesis from ADP in the presence of malate/glutamate (RCI substrates), succinate (RCII substrate) or N,N,N′,N′-tetramethyl-p-phenylenediamine (TMPD) /ascorbate (artificial RCIV substrates) was comparable in two of the three pairs of tumor and normal tissues as shown in Fig. 3.2.1a and Fig. 3.2.1b. However, less ATP was generated from all substrates examined for the sample #4T shown in Fig. 3.2.1c which was probably due to the extensive areas of hemorrhage and necrosis as revealed by the pathological analysis (Table 1).

Enzymatic activity of respiratory complex I (NADH dehydrogenase) was shown to be lower in the mitochondrial extract of sample #1T; however, ATP formation given rise from RCI substrates, malate/glutamate was surprisingly not affected as shown in Fig. 3.2.1a.

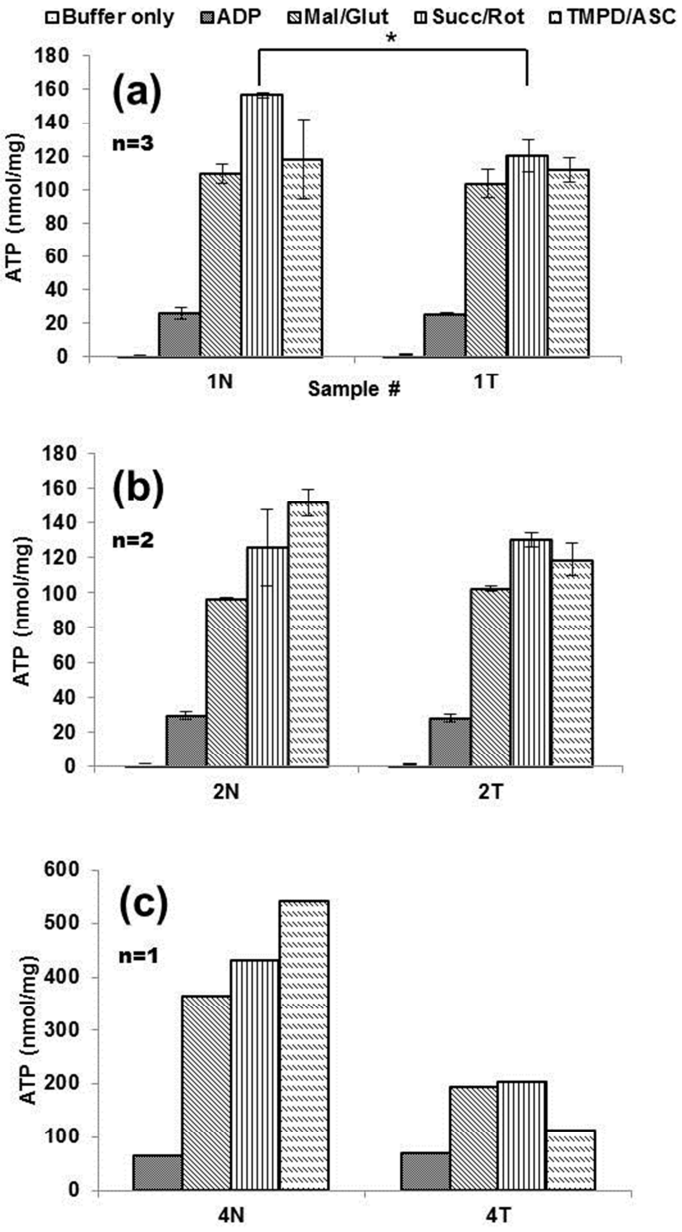

Fig. 3.2.1 Biosynthesis of ATP in intact mitochondria isolated from ccRCC tumor and patient-matched normal tissue.
5mM each malate/glutamate (RCI substrates), 10mM succinate (RCII substrate)/5µM rotenone and 1mM TMPD/5mM ascorbate (artificial electron donors for RCIV)/2µg/ml antimycin A were used. 125µM ADP was added in all conditions containing respiratory substrates. The rate of ATP biosynthesis was only compared for sample #1 as shown in Fig. (a) for n=3; *p<0.05. No significant difference was observed except that for succinate.

3.2.2 ccRCC tumor mitochondria exhibit comparable oxygen consumption rate

The capacity and function of the intact mitochondria isolated from ccRCC tumor tissues and their normal counterparts were also determined using polarographic-based measurements of oxygen consumption. The flux control ratio which represented the oxygen consumption rate was depicted in Fig. 3.2.2.

State 4 respiration was achieved by the oxidation of succinate plus rotenone without ADP, labeled as S(ROT). In this case, rotenone was added to inhibit NADH dehydrogenase and therefore prevent the formation of oxaloacetate from malate by the action of malate dehydrogenase that required NAD^+ as a cofactor. Accumulation of oxaloacetate (which is a potent competitive inhibitor of succinate dehydrogenase (Wojtczak et al., 1969) due to its inability to permeate the mitochondrial inner membrane will lead to the inhibition of succinate dehydrogenase which is unfavorable under this assay setup. On the other hand, State 3 respiration was attained with saturated amount of ADP for the estimation of coupled OXPHOS capacity.

A comparable degree of OXPHOS was observed in all three sets of samples (Fig. 3.2.2) except for minimal State 4 respiration of succinate which was lower in tumor sample labeled as #4T.

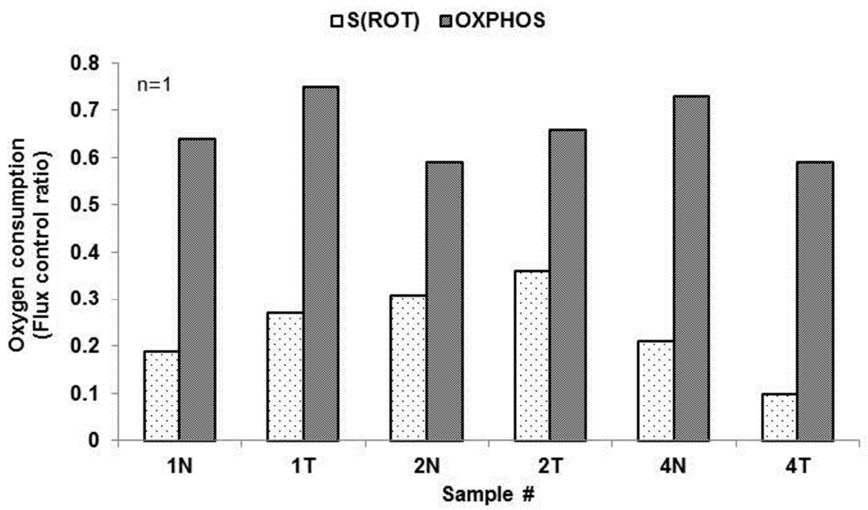

Fig. 3.2.2 Oxygen consumption in intact mitochondria isolated from ccRCC tumor and corresponding normal tissue.

A comparable degree of oxygen flux (rate of oxygen consumption) control ratio was evident in both tissues using 10mM succinate as respiratory substrate in the presence of 0.5μM rotenone, an inhibitor of NADH dehydrogenase, except for tumor sample #4. OXPHOS which was measured in the presence of 250μM ADP was comparable in mitochondria isolated from normal (N) and ccRCC tumor (T) tissues. However, state 4 respiration of succinate plus rotenone appeared compromised in sample #4T.

3.2.3 Mitochondria from ccRCC tumor exhibit higher basal mitochondrial membrane potential (MMP)

The JC-1 fluorescent probe was used as a semi-quantitative method to evaluate the capacity of mitochondria to induce membrane potential (MMP) by sequential additions of respiratory substrates followed by de-energization with the inhibitors. JC-1 is a lipophilic, cationic probe and it is taken up into the mitochondria due to the negative transmembrane potential in the matrix. When more of the JC-1 green monomers enter the mitochondria due to the polarization of mitochondrial membrane, they form aggregates which have a red fluorescence causing a shift in the emission wavelength from 535nm to 595nm. This is also reflected by the reciprocal change of the green and red fluorescence. ADP was initially introduced to the assay system in order to deplete the endogenous substrates present in the isolated mitochondria (Chance and Williams, 1955) by promoting the coupling between oxidation and phosphorylation.

Of note, the term "basal MMP" used throughout this thesis corresponds to State 2 respiration in which the MMP was measured in the presence of ADP but without addition of any respiratory substrates/inhibitors. In contrast, the term "inherent or endogenous MMP" is the MMP of mitochondria in the assay buffer containing phosphate but without addition of ADP and respiratory substrates/inhibitors which corresponds to State 1 respiration.

Higher basal MMP was detected in mitochondria isolated from ccRCC tumor (dotted line) when compared to the matched normal tissue (solid line) as shown by steeper gradients marked by asterisks in Fig. 3.2.3b, 3.2.3d and 3.2.3f in

the presence of ADP. The MMP was further increased by substrates of respiratory complex I (also known as NADH dehydrogenase), malate and glutamate (Mal/Glut) followed by inhibition of NADH dehydrogenase by rotenone. The effect of subsequent addition of complex II substrates, succinate (Succ) was comparable in the normal samples (Fig. 3.2.3a, 3.2.3c and 3.2.3e but variable in the three tumor samples shown in Fig. 3.2.3b, 3.2.3d and 3.2.3f with the last showing the least response. The MMP was eventually collapsed by the addition of antimycin A (AA), an inhibitor of respiratory complex III.

Overall, intact mitochondria isolated from ccRCC tumor tissues are able to carry out the essential mitochondrial activities involved in OXPHOS. Energization of MMP by respiratory substrates indicates the intactness and functionality of the mitochondria isolated from ccRCC. The observations of ATP biosynthesis and increase in the oxygen flux in response to ADP demonstrate the coupling of oxidation of succinate to phosphorylation of ADP. However, it must be iterated that exogenous ADP and respiratory substrates were added in all the measurements of OXPHOS; thus the results represent the potential of the isolated mitochondria to perform OXPHOS when substrates are available. On a side note, the aberrant ATP biosynthesis, oxygen flux and MMP were noted with succinate in the tumor sample #4 which could be due to the presence of extensive necrosis (Table 1).

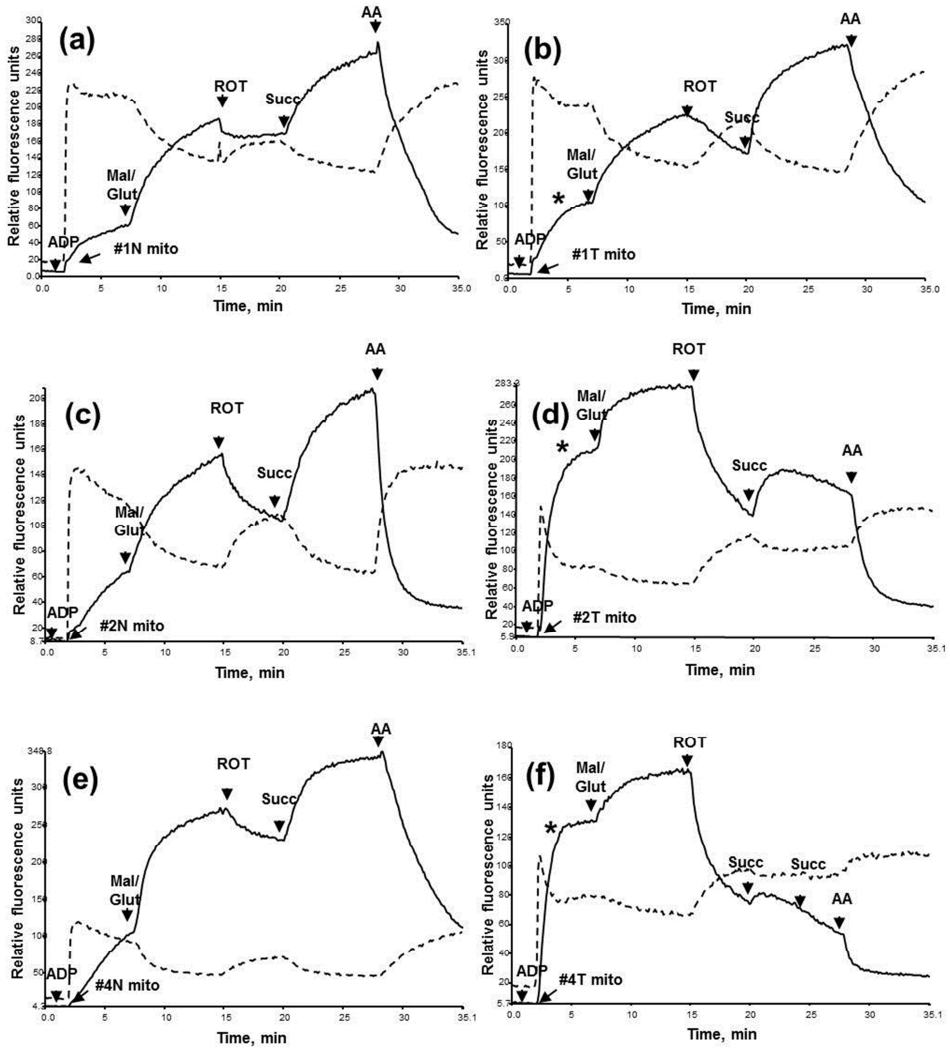

Fig. 3.2.3 Mitochondrial membrane potential in intact mitochondria isolated from ccRCC tumor and corresponding normal tissue.

The basal MMP, evident in the presence of 125μM ADP but before the addition of mal/glut was higher in mitochondria isolated from ccRCC tumor tissues as shown by the asterisks in Fig. (b), (d) and (f) as compared to the matched adjacent normal tissues in Fig. (a), (c) and (e). X- and y- axes represent, respectively, the intensity of fluorescence and time (min). Solid lines denote the red fluorescence of the JC-1 aggregates and dotted lines the green fluorescence of the monomers; these two measurements showed a reciprocal relationship. The MMP was induced by addition of 5mM each malate and glutamate (Mal/Glut) which was inhibited by 5μM rotenone (ROT) followed by re-energization by 10mM succinate (Succ) with subsequent inhibition with 4μg/ml antimycin A (AA, an inhibitor of respiratory complex III) which finally collapsed the MMP.

3.2.4 ccRCC tumor mitochondria produced higher reactive oxygen species (ROS)

The high basal MMP observed in the ccRCC tumor creates resistance for the electrons to be passed down the electron transport chain. This could lead to higher formation of superoxide. Measurement of ROS produced by normal and ccRCC tumor mitochondria were performed using the oxidative stress sensitive probe, 2′,7′-dichlorofluorescin diacetate (DCFDA) which detects a range of radicals including peroxynitrite ($ONOO^-$), hydrogen peroxide (H_2O_2) in combination with cellular peroxidases and hydroxyl radical (·OH) (Myhre et al., 2003). Result in Fig. 3.2.4 showed that under basal condition (in phosphate buffered saline), tumor mitochondria of sample #6 and #9 produced higher level of ROS as compared to its normal counterpart.

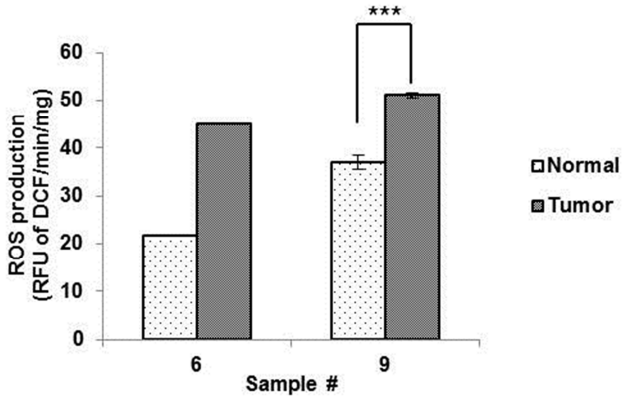

Fig. 3.2.4 ROS production in intact mitochondria isolated from ccRCC tumor and patient-matched normal tissues.

ROS production was examined by using the fluorescence probe, 2′, 7′-dichlorofluorescin diacetate (DCFDA) which could be oxidized by various ROS including peroxynitrite ($ONOO^-$), hydrogen peroxide (H_2O_2) in combination with cellular peroxidases and hydroxyl radical (·OH). ccRCC tumor mitochondria generated higher level of ROS in the phosphate-buffered saline (PBS) and it is shown to be statistically significant in sample #9 with ***p <0.005 for n=3.

3.2.5 The higher ROS generated by ccRCC tumor mitochondria is supported by oxygen radicals other than hydrogen peroxide

To further dissect if the higher ROS production was also reflected in hydrogen peroxide production, H_2O_2 released by the mitochondria was captured using the Amplex red™ reagent. Surprisingly, rate of H_2O_2 generation was significantly lower in ccRCC tumor mitochondria of sample #9 and that was also true in sample #8 which was an unclassified renal cell carcinoma (Fig. 3.2.5). Therefore, the higher ROS production in ccRCC tumor mitochondria was unlikely to be contributed by hydrogen peroxide.

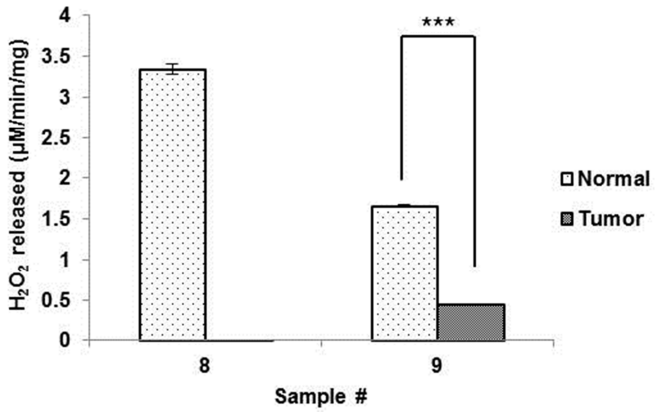

Fig. 3.2.5 Hydrogen peroxide released by intact mitochondria isolated from ccRCC tumor and patient-matched normal tissues.
Amplex ® red reagent in combination of peroxide was employed to specifically detect the release of hydrogen peroxide from mitochondria. Lower level of hydrogen peroxide production was detected in the ccRCC tumor mitochondria, sample #9. The unclassified renal cell carcinoma, sample #8 showed the same effect. Statistical analysis revealed the significance in sample #9 with ***p<0.005 for n=3.

3.2.6 Protein expression of MnSOD is higher in ccRCC tumor lysate

In order to find out why the production of hydrogen peroxide is lower in ccRCC tumor mitochondria, the protein expression of MnSOD which is found specifically in the mitochondria was examined. 77.8% of ccRCC tumor showed higher MnSOD expression (Fig. 3.2.6). In spite of its higher protein expression, formation of hydrogen peroxide was lower in the tumor mitochondria of #6 and #9 (Fig. 3.2.5).

However, overexpression of MnSOD does not guarantee the higher production of hydrogen peroxide. The rates of superoxide production and H_2O_2 removal determine if additional hydrogen peroxide will be detected in a MnSOD overexpression system, in this case the ccRCC tumor mitochondria. SODs are present far in excess than it substrate (superoxide) and thus SODs are more than sufficient to convert the superoxide into hydrogen peroxide provided that superoxide production is not limited. Therefore, it is the generation of superoxide but not the expression level of MnSOD that controls the H_2O_2 production. The low H_2O_2 levels could also be contributed by its rapid scavenging by catalase (one of the fastest enzyme), glutathione peroxidases and peroxidredoxins.

Alternatively, H_2O_2 can be converted to superoxide and then peroxynitrite in a reverse reaction of MnSOD when nitric oxide is available (MacMillan-Crow and Crow, 2011) which were depicted in Fig. 3.2.6. In this case, the overexpression of MnSOD might not result in higher H_2O_2 production in ccRCC.

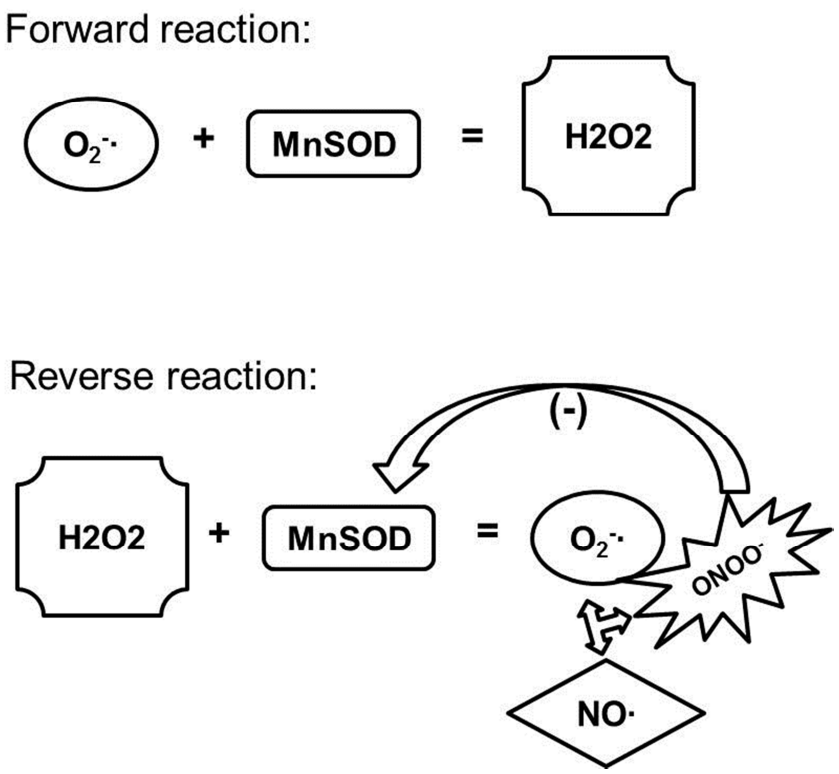

Fig. 3.2.6a The forward and reverse reactions of MnSOD. Superoxide produced in the reverse reaction reacts with nitric oxide and give rise to peroxynitrite, leading to MnSOD inactivation.

This provides the explanation for the higher DCF fluorescence but low H_2O_2 formation despite the upregulated MnSOD expression in ccRCC tumor mitochondria. Further investigations involving determination of superoxide and nitric oxide as well as enzymatic activities of catalase, glutathione peroxidases and peroxidredoxins would be useful to provide insights into the mechanism responsible for the high MnSOD expression but low H_2O_2 production observed in ccRCC mitochondria.

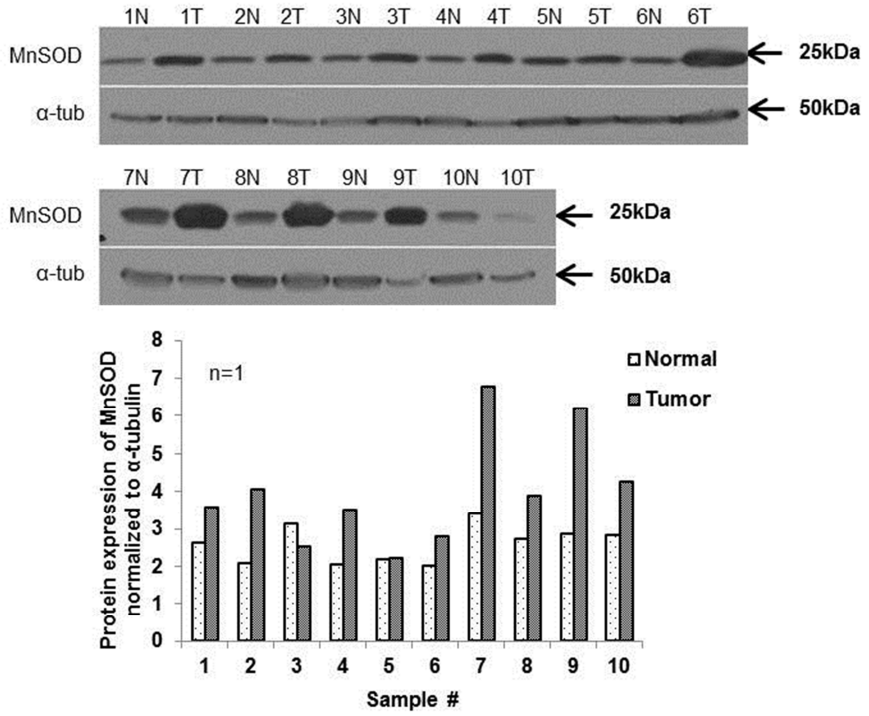

Fig. 3.2.6b Western blot analysis of MnSOD in lysate of ccRCC tumor and adjacent normal tissue.
MnSOD is synthesized as a precursor protein in the cytosol and translocated into the mitochondria driven by the mitochondrial targeting sequence. Higher expression level of MnSOD was found in the ccRCC tumor as compared to their corresponding control, except sample #3 and #5.

CHAPTER 4 THE HIGHER BASAL MMP IN MITOCHONDRIA ISOLATED FROM CLEAR CELL RENAL CELL CARCINOMA (CCRCC)

4.1 Introduction

4.1.1 Mitochondrial membrane potential

Whilst electrons are passed down the series of respiratory complexes at the electron transport chain, protons are pumped from mitochondrial matrix to the intermembrane space causing the accumulation of H^+ in that region. This creates a proton gradient across the inner mitochondrial membrane (IMM) leading to the establishment of the mitochondrial membrane potential ($\Delta\Psi m$, an electrical gradient) and mitochondrial pH gradient (ΔpHm, an H^+ chemical gradient) (Boyer et al., 1977; Mitchell, 1966; Murphy and Brand, 1987). The former is manifested by the positively charged proton and the latter is due to the acidity caused by protons.

The energy stored in the electrochemical gradient (Δp) is used to drive the ATP synthesis at ATP synthase (Complex V) in which protons flow back to the matrix against its gradient since the IMM is impermeable to proton. $\Delta\Psi m$ is highly negative with a typical value range from 150-180mV and ΔpHm of 0.5 to 1 unit giving rise to 30-60mV; therefore, Δp which is a sum of both ranges from 180-220mV. The ratio of contribution by both components on the proton gradient varies from cell line to cell line with unknown reason (Tzagoloff, 1982).

The proton gradient regulates the transport of ions and metabolites (LaNoue and Schoolwerth, 1979), the translocation of precursor enzymes (Chen and Douglas, 1987; Horwich et al., 1987; Schleyer et al., 1982; Verner and Schatz,

1987), the synthesis of mitochondrial protein (Abou-Khalil et al., 1986; Rabinovitz et al., 1977) and apoptosis (Ly et al., 2003). The mitochondrial membrane potential was also reported to be associated with cell growth. Higher MMP was observed in cells in exponential growth phase than those in stationary phase (Benel et al., 1986; Bertoncello et al., 1985; Darzynkiewicz et al., 1981; Doolittle et al., 1987; Mulder and Visser, 1987). Cell differentiation increases or decreases the MMP depending on the energy expenditure in the differentiated cells (Collins and Foster, 1983; James and Bohman, 1981; Summerhayes et al., 1982). The proton potential is also required for cell motility since cells along the edges of a healing wound exhibited higher MMP (Johnson et al., 1981) which was restored to resting level after the wound was covered up.

Higher MMP in cancer cells was previously reported in a study comparing normal epithelial cells and cancer cells derived from tumors of various tissues (Lampidis et al., 1983; Summerhayes et al., 1982; Wiseman et al., 1985). There is at least 60mV difference in MMP between the normal epithelial cells and carcinoma cells (Modica-Napolitano and Aprille, 1987) but the mechanism responsible is unknown.

4.1.2 Uncoupling proteins (UCPs)

Uncoupling proteins (UCPs) are proton transporters that reside in the inner mitochondrial membrane. UCP was first used to describe UCP1 which is uniquely found in the mitochondria of brown adipocytes. Activation of UCP1 by free fatty acid uncouples the ATP production from the mitochondrial respiration and dissipates the energy of proton gradient as heat.

UCP2 and UCP3 are two homologues of UCP1 that share ~56% of their amino acid sequence. UCP2 is ubiquitously expressed whereas UCP3 is mainly detected in skeletal muscle. The involvement of UCP2 and UCP3 in regulating the proton electrochemical gradient is suggested in yeast (Fleury et al., 1997; Gimeno et al., 1997; Hinz et al., 1999a; Hinz et al., 1999b; Zhang et al., 1999) and mammalian cells (Fink et al., 2002; Hong et al., 2001). However, controversial studies show UCP2 and UCP3 do not mimic the role of UCP1 in uncoupling and thermogenesis (Golozoubova et al., 2001; Stuart et al., 2001). Besides regulating the free radical levels in cells, UCP2 and UCP3 have been suggested to be involved in insulin secretion (Hong et al., 2001) and fatty acid metabolism (MacLellan et al., 2005) respectively.

By uncoupling the oxidative phosphorylation (OXPHOS), UCPs collapse the mitochondrial membrane potential since protons are shuttled across the IMM freely; therefore, it is pertinent to examine the relationship between UCPs and higher MMP in mitochondria of ccRCC tumor.

4.1.3 Glutaminolysis

In addition to uncoupling proteins, respiratory substrates which feed electrons to the respiratory chain are important for the establishment and maintaining of MMP.

Owing to the glucose addiction and diversion of pyruvate-derived carbon to lactate production especially during the loss of PDH activity mediated by HIF1α, cancer cells seek alternative carbon source to generate building blocks for their active proliferation. Glutamine (Gln) which is the most abundant amino acid present in the plasma and most tissues (Van Slyke et al., 1973) is the ideal candidate to fuel the rapidly dividing cells via the mitochondrial pathway of glutaminolysis.

First of all, glutamine has to be transported from the extracellular compartment into the mitochondria in order for glutaminolysis to occur (McGivan and Bungard, 2007). In fact, glutamine transporters have been identified on the inner mitochondrial membrane (Mates et al., 2009).

During glutaminolysis, glutamine (Gln) is deaminated to form glutamate (Glut) and ammonia via the action of glutaminase. This is followed by the deamination of glutamate to produce α-ketoglutarate (α-KG) which is a TCA cycle intermediate. By replenishing the Krebs cycle, glutamine enables the production of pyruvate and NADPH by the action of malic enzyme. Pyruvate is then converted into acetyl-CoA (if the functional pyruvate dehydrogenase is present) which forms citrate in combination with oxaloacetate that produced from glutamine-derived α-ketoglutarate. NADPH regeneration leads to the reduction of

glutathione for ROS scavenging (Medina, 2001; Tong et al., 2009). However, in cases like ccRCC, citrate is probably generated from glutamine-derived α-ketoglutarate via the reverse TCA cycle due to the diminution of PDH expression and activity.

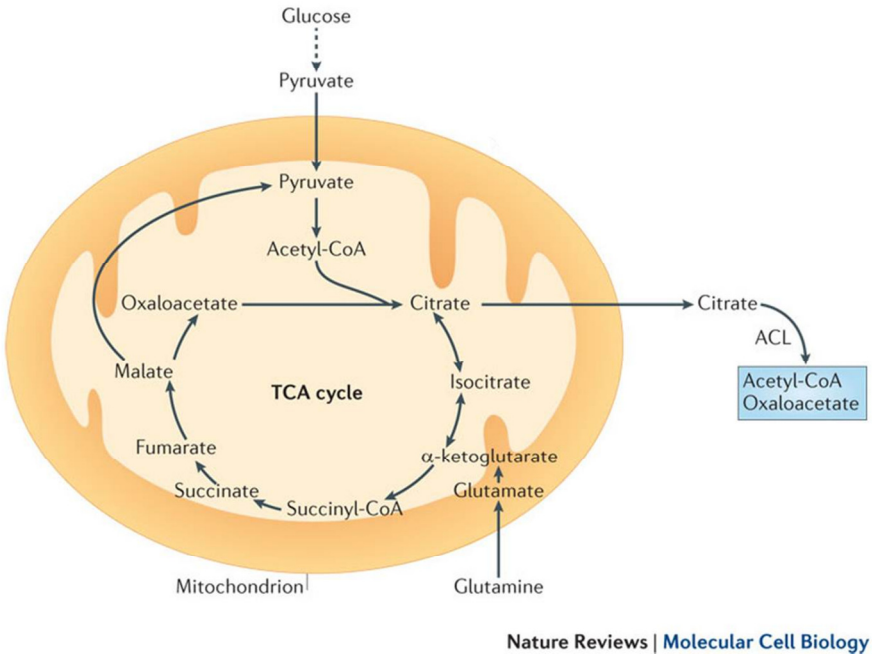

Fig. 4.1.3 Anaplerosis of TCA cycle via glutaminolysis. Reproduced from Nature Reviews Molecular Cell Biology, 13, Wellen KE and Thompson CB, A two-way street: reciprocal regulation of metabolism and signaling, page 271, 2012, with permission from Nature Publishing Group (License Number: 3445710152912).

Glutaminase exists as two isozymes, kidney-type and liver-type. They are different on the requirement for phosphate, Km for glutamine and pH optima (Horowitz et al., 1968; Katunuma et al., 1967; Katunuma et al., 1973). Liver-type glutaminase requires low phosphate but high glutamine for its activity (*K*m=28 to 42mM) as compared to the kidney-type which demonstrated a *K*m of 22mM and 2.2mM for phosphate and glutamine respectively (Horowitz et al., 1968; Huang

and Knox, 1976; Katunuma et al., 1967; Pinkus and Windmueller, 1977). Glutaminase activity found in extracts of cells and tissues are generally the phosphate-dependent, kidney type isozyme (Katunuma and Okada, 1963). Tumors of kidney (Katunuma et al., 1972), mammary gland and fetal liver (Knox, 1976) exhibit higher phosphate-activated glutaminase activity. The correlation between glutaminase activity and the degree of malignancy and growth rates was observed in the Morris hepatomas (Knox et al., 1969; Knox et al., 1967; Linder-Horowitz et al., 1969). The role of glutamine in supporting the anaplerosis of TCA cycle of tumor cells was also revealed by using ^{13}C NMR spectroscopy (DeBerardinis et al., 2007).

4.2 Results and Discussions

4.2.1 The role of uncoupling proteins (UCPs)

4.2.1.1 The protein expressions of UCPs in tissue lysate of ccRCC tumor and the corresponding patient-matched normal

UCP1 is normally expressed in the brown adipocytes; therefore, it is not surprising to detect negligible UCP1 expression in the normal, human kidney tissue lysate. However, higher protein expression was observed in the tumor of sample #2, #5, #6 and #7 as compared to their adjacent normal tissue (Fig. 4.2.1.1a). UCP2 was completely absent in all the ccRCC tumor except sample #7 (Fig. 4.2.1.1b) and it was accompanied by a reciprocal increase in the protein expression of UCP3L (Fig. 4.2.1.1c). UCP3 mRNA exists as two transcripts, UCP3L and UCP3S which were generated from a single gene through alternative splicing. UCP3S which lacks the last 37 amino acids that represent the region for fatty acid and guanine nucleotide regulation (Miroux et al., 1993) is believed to have no uncoupling activity (Millet et al., 1998). Although the inverse relationship between the UCP2 and UCP3L is interesting, it is not covered here.

In this thesis, focus has been placed on UCP2 which is normally found to be upregulated in cancers such as hepatocarcinoma (Carretero et al., 1998), cholangiocarcinoma and oxyphilic thyroid tumor (Baffy, 2010), colon cancer (Horimoto et al., 2004; Kuai et al., 2010) and almost all human cancers examined (Ayyasamy et al., 2011). Our finding on the loss of UCP2 indicated its uniqueness to ccRCC and it could contribute to the higher mitochondrial

membrane potential observed in the ccRCC tumor. The role of UCP2 in supporting mitochondrial membrane potential was therefore examined.

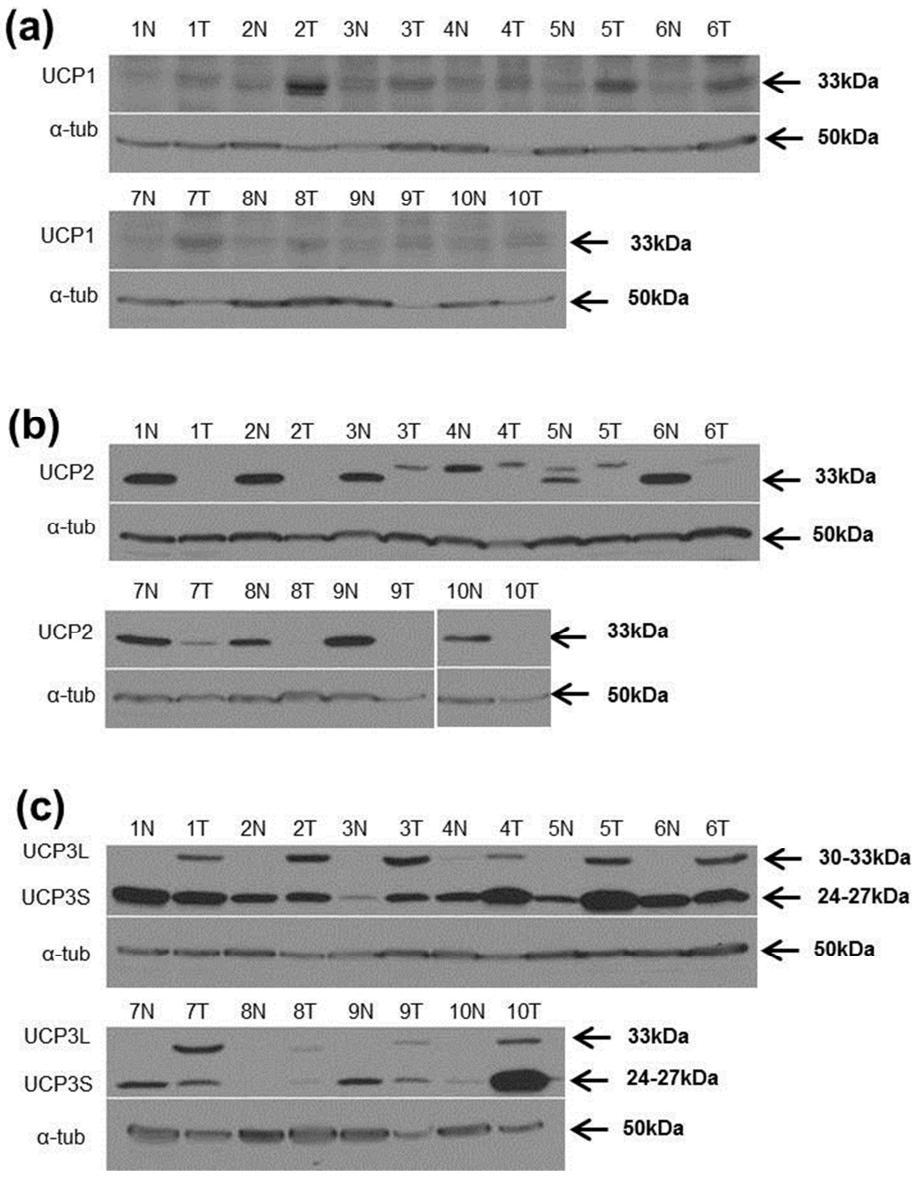

Fig. 4.2.1.1 Protein expressions of uncoupling proteins (UCPs) in lysate of ccRCC tumor and adjacent normal tissue.

Tissue lysates prepared from ccRCC tumors and their corresponding normal counterparts were probed for uncoupling proteins. Intensity of bands was quantified using the ImageJ software and expressed as relative to α-tubulin.

(a) UCP1 Negligible UCP1 expression was seen in the normal kidney tissue and it was seen to be upregulated in tumor of sample #2, #5 and #7.

(b) UCP2 UCP2 was near to absent in the ccRCC tumors.

(c) UCP3 Two bands were detected for the UCP3 due to the presence of two spliced variants, UCP3L and UCP3S. UCP3S lacks the sequence which is critical for uncoupling activity and therefore is not discussed here. UCP3L was upregulated in all the ccRCC tumor sample.

4.2.1.2 Effect of genipin, a UCP2 inhibitor on MMP of mitochondria isolated from normal tissue

Genipin, an extract from *Gardenia jasminoides* is a highly specific inhibitor of UCP2 (Mailloux et al., 2010). It has been demonstrated to decrease the proton leak mediated by UCP2 in brain tissue, pancreatic β-cells and kidney mitochondria (Parton et al., 2007; Zhang et al., 2006). Therefore, the effect of genipin on the energization of mitochondrial membrane potential was examined in normal, intact mitochondria of sample #10 since there was negligible level of UCP2 present in this ccRCC tumor. In Fig. 4.2.1.2, 50μM genipin (represented as dotted line) or 0.1% DMSO (vehicle control in solid line) was added before ADP, followed by the addition of respiratory substrates and inhibitors. No difference was seen between the MMP of control and genipin-treated mitochondria suggesting UCP2 might not be involved in MMP regulation. However, only one sample was examined.

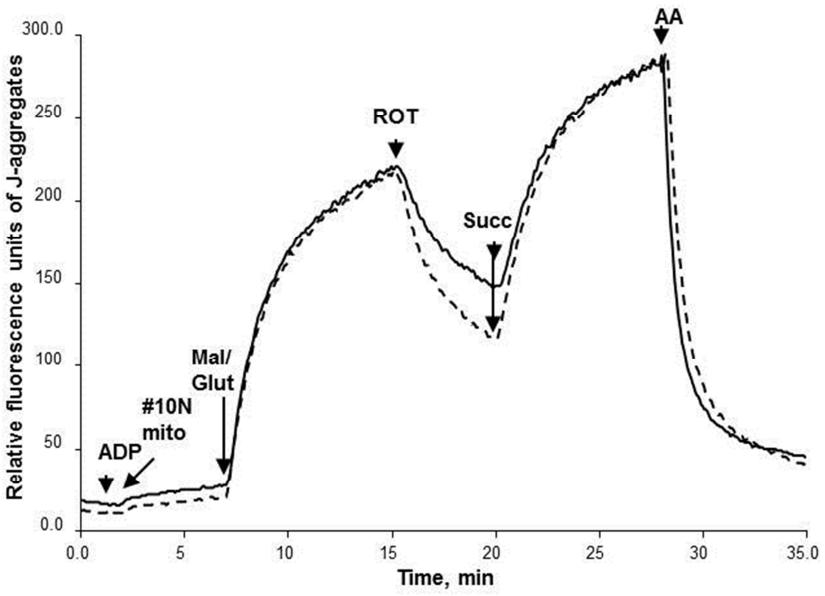

Fig. 4.2.1.2 Effect of genipin, a UCP2 inhibitor on the MMP of normal, intact mitochondria isolated from sample #10.
50µM genipin or DMSO (vehicle control) was added to the assay cuvette in the beginning of the run followed by JC-1 dye, 125µM ADP and mitochondria. The MMP was then induced by addition of 5mM each mal/glut which was inhibited by 5µM rotenone (ROT) followed by re-energization by 10mM succinate (Succ) with subsequent inhibition with 4µg/ml antimycin A (AA, an inhibitor of respiratory complex III) which finally collapsed the MMP. Only the traces of the red aggregates were presented and the solid line denotes the control and dotted line for genipin-treated. No effect was seen on the MMP since the two traces showed little to no difference.

4.2.1.3 Effect of genipin, a UCP2 inhibitor on MMP of 786-O cells

786-O is a kidney cell line derived from primary clear cell adenocarcinoma and the use of this cell line is to mimic the condition of ccRCC tumor. UCP2 protein is present in the 786-O cells as shown by the western blot analysis using the whole cell lysate (Fig. 4.2.1.3a). Genipin inhibits UCP2 and resulted in increase of MMP by 41% when 786-O cells were treated with 200μM genipin for 3h. No effect was seen with 50μM genipin (Fig. 4.2.1.3b).

With reference to this, higher concentrations of genipin might be required to show an effect in mitochondria isolated from tissue (Fig. 4.2.1.2). Alternatively, the discrepancy between the effect of genipin in isolated mitochondria of normal tissue and 786-O cells could be due to the lack of activator in the former. It is reported that UCP2 and UCP3 require the presence of activators such as superoxide (Brand et al., 2004; Talbot et al., 2003) and reactive alkenals (Echtay et al., 2003) in order for it to transport protons and UCP3 knockout exerted no effect on the basal proton conductance of isolated mouse mitochondria (Cadenas et al., 2002). Mitochondria isolated from patient-matched normal tissue apparently have low levels of these activators. Moreover, genipin failed to inhibit the exchange of C4 metabolites with radiolabelled phosphate by UCP2 (Vozza et al., 2014) which could explain its limited effect on the MMP in this case.

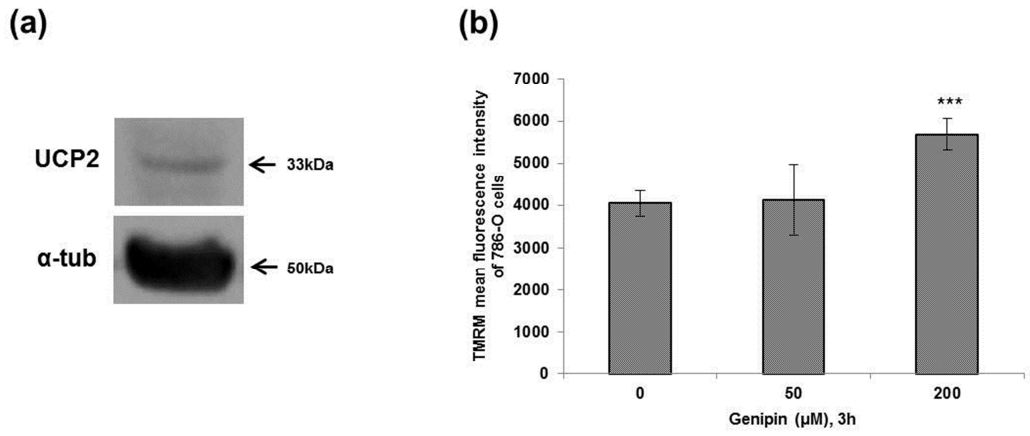

Fig. 4.2.1.3 UCP2 regulates MMP in 786-O cells.

(a) Western blot analysis of UCP2 protein expression of 786-O cell lysate, n=3.

(b) 786-O cells were treated with genipin for 3h in culture medium and the mitochondrial membrane potential (MMP) was measured by TMRM fluorescence using flow cytometer. The MMP was increased when cells are treated with 200μM genipin but no effect was seen with 50μM genipin with ***p<0.005 for n=4.

4.2.1.4 UCP2 overexpression decreases MMP of 786-O cells

UCP2 was overexpressed in the 786-O cells following 24h transfection with Myc-DDK-tagged human UCP2 plasmid (pCMV-UCP2) (Fig. 4.2.1.4a). Our recent preliminary study showed that UCP2 overexpression led to the reduction of MMP (Fig. 4.2.1.4b). However, statistical significance was not tested as only duplicates were performed. Effort to reproduce the results with more replicates to achieve statistical significance is now undergoing. Together with higher MMP induced by genipin (an inhibitor of UCP2), our results suggested that UCP2 is a negative regulator of MMP in ccRCC cells.

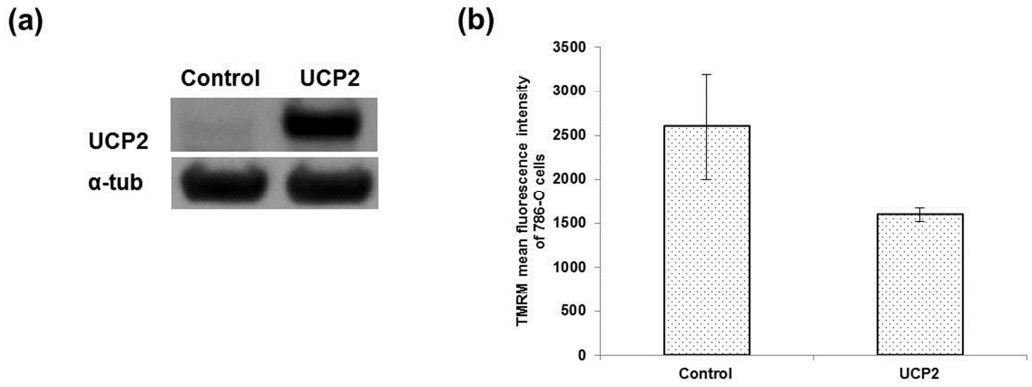

Fig. 4.2.1.4 Overexpression of UCP2 decreased MMP of 786-O cells.
(a). Western blot analysis showed the overexpression of UCP2 at protein level in the 786-O cell lysate following 24h transfection using empty vector (labeled as Control) or pCMV-UCP2 vector (C-terminal Myc-DDK-tagged, labeled as UCP2). α-tubulin served as loading control.
(b). Mitochondrial membrane potential (MMP) of UCP2-overexpressed and control cells (transfected with empty vector) was measured by TMRM fluorescence using flow cytometer. MMP was decreased when UCP2 was overexpressed, n=2.

4.2.2 The role of ADP and glutamine-derived respiratory substrates in supporting basal MMP in ccRCC tumor mitochondria

4.2.2.1 ADP

Higher basal MMP in the presence of ADP was repeatedly seen in the tumor mitochondria (Fig. 3.2.3). In order to find out if the MMP is inherently higher in the tumor mitochondria or it is due to the effect of fortified ADP, normal and tumor mitochondria were added into cuvette containing only the assay buffer and JC-1 probes. Only the traces of the JC-1 red aggregates were shown here, with solid and dotted lines representing the MMP of normal and tumor mitochondria respectively.

The inherent MMP appeared to be higher in the tumor mitochondria as compared to the normal even when ADP was not added in the beginning of the run (Fig. 4.2.2.1a and 4.2.2.1b). In fact, there was no evidence of MMP in mitochondria isolated from two different normal samples. However, the high MMP in tumor mitochondria was not sustainable and showing a decrease 2-5min later. The declining MMP was stopped by introducing exogenous ADP suggesting the role of ADP in maintaining the inherent basal MMP in tumor mitochondria. The addition of ADP would normally decrease the MMP since it promotes the return of proton into the matrix via the Fo portion of ATP synthase. However, we hypothesized that ADP would have inhibited the UCP3 which is upregulated in ccRCC tumor as shown in Fig. 4.2.2.1 based on the findings of Echtay *et al*. (Echtay et al., 2001) and therefore ADP leads to the increase in MMP in ccRCC tumor.

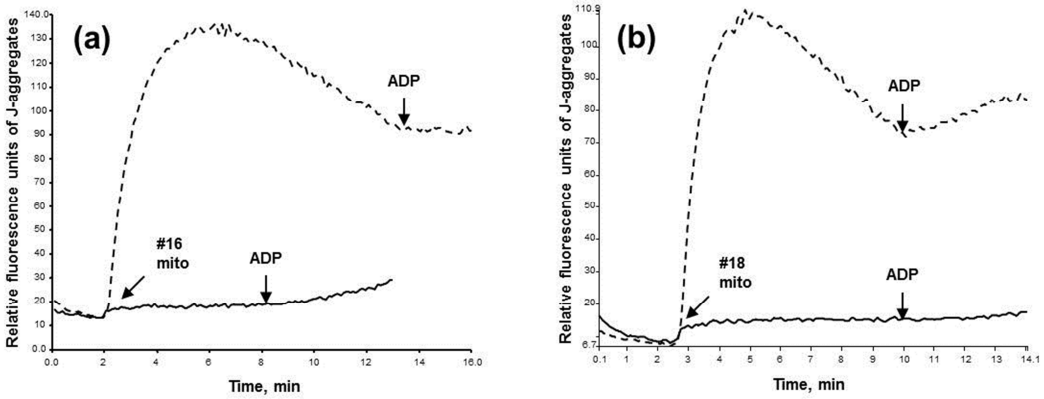

Fig. 4.2.2.1 Endogenous MMP in mitochondria isolated from ccRCC tissues. Endogenous MMP in the absence of added ADP and respiratory substrate. Mitochondria isolated from ccRCC tumor sample (a). #16 and (b). #18 (dotted line) but not from patient-matched normal tissues (solid line) exhibited an MMP without the addition of ADP and respiratory substrate. Only the intensity of the red fluorescence of the J-aggregates is shown. This endogenous MMP was maintained for about 2-5min and its subsequent decline was prevented by addition of ADP.

4.2.2.2 Complex I-dependent substrate

If ADP is present to promote the coupling of OXPHOS, there must be some endogenous respiratory substrates that provide the reducing equivalents for the oxidation to occur. Lower energization with succinate was detected in tumor mitochondria suggesting succinate dehydrogenase activity was compromised in two of three samples (Fig. 3.2.2d & 3.2.2f). Therefore, the higher basal MMP in tumor could probably be contributed by complex I- instead of complex II-dependent substrates. This was supported by the observation when rotenone, a complex I inhibitor collapsed the basal MMP in tumor mitochondria. It was noted that the vehicle control containing 0.5% ethanol also slightly reduced the MMP (Fig. 4.2.2.2).

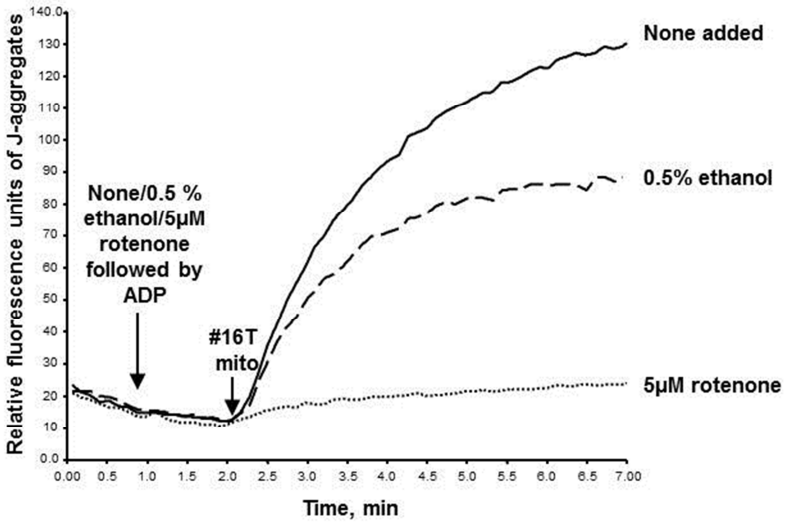

Fig. 4.2.2.2 Inhibition of basal MMP in mitochondria isolated from ccRCC tumor.
5μM rotenone, an inhibitor of respiratory complex I, effectively inhibited the basal MMP. Part of the inhibition was due to ethanol which was used to dissolve rotenone. Only the intensity of the red fluorescence of the J-aggregates is shown.

4.2.2.3 Energization of MMP in mitochondria isolated from ccRCC tumor tissues by glutamine and its derived respiratory substrates

The inhibition of rotenone shown in Fig. 4.2.2.2 inferred that complex I-dependent substrates are involved in supporting the basal MMP of tumor mitochondria. However, PDH activity has been shown to be negligible/absent in the tumor mitochondria (Fig. 2.2.3b); thus substrates derived from the TCA cycle would therefore be minimal. The alternative carbon source that fuels the Krebs cycle comes from glutaminolysis. Therefore, the ability of mitochondria isolated from ccRCC tumor in utilizing glutamine and its derived, complex I-dependent respiratory substrates, namely the glutamine, glutamate, α-ketoglutarate and isocitrate was examined.

Fig. 4.2.2.3 showed the traces of the red fluorescence of the JC-1 aggregates, illustrating the induction of MMP by (a) glutamine, (b) glutamate, (c) α-KG and (d) isocitrate in sample #15, #16 and #18. Glutamine was included as it is known that glutaminase activity is high in renal cells (Curthoys and Watford, 1995). All these substrates were effective in eliciting the MMP in mitochondria isolated from both normal and ccRCC tumor tissues. Of note, the higher basal MMP in tumor mitochondria prior to the addition of each of these four respiratory substrates as indicated by asterisks was noted before in Fig. 3.2.2b, 3.2.2d and 3.2.2f.

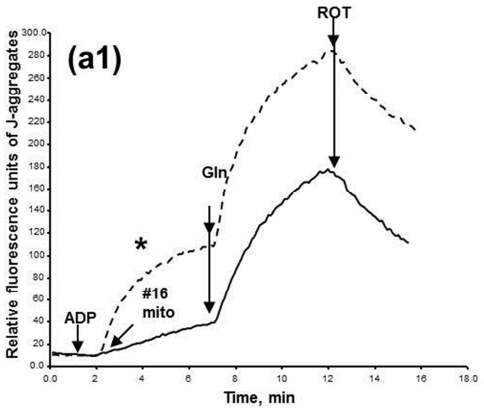
(a1)
ROT
Gln
*
#16
mito
ADP
Relative fluorescence units of J-aggregates
Time, min

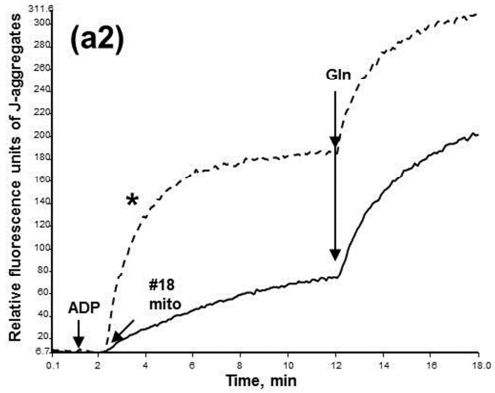
(a2)
Gln
*
#18
mito
ADP
Relative fluorescence units of J-aggregates
Time, min

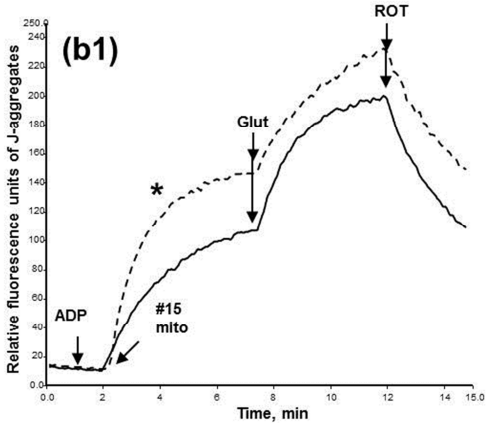
(b1)
ROT
Glut
*
#15
mito
ADP
Relative fluorescence units of J-aggregates
Time, min

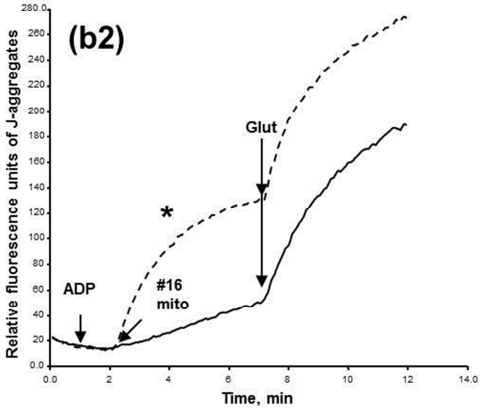
(b2)
Glut
*
#16
mito
ADP
Relative fluorescence units of J-aggregates
Time, min

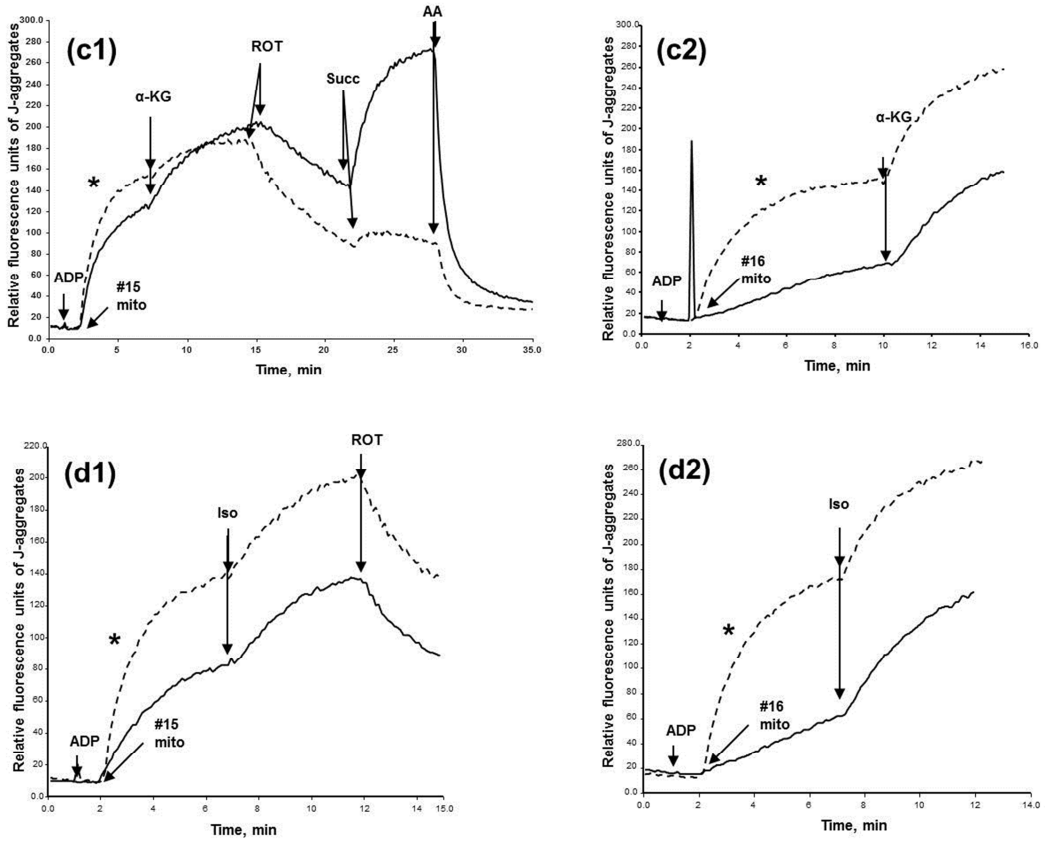

Fig. 4.2.2.3 Mitochondrial membrane potential (MMP) from glutamine and its derived respiratory substrates.

(a). Glutamine (Gln), (b). glutamate (Glut), (c). α-ketoglutarate (α-KG) and (d). isocitrate (Iso) were able to energize mitochondria to produce an increased MMP. In some case, rotenone (ROT), succinate (SUCC) and/or antimycin A (AA) were also introduced. The intensity of the red fluorescence of the J-aggregates is shown with solid lines for the normal tissues and dotted lines for tumor tissues. In all traces, the MMP prior to the addition of the respiratory substrate was always higher in mitochondria isolated from ccRCC (indicated by asterisks) which was also shown previously in Fig. 3.2.2.3. Left and right panels (numbered as 1 & 2) are traces obtained from isolated mitochondria from different tissue samples (labelled as #).

4.2.2.4 ccRCC tumor mitochondria are able to utilize glutamine and its derived respiratory substrates for ATP biosynthesis

In addition to measurement of MMP, ATP biosynthesis derived from glutamine, glutamate, α-KG and isocitrate was also investigated. The rate of ATP biosynthesis from ADP only, glutamate, α-KG and isocitrate was higher in ccRCC tumor compared to patient matched normal tissues (Fig. 4.2.2.4). The significantly higher rate of ATP synthesis with only ADP in tumor mitochondria suggesting either a higher level of endogenous respiratory substrate or higher activity of mitochondrial kinases e.g. adenylate kinase (AK) or creatinine kinase (CK) (Noma et al., 2001; Payne and Strauss, 1994) which converts ATP and AMP to ADP, vice versa. These kinases were however not measured in our study.

In contrast, tumor has a lower rate of ATP production from glutamine but achieving 79% of that in normal. As compared to mitochondria isolated from normal tissue, the loss of ability to generate more ATP from glutamine than other glutamine-derived substrates in the tumor mitochondria suggested a lower mitochondrial uptake of glutamine or compromised glutamine conversion to glutamate. However, both have been suggested to be upregulated in cancers (Fuchs and Bode, 2005; Hensley et al., 2013; Wise et al., 2008). It is noteworthy that the result was obtained with only one sample and this experiment need to be repeated in future samples.

Interestingly, 2mM glutamine produced a higher rate of ATP biosynthesis compared to 5mM glutamate, 2.5mM α-KG or 5mM isocitrate in normal mitochondria. This could be due to the more rapid entry of glutamine through the

kidney mitochondrial membrane as compared to glutamate which penetrates very slowly (Kovacevic et al., 1970).

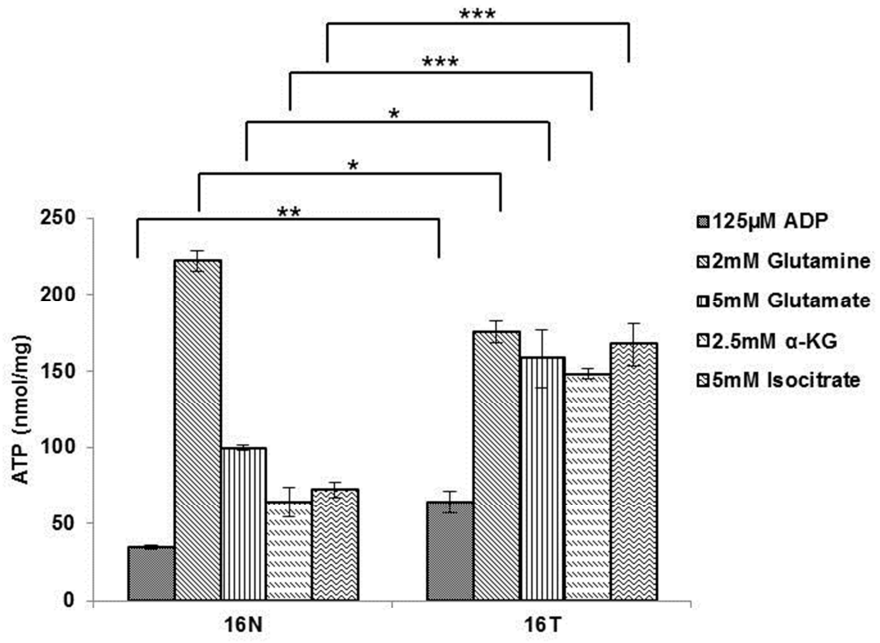

Fig. 4.2.2.4 ATP synthesis from glutamine and its derived respiratory substrates. The rate of ATP biosynthesis from the oxidation of glutamate, α-ketoglutarate and isocitrate (but not of glutamine) in the presence of 125μM ADP was higher in mitochondria isolated from ccRCC tumor when compared to the normal tissues (*p<0.05, **p<0.01, ***p<0.005 with n=3). It was noted that ATP produced from 2mM glutamine was significantly more than that produced by 5mM glutamate, 2.5mM α-ketoglutarate and 5mM isocitrate in normal (p<0.005).

4.2.2.5 Glutaminolysis in ccRCC tumor

Role of glutaminolysis as the alternate energy source in ccRCC tumor was further examined by measuring the protein expression of kidney-type (K-type) mitochondrial glutaminase (KGA/GLS1). KGA is a phosphate-activated amidohydrolase that catalyzes the hydrolysis of glutamine to glutamate and ammonia. Of the ten samples analyzed, 4 showed higher expression levels of KGA in tumor than their corresponding normal counterparts whereas 6 had comparable levels of expression (Fig. 4.2.2.5a). Result on glutaminase enzymatic activity in the mitochondrial extracts of sample #9, #15 and #16 however was variable (Fig. 4.2.2.5b). The higher levels of KGA protein expressions in tumor of sample #9 did not translate into higher glutaminase enzymatic activity.

It would be interesting to examine the glutaminolysis flux in the ccRCC and patient-matched normal tissues by profiling its metabolites using mass spectrometry.

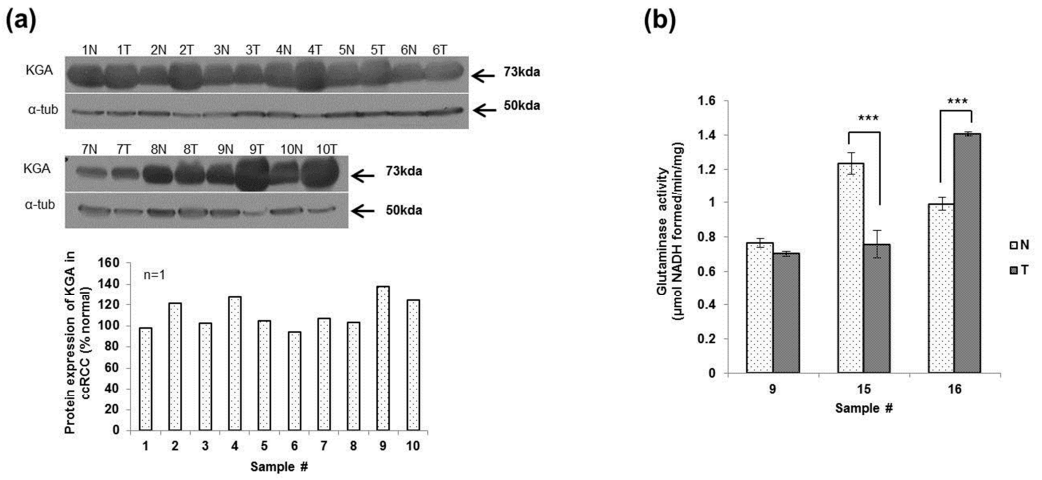

Fig. 4.2.2.5 Protein expression and enzymatic activity of the glutaminase.

(a) The protein expression of human kidney-type glutaminase (KGA) was higher in 4/10 and comparable in 5/10 of ccRCC samples as compared to the corresponding patient-matched normal tissue samples. α-Tubulin was the loading control.

(b) Determination of glutaminase activity in the mitochondrial extracts of sample #9, #15 and #16 showed varying results (***p<0.005 with n=3). Higher protein expression of KGA in sample #9 was not reflected in the enzymatic activity.

CHAPTER 5 LIMITATIONS, CONCLUSIONS AND FUTURE DIRECTIONS

5.1 Limitations of this study

The main limitation of our study is the small quantity of mitochondria that could be isolated from limited freshly resected human specimen, causing the lack of replicates in many sets of data and resulting in semi-quantitative analysis. Enzymatic activities such as NADH, Fo-ATPase, CS and MDH were measured in freeze-thawed mitochondrial extracts obtained from remaining intact mitochondrial preparations. Understandably, these extracts were limited due to the reasons above, which explained the lack of replicates in the data assays as shown in Fig 2.2.5.

During the course of the study, new ideas were generated based on the data accrued. It seemed therefore more meaningful to perform different sets of other experiments to test our hypotheses rather than to repeat those carried out previously. This explained why all the protocols were not used on all tissue samples. Besides, when similar sets of data were obtained from two or three tissue samples, it appeared not prudent to continue to measure these same parameters. Therefore, only certain samples were used instead of the whole panel, consisting of 18 samples. Furthermore, three out of the 18 samples were not classified as clear cell renal cell carcinoma in which the pathologists' reports of tissues were only completed after the experiments on freshly isolated, intact mitochondria had been performed on the day of surgery.

No experimental replicates were performed for Western blot analysis of tumor lysate as it was intended as an overview of their protein levels between patient-matched paired samples and also due to the scarcity of lysate available for screening of multiple proteins. The JC-1 assay employed provides only semi-quantitative analysis of MMP which suffices to complement the other two OXPHOS parameters measured.

5.2 Conclusions

The enhanced aerobic glycolysis in cancer cells was proposed to be an outcome of impaired respiration by Otto Warburg. This study confirmed the glycolytic phenotype in ccRCC as shown by the increased protein expression of HIF1α and HIF2α as well as their downstream targets, namely HKII, LDH5 and PDHK1. In addition, the reduced expression and activity of mitochondrial respiratory complexes resulted from an attenuation of mitochondrial biogenesis suggested a deficit of OXPHOS in ccRCC as stipulated in Warburg effect.

Enzyme activity of PDH, a crucial enzyme that links glycolysis and OXPHOS was found to be lost in the ccRCC tumors examined. There is evidence of inhibition of PDHc activity brought upon by the phosphorylation of PDHK1. However, reports on the status of PDH expression in human cancer tissue has not been reported, not to mention the measurement of its enzymatic activity which requires the isolation of mitochondria from the human specimen. Most studies on cancer cell bioenergetics depend on the use of immortalized cell lines which are fortified with excessive nutrients during their culture under atmospheric level of oxygen. However, these culture conditions do not reflect the tumor

microenvironment with limited oxygen and nutrients. Human cancer tissue is therefore a better alternative in accessing the *in vivo* condition.

Our measurement of OXPHOS capacity with three different parameters in the isolated, intact mitochondria unveils their respiratory competency in ccRCC tumors when exogenous substrates are provided. Our finding of a higher basal MMP of mitochondria isolated from ccRCC tumor concurs with hyperpolarized mitochondria reported in human cell lines, A549, M059K and MCF-7 (Bonnet, 2007, 11, 37-51). The regulation of MMP by UCP2 and glutamine-derived substrates provide plausible mechanisms underpinning the higher MMP in ccRCC tumor mitochondria. Furthermore, the inherent MMP in mitochondria isolated from ccRCC tumor tissue which is absent in the normal mitochondria supports the use of lipophilic, cationic drugs that selectively accumulate within the cancer mitochondria due to the negative charge in the matrix. In addition, the loss of UCP2 expression and the reciprocal increase in UCP3 make them potential prognostic markers for ccRCC.

Overall, we propose the metabolic switch of ccRCC from glucose-derived to glutamine-derived carbon source due to the deficiency of PDH leads to the higher MMP in tumor through the loss of UCP2 and anaplerosis of TCA cycle.

5.3 Future directions

This study provided evidence for the presence of respiratory competent mitochondria in the ccRCC tumor which coincides with our earlier finding using mitochondria isolated from ovarian and peritoneal tumor (Lim et al., 2011). It would be interesting to find out if other types of cancers also harbor the functional

mitochondria. Mitochondria isolated from ccRCC tumor exhibited higher ROS production but the type of ROS was not conclusively evaluated. Although we found that hydrogen peroxide was not responsible for the elevated ROS, assays determining the level of superoxide and other ROS should be carried out in future. With the crucial role of mitochondria play in energy metabolism, apoptosis and ROS production, understanding the mitochondrial functions in tumor warrants cancer therapy with greater efficiency.

UCP2 protein was found to be lost in the ccRCC tumor; however, how and at which level (transcriptional or translational) it is regulated was not studied. It would be worthwhile to look out the mechanism responsible for the loss of UCP2 and the reciprocal increase of UCP3 which might be unique to ccRCC. The use of UCP2 inhibitor, genipin and the UCP2 expression in 786-O cells demonstrated the role of UCP2 in compromising mitochondrial membrane potential, suggesting its role in uncoupling OXPHOS. However, it remains to be elucidated if UCP2 does increase the proton conductance which is a more direct method in ascertaining its uncoupling action. On the other hand, functions of UCP3 which was increased in the ccRCC tumor have to be examined. If UCP3 also governs the transport of proton, it would be interesting to study the interplay between UCP2 and UCP3 in respect to the higher MMP in ccRCC as well as other tumors.

The ability of mitochondria isolated from ccRCC tumor in metabolizing glutamine and its derived substrates together with the compromised PDH activity suggested a metabolic switch towards glutaminolysis. Given that PDH is deficient in the ccRCC tumor, reverse TCA cycle flux would be anticipated for

replenishing the acetyl CoA and oxaloacetate via the action of ATP citrate lyase. In fact, the preferential use of reductive carboxylation for lipogenesis is predominant in cells grown under hypoxia (Filipp et al., 2012; Metallo et al., 2012). Determination of the intracellular metabolites involved in the several pathways, namely glycolysis, TCA cycle, glutaminolysis and fatty acid synthesis will provide clues on the metabolic flux engaged by the ccRCC tumor. We demonstrated that the higher inherent MMP in mitochondria isolated from ccRCC could be supported by ADP and complex I, glutamine-derived respiratory substrates. However, if the ccRCC tumor possesses higher level of ADP than its normal counterpart and whether glutamine addiction changes MMP remain to be solved.

The increased reliance on glutaminolysis in cancer cells has prompted the development of drug targeting at glutaminase. In fact, glutaminase inhibitors such as CB-839, BPTES (bis-2-(5-phenylacetamido-1, 2, 4-thiadiazol-2-yl) ethyl sulfide) and compound 968 have been reported to inhibit cancer cell growth (Gross et al., 2014; Seltzer et al., 2010; Wang et al., 2010). In fact, a clinical trial involving the study the effect of CB-839 in solid tumors including renal cell carcinoma is undertaken by the pharmaceutical company, Calithera Biosciences, Inc (South San Francisco, CA, USA). Our finding on the higher inherent MMP in mitochondria of ccRCC tumor could open avenues for targeted delivery of glutaminase inhibitors.

CHAPTER 6 MATERIALS AND METHODS

6.1 Materials

Cell cultures – Roswell Park Memorial Institute (RPMI) 1640 medium, trypsin and penicillin-streptomycin mixture were purchased from Gibco®, Life Technologies (Carlsbad, CA, USA). Sodium bicarbonate was purchased from Sigma Aldrich Co. Ltd (St Louis, MO, USA). Fetal bovine serum (FBS) was purchased from Hyclone, Thermo Scientific (Waltham, MA, USA).

Chemicals – 5,5',6,6'-tetrachloro 1,1, 3,3' tetraethylbenzimidazolcarbocyanine iodide (JC-1), the Amplex™ Red hydrogen peroxide/peroxidase assay kit, were Molecular Probes Inc. (Eugene, OR, USA). Nonidet P-40 was purchased from Calbiochem (San Diego, CA, USA). The following were purchased from Sigma Aldrich Co. Ltd (St Louis, MO): ADP, ATP, 2',7'-dichlorofluorescein diacetate, tetramethylrhodamine methyl ester (TMRM), carbonyl cyanide p-trifluoromethoxyphenylhydrazone (FCCP), L-glutamic acid, L-malic acid, glutamine, isocitric acid, α-ketoglutarate, TMPD, ascorbic acid, horseradish peroxidase type VI, (298U/mg), LDH (5.3 kU/ml), PK, NAD+, NADH, DTNB, acetyl-coA, hydrazine, decylubiquinone, phosphoenolpyruvate (PEP), rotenone, malonate, antimycin A, FL-ASC Bioluminescent cell assay kit, phenylmethylsulfonyl fluoride (PMSF), protease inhibitor cocktail, phosphatase inhibitor cocktail; Tween-20 was from Sinopharm Chemical Reagent Co. Ltd (Shanghai, CHN). Disodium succinate hexahydrate was purchased from Merck & Co. (Whitehouse Station, NJ, USA).

Antibodies used for western blotting – mouse monoclonal anti-HIF1α and rabbit polyclonal anti-HIF2α were from Novus Biologicals (Littleton, CO, USA); MitoProfile® Total OXPHOS Rodent WB Antibody Cocktail (MS604) was from MitoSciences (Eugene, OR, USA); goat polyclonal anti-mtTFA, rabbit polyclonal anti-PGC1α and NRF-1, goat polyclonal anti-HKII, mouse monoclonal anti-KGA, goat polyclonal anti-UCP2 were from Santa Cruz Biotechnology (Santa Cruz, CA, USA); rabbit polyclonal anti-Lactate dehydrogenase isoenzyme V (LDH-V) from Abcam (Cambridge, UK); rabbit monoclonal antibodies for pyruvate dehydrogenase kinase 1 (PDHK1) was from Cell Signaling Technology (Beverly, MA, USA); Manganese SOD (MnSOD) was from BD Transduction Lab (Franklin Lakes, NJ, USA); rabbit polyclonal antibodies for UCP2 from Alpha Diagnostic (San Antonio, TX, USA), UCP1 and UCP3 from CHEMICON International Inc. (Temecula, CA, USA); mouse monoclonal anti-PDHE1α from Invitrogen (Carlsbad, CA, USA); mouse monoclonal anti-Actin, pan Ab-5 from NeoMarkers (Fremont, CA, USA); mouse monoclonal anti-α-tubulin from Sigma-Aldrich (St. Louis, MO, USA). All secondary antibodies were conjugated with horseradish peroxidase and purchased from Santa Cruz Biotechnology (Santa Cruz, CA, USA).

6.2 Methods

6.2.1 Human tissues from ccRCC

Freshly resected, paired normal renal and tumor samples were collected from 18 patients after the nephrectomy procedure in National University of Singapore under the approval and patients' consent obtained from National University

Health Services (DSRB B/11/158). Pathological analysis confirmed that all the tumor samples were clear cell renal cell carcinoma of various histological grades except samples #8, #11 and #14 which are respectively, unclassified renal cell carcinoma, epithelioid angiomyolipoma and chromophobe renal cell carcinoma. Particulars of samples are shown in Table 1. Preparation of mitochondria was carried out within 1h after excision using the method described below.

6.2.2 Isolation of intact mitochondria, mitochondrial and cytosolic fractions

The tissues were first trimmed of fat and connective tissues and rinsed in an isolation buffer (at a ratio of 1g tissue to 3ml buffer) containing 2mM Tris, 250mM sucrose, 4mM KCl, 2mM EGTA, pH 7.5. This was followed by homogenization by hand with a tight fitting glass–glass homogenizer using 15 up-and-down passes. The homogenate was centrifuged at 1000*g* for 10min at 4°C. The supernatant was collected and centrifuged twice at 10,000*g* for 10min each time to obtain the mitochondrial pellet which was finally resuspended in the same isolation buffer. The pooled supernatant was centrifuged at 100,000*g* for 1h to obtain the cytosolic fraction which was routinely frozen at −80°C for subsequent assays. Protein determination was carried out by the method reported (Bradford, 1976).

6.2.3 Preparation of tissue lysate

Snap-frozen tissue was kept in -80°C freezer till the day of lysate preparation. The tissues were thawed followed by the addition of lysis buffer (at a ratio of 1g tissue to 3ml buffer) containing 20mM Tric-HCl, pH7.4, 150mM NaCl, 1mM EDTA, 1% Triton X-100, 1% sodium deoxycholate, 0.1% SDS, 1mM PMSF, 1X inhibitor

cocktails for protease and phosphatase (both from Sigma Aldrich Co. Ltd, St Louis, MO, USA). The tissues were cut into small pieces and homogenized. The homogenate was left on ice for 2h with frequent vortexing followed by centrifugation at 16000*g* for 20min at 4°C. The supernatant was collected as tissue lysate and kept at -80°C freezer till use.

6.2.4 Cell culture and genipin treatment

786-O cells were obtained from American Type Culture Collection (ATCC, Manassas, VA, USA), and were cultured in RPMI supplemented with 10% fetal bovine serum, 100 U/ml of penicillin and 100µg/ml streptomycin at 37°C and 5% CO2. 0.2mil cells were seeded into each well of 6-well plate and left to grow overnight in the CO_2 incubator. On the next day, genipin (50 and 200µM) or 0.1% DMSO (final concentration, serves as vehicle control) prepared in the culture medium was added to the cells which were harvested for MMP measurement after 3h incubation in the CO_2 incubator.

6.2.5 Preparation of whole cell lysate

786-O cells were washed with ice-cold PBS followed by the addition of lysis buffer (0.5% Triton X-100, 150mM NaCl, 10mM Tris pH 7.4, 1mM EDTA, 0.5% NP-40, 2mM sodium orthovanadate) containing 1X protease and phosphatase inhibitor cocktail (Sigma-Aldrich, St Louis, MO, USA). The cells were scraped off with a rubber policeman and vortexed for 10sec every 5min for 20min. In between, the cell lysate was put on ice. This was followed by centrifugation at 14,000*g* for 15min at 4°C. The supernatant was collected and subjected to protein determination or western blot analysis.

6.2.6 Western blot analysis in tissue lysate or whole cell lysate

10 to 50µg lysate were resolved on 8 to 15% sodium dodecyl sulfate-polyacrylamide gel and electroblotted onto nitrocellulose for 1h at 4°C. After blocking with 5% milk (or BSA for phospho protein) in TBST, the membranes were incubated with primary antibodies at a ratio of 1:1000 in 0.5% BSA for overnight at 4°C. The membrane was washed and incubated with horseradish peroxidase-conjugated secondary antibody at 1:15000 (Santa Cruz) for 1 h at room temperature in 5% milk (or BSA for phospho protein) in TBS with 0.1% Tween-20. Detection was performed via SuperSignal West Pico or Femto Maximum sensitivity substrate (Pierce, Rockford, IL, USA).

6.2.7 Enzyme activities in freeze-thawed mitochondrial extract

6.2.7.1 Complex I (NADH dehydrogenase) activity

Complex I activity was measured by the oxidation of NADH. The assay mixture contained 25mM potassium phosphate (pH 7.2), 5mM $MgCl_2$, 0.064mM decylubiquinone, 2mg/ml albumin, 2mM KCN and 5mM NADH. The reaction was started upon addition of mitochondrial extract and the NADH fluorescence was followed at Ex/Em 352/464nm in a luminescence spectrophotometer (LS55, PerkinElmer Waltham, MA, USA). Changes in the velocity were tabulated according to the standard curve by adding known amount of NADH.

6.2.7.2 Complex V (FoF1-ATPase) activity

ATPase activity was coupled to the reactions of lactate dehydrogenase and pyruvate kinase and the oxidation of NADH was followed at 340nm. The reaction

mixture contained 50mM Tris, pH8.0, 5mg/ml BSA, 20mM $MgCl_2$, 50mM KCl, 10mM phosphoenolpyruvate (PEP), 2.5mM ATP, 4 units lactate dehydrogenase, 4 units pyruvate kinase and 1mM NADH. The reaction was started by adding the reaction mixture into the wells containing the enzyme extract, both of which were separately pre-incubated at 37°C for 5min.

6.2.7.3 Pyruvate dehydrogenase complex (PDHc) activity

Both active (dephosphorylated) and total (phosphorylated and dephosphorylated) PDHc activities were determined following the reported protocol (Eboli and Pasquini, 1994).

6.2.7.4 Citrate synthase activity

The assay was started by adding 0.5 mM oxaloacetate to a mixture containing 0.1 mM DTNB (5, 5′-dithiobis-(2-nitrobenzoic acid), 0.3 mM acetyl CoA and an aliquot of mitochondrial extract containing 0.1 mg protein. The absorbance was followed for 5 min at 412 nm at 37 °C (Trounce et al., 1996).

6.2.7.5 Malate dehydrogenase (MDH) activity

The assay was started by adding 5mM malate to a mixture containing 100mM KH_2PO_4 pH7.40, 0.16% Triton X-100, 1mM NAD^+ and an aliquot of mitochondrial extract containing 0.01mg protein. Fluorescence of NADH was followed at Ex/Em 352/464nm in a luminescence spectrophotometer (LS55, PerkinElmer Waltham, MA, USA) (Heyde and Ainsworth, 1968).

6.2.7.6 Glutaminase activity

The glutaminase activity was measured by a two-step assay. 5 µl mitochondrial extract containing glutaminase was added to the first assay mixture containing 20mM glutamine, 150mM KH_2PO_4, 0.2mM EDTA, 50mM Tris-HCL, pH8.60 in a final volume of 20µl. The samples were incubated for 30min at 37°C followed by addition of 2µl of 3M HCl to stop the reaction. 200µl of the second mixture containing 0.08mg/ml GDH, 80mM Tris-HCl, pH9.40, 200mM hydrazine, 2.5mM ADP, 0.2mM NAD^+ was then added. The formation of NADH was followed at 340nm using the absorbance microplate reader, Spectramax 190 (Molecular Devices Corporation, Sunnyvale, CA, USA) and the initial velocity was used to calculate the specific enzyme activity. Blank with HCl added into the first mixture prior to the addition of mitochondria extract showed no activity.

6.2.8 Mitochondrial membrane potential (MMP) of isolated mitochondria

The MMP of freshly isolated mitochondria was examined using the specific mitochondrial probe, JC-1 by following its fluorescence at Ex/Em of 485nm/535nm for the green monomer and 485nm/595nm for the red aggregate as described previously in our reports (Lim et al., 2011; Ng et al., 2006; Zhang et al., 2004). 125µM ADP was added into intact mitochondria containing 0.05 to 0.2mg protein, followed by the respiratory substrates and inhibitors: 5mM each malate/glutamate (Mal/Glut), 5µM rotenone (ROT), 10mM succinate (Succ) and 4µg/ml antimycin A (AA). For glutamine and its derived substrates, 2mM glutamine (Gln), 5mM glutamate (Glut), 2.5mM α-ketoglutarate (α-KG) or 5mM isocitrate (Iso) was added.

6.2.9 MMP determination of 786-O cells using TMRM and flow cytometry

In order to measure the MMP, 786-O cells were probed with tetramethylrhodamine methyl ester (TMRM) which selectively accumulates in the mitochondria due to its positive charge. After treated with genipin or transfected with UCP2 vector, cells were dislodged by treatment of trypsin-EDTA. 0.15million cells were incubated with 150µl of Hank's Balanced Salt Solution (HBSS) containing 1mg/ml glucose supplemented with 100nM TMRM (Sigma Aldrich Co. Ltd, St Louis, MO, USA) for 15min at 37°C. Positive control was achieved by treating the cells with 1µM FCCP and subjected to the same incubation conditions. After which, the TMRM-containing buffer was removed by centrifugation and cells were resuspended in HBSS/glucose buffer followed by flow cytometry analysis on a FACSCanto™ II (BD Biosciences, Franklin Lakes, NJ, USA). The cells were excited with an air-cooled argon 488nm laser and the fluorescence of TMRM was monitored in the PE channel, 10000 events per condition were collected for each histogram.

6.2.10 ATP biosynthesis

ATP synthesis from exogenous ADP and respiratory substrates was measured in isolated mitochondria. Routinely, mitochondria containing 0.05mg protein were added to 0.5ml of buffer (100mM KCl, 12.5mM KH_2PO_4, 10mM Tris, pH7.60) containing 125 µM ADP and the following respiratory substrates ± inhibitor: 5mM each malate/glutamate, 10mM succinate + 5µM rotenone, 5mM ascorbate and 1mM TMPD+2µg/ml antimycin A, 2mM glutamine, 5mM glutamate, 2.5mM α-ketoglutarate or 5mM isocitrate. The assay mixture was incubated for 5min at

37°C before ATP production was stopped by placing the tubes in boiling water for 3 min followed by centrifugation at 20,000*g* for 10min in a microfuge. The amount of ATP produced was determined by the luciferin/luciferase assay as described previously (Zhang et al., 2004) and the chemiluminescence generated was read in a luminometer (Victor 3, PerkinElmer Waltham, MA, USA) as described previously (Ng et al., 2006).

6.2.11 Oxygen consumption

Mitochondrial oxygen consumption was measured using the O2K, Oroboros (Innsbruck, Austria). Air calibration was performed with MiR05 containing 0.5mM EGTA, 3mM $MgCl_2$.6H2O, 60mM K-lactobionate, 20mM Taurine, 10mM KH_2PO_4, 20mM HEPES, 110mM sucrose, 1g/L BSA, pH 7.1. The chambers were closed after air calibration and mitochondria containing 0.05mg protein were added. State 4 respiration was induced by the addition of 0.5µM rotenone and 10mM succinate, two doses of 0.25mM ADP were added to obtain the State 3 respiration. A maximal capacity of the electron transport system (ETS) of the mitochondria was achieved by titrating sequentially with 0.1µL-1µL aliquots of 1mM FCCP until a maximal response was achieved as described (Gnaiger et al., 2000).

6.2.12 ROS production in isolated mitochondria

ROS production of isolation mitochondria was measured using the fluorescence probe, 2′,7′-dichlorofluorescin diacetate (DCFDA) which could be oxidized by various ROS including peroxynitrite ($ONOO^-$), hydrogen peroxide (H_2O_2) in combination with cellular peroxidases and hydroxyl radical (·OH). The assay

mixture contained 0.5mg/ml mitochondria, 1U/ml horseradish peroxidase (HRP) and 1μM DCFDA in PBS. The fluorescence of DCF was followed at Ex/Em 490/526nm for 30min at 37°C using the multimode microplate reader, Varioskan™ Flash (Thermo Scientific, West Palm Beach, FL, United States).

6.2.13 Hydrogen peroxide production in isolated mitochondria

H_2O_2 production of isolated mitochondria was measured using the Amplex Red™ hydrogen peroxide/peroxidase assay kit following manufacturer's instructions.

6.2.14 Plasmid constructs and transfection

Myc-DDK-tagged human uncoupling protein 2 plasmid (pCMV-UCP2) was purchased from Origene (Rockville, MD) and validated by sequencing. The empty vector was created by cutting the pCMV-UCP2 vector with *BamH I/Xho I* followed by blunting the edges before ligating the ends. Subconfluent 786-O cells were transfected with either control or pCMV-UCP2 vector using Lipofectamine 3000 (Invitrogen Life Technologies, Carlsbad, CA, USA) according to the manufacturer's instructions. Cells were harvested 24hr after transfection and used for MMP measurement and western blot analysis.

6.2.15 Statistical analysis

Data were presented as means ± SD, and were analyzed by the Student's *t* test where a p value of < 0.05 was considered to be significant for n=3.

BIBLIOGRAPHY

Abou-Khalil, W.H., Arimura, G.K., Yunis, A.A., Abou-Khalil, S., 1986. Inhibition by rhodamine 123 of protein synthesis in mitochondria of normal and cancer tissues. Biochemical and biophysical research communications 137, 759-765.

Arora, K.K., Pedersen, P.L., 1988. Functional significance of mitochondrial bound hexokinase in tumor cell metabolism. Evidence for preferential phosphorylation of glucose by intramitochondrially generated ATP. The Journal of biological chemistry 263, 17422-17428.

Ayyasamy, V., Owens, K.M., Desouki, M.M., Liang, P., Bakin, A., Thangaraj, K., Buchsbaum, D.J., LoBuglio, A.F., Singh, K.K., 2011. Cellular model of Warburg effect identifies tumor promoting function of UCP2 in breast cancer and its suppression by genipin. PloS one 6, e24792.

Baba, M., Hong, S.B., Sharma, N., Warren, M.B., Nickerson, M.L., Iwamatsu, A., Esposito, D., Gillette, W.K., Hopkins, R.F., 3rd, Hartley, J.L., Furihata, M., Oishi, S., Zhen, W., Burke, T.R., Jr., Linehan, W.M., Schmidt, L.S., Zbar, B., 2006. Folliculin encoded by the BHD gene interacts with a binding protein, FNIP1, and AMPK, and is involved in AMPK and mTOR signaling. Proceedings of the National Academy of Sciences of the United States of America 103, 15552-15557.

Baffy, G., 2010. Uncoupling protein-2 and cancer. Mitochondrion 10, 243-252.

Baggetto, L.G., 1992. Deviant energetic metabolism of glycolytic cancer cells. Biochimie 74, 959-974.

Baggetto, L.G., Lehninger, A.L., 1987. Formation and utilization of acetoin, an unusual product of pyruvate metabolism by Ehrlich and AS30-D tumor mitochondria. The Journal of biological chemistry 262, 9535-9541.

Barja, G., 1999. Mitochondrial oxygen radical generation and leak: sites of production in states 4 and 3, organ specificity, and relation to aging and longevity. Journal of bioenergetics and biomembranes 31, 347-366.

Baysal, B.E., Ferrell, R.E., Willett-Brozick, J.E., Lawrence, E.C., Myssiorek, D., Bosch, A., van der Mey, A., Taschner, P.E., Rubinstein, W.S., Myers, E.N., Richard, C.W., 3rd, Cornelisse, C.J., Devilee, P., Devlin, B., 2000. Mutations in SDHD, a mitochondrial complex II gene, in hereditary paraganglioma. Science 287, 848-851.

Beckman, J.S., Koppenol, W.H., 1996. Nitric oxide, superoxide, and peroxynitrite: the good, the bad, and ugly. The American journal of physiology 271, C1424-1437.

Benel, L., Ronot, X., Kornprobst, M., Adolphe, M., Mounolou, J.C., 1986. Mitochondrial uptake of rhodamine 123 by rabbit articular chondrocytes. Cytometry 7, 281-285.

Bertoncello, I., Hodgson, G.S., Bradley, T.R., 1985. Multiparameter analysis of transplantable hemopoietic stem cells: I. The separation and enrichment of stem cells homing to marrow and spleen on the basis of rhodamine-123 fluorescence. Experimental hematology 13, 999-1006.

Betarbet, R., Sherer, T.B., Greenamyre, J.T., 2002. Animal models of Parkinson's disease. BioEssays : news and reviews in molecular, cellular and developmental biology 24, 308-318.

Birt, A.R., Hogg, G.R., Dube, W.J., 1977. Hereditary multiple fibrofolliculomas with trichodiscomas and acrochordons. Archives of dermatology 113, 1674-1677.

Boffetta, P., Dosemeci, M., Gridley, G., Bath, H., Moradi, T., Silverman, D., 2001. Occupational exposure to diesel engine emissions and risk of cancer in Swedish men and women. Cancer causes & control : CCC 12, 365-374.

Bonora, E., Porcelli, A.M., Gasparre, G., Biondi, A., Ghelli, A., Carelli, V., Baracca, A., Tallini, G., Martinuzzi, A., Lenaz, G., Rugolo, M., Romeo, G., 2006. Defective oxidative phosphorylation in thyroid oncocytic carcinoma is associated with pathogenic mitochondrial DNA mutations affecting complexes I and III. Cancer research 66, 6087-6096.

Boyer, P.D., Chance, B., Ernster, L., Mitchell, P., Racker, E., Slater, E.C., 1977. Oxidative phosphorylation and photophosphorylation. Annual review of biochemistry 46, 955-966.

Bradford, M.M., 1976. A rapid and sensitive method for the quantitation of microgram quantities of protein utilizing the principle of protein-dye binding. Analytical biochemistry 72, 248-254.

Brand, M.D., Affourtit, C., Esteves, T.C., Green, K., Lambert, A.J., Miwa, S., Pakay, J.L., Parker, N., 2004. Mitochondrial superoxide: production, biological effects, and activation of uncoupling proteins. Free radical biology & medicine 37, 755-767.

Bravo, C., Minauro-Sanmiguel, F., Morales-Rios, E., Rodriguez-Zavala, J.S., Garcia, J.J., 2004. Overexpression of the inhibitor protein IF(1) in AS-30D hepatoma produces a higher association with mitochondrial F(1)F(0) ATP synthase compared to normal rat liver: functional and cross-linking studies. Journal of bioenergetics and biomembranes 36, 257-264.

Briscoe, D.A., Fiskum, G., Holleran, A.L., Kelleher, J.K., 1994. Acetoacetate metabolism in AS-30D hepatoma cells. Molecular and cellular biochemistry 136, 131-137.

Bruder, E., Passera, O., Harms, D., Leuschner, I., Ladanyi, M., Argani, P., Eble, J.N., Struckmann, K., Schraml, P., Moch, H., 2004. Morphologic and molecular characterization of renal cell carcinoma in children and young adults. The American journal of surgical pathology 28, 1117-1132.

Bruning, T., Pesch, B., Wiesenhutter, B., Rabstein, S., Lammert, M., Baumuller, A., Bolt, H.M., 2003. Renal cell cancer risk and occupational exposure to trichloroethylene: results of a consecutive case-control study in Arnsberg, Germany. American journal of industrial medicine 43, 274-285.

Bustamante, E., Pedersen, P.L., 1977. High aerobic glycolysis of rat hepatoma cells in culture: role of mitochondrial hexokinase. Proceedings of the National Academy of Sciences of the United States of America 74, 3735-3739.

Cadenas, S., Echtay, K.S., Harper, J.A., Jekabsons, M.B., Buckingham, J.A., Grau, E., Abuin, A., Chapman, H., Clapham, J.C., Brand, M.D., 2002. The basal proton conductance of skeletal muscle mitochondria from transgenic mice overexpressing or lacking uncoupling protein-3. The Journal of biological chemistry 277, 2773-2778.

Carew, J.S., Huang, P., 2002. Mitochondrial defects in cancer. Molecular cancer 1, 9.

Carretero, M.V., Torres, L., Latasa, U., Garcia-Trevijano, E.R., Prieto, J., Mato, J.M., Avila, M.A., 1998. Transformed but not normal hepatocytes express UCP2. FEBS letters 439, 55-58.

Ceccarini, C., Eagle, H., 1971. pH as a determinant of cellular growth and contact inhibition. Proceedings of the National Academy of Sciences of the United States of America 68, 229-233.

Chance, B., Williams, G.R., 1955. Respiratory enzymes in oxidative phosphorylation. III. The steady state. The Journal of biological chemistry 217, 409-427.

Chen, J., Futami, K., Petillo, D., Peng, J., Wang, P., Knol, J., Li, Y., Khoo, S.K., Huang, D., Qian, C.N., Zhao, P., Dykema, K., Zhang, R., Cao, B., Yang, X.J., Furge, K., Williams, B.O., Teh, B.T., 2008. Deficiency of FLCN in mouse kidney led to development of polycystic kidneys and renal neoplasia. PloS one 3, e3581.

Chen, W.J., Douglas, M.G., 1987. Phosphodiester bond cleavage outside mitochondria is required for the completion of protein import into the mitochondrial matrix. Cell 49, 651-658.

Chow, W.H., Devesa, S.S., Warren, J.L., Fraumeni, J.F., Jr., 1999. Rising incidence of renal cell cancer in the United States. JAMA : the journal of the American Medical Association 281, 1628-1631.

Chowdhury, R., Hardy, A., Schofield, C.J., 2008. The human oxygen sensing machinery and its manipulation. Chemical Society reviews 37, 1308-1319.

Collins, J.M., Foster, K.A., 1983. Differentiation of promyelocytic (HL-60) cells into mature granulocytes: mitochondrial-specific rhodamine 123 fluorescence. The Journal of cell biology 96, 94-99.

Curthoys, N.P., Watford, M., 1995. Regulation of glutaminase activity and glutamine metabolism. Annual review of nutrition 15, 133-159.

Dahl, H.H., Hunt, S.M., Hutchison, W.M., Brown, G.K., 1987. The human pyruvate dehydrogenase complex. Isolation of cDNA clones for the E1 alpha subunit, sequence analysis, and characterization of the mRNA. The Journal of biological chemistry 262, 7398-7403.

Darzynkiewicz, Z., Staiano-Coico, L., Melamed, M.R., 1981. Increased mitochondrial uptake of rhodamine 123 during lymphocyte stimulation. Proceedings of the National Academy of Sciences of the United States of America 78, 2383-2387.

DeBerardinis, R.J., Mancuso, A., Daikhin, E., Nissim, I., Yudkoff, M., Wehrli, S., Thompson, C.B., 2007. Beyond aerobic glycolysis: transformed cells can engage in glutamine metabolism that exceeds the requirement for protein and nucleotide synthesis. Proceedings of the National Academy of Sciences of the United States of America 104, 19345-19350.

Decastro, G.J., McKiernan, J.M., 2008. Epidemiology, clinical staging, and presentation of renal cell carcinoma. The Urologic clinics of North America 35, 581-592; vi.

Denko, N.C., Fontana, L.A., Hudson, K.M., Sutphin, P.D., Raychaudhuri, S., Altman, R., Giaccia, A.J., 2003. Investigating hypoxic tumor physiology through gene expression patterns. Oncogene 22, 5907-5914.

Dietrich, J., Henning, U., 1970. Regulation of pyruvate dehydrogenase complex synthesis in Escherichia coli K 12. Identification of the inducing metabolite. European journal of biochemistry / FEBS 14, 258-269.

Dietzen, D.J., Davis, E.J., 1993. Oxidation of pyruvate, malate, citrate, and cytosolic reducing equivalents by AS-30D hepatoma mitochondria. Archives of biochemistry and biophysics 305, 91-102.

Doolittle, M., Bohman, R., Durstenfeld, A., Cascarano, J., 1987. Identification and characterization of liver nonparenchymal cells by flow cytometry. Hepatology 7, 696-703.
Eble J, S.G., Epstein J.I., Sesterhenn I.A., 2004. Pathology and Genetics of Tumours of the Urinary System and Male Genital Organs. IARC Press, Lyon.

Eboli, M.L., Pasquini, A., 1994. Transformation linked decrease of pyruvate dehydrogenase complex in human epidermis. Cancer letters 85, 239-243.

Echtay, K.S., Esteves, T.C., Pakay, J.L., Jekabsons, M.B., Lambert, A.J., Portero-Otin, M., Pamplona, R., Vidal-Puig, A.J., Wang, S., Roebuck, S.J., Brand, M.D., 2003. A signalling role for 4-hydroxy-2-nonenal in regulation of mitochondrial uncoupling. The EMBO journal 22, 4103-4110.

Echtay, K.S., Winkler, E., Frischmuth, K., Klingenberg, M., 2001. Uncoupling proteins 2 and 3 are highly active H(+) transporters and highly nucleotide sensitive when activated by coenzyme Q (ubiquinone). Proceedings of the National Academy of Sciences of the United States of America 98, 1416-1421.

Faivre, S., Kroemer, G., Raymond, E., 2006. Current development of mTOR inhibitors as anticancer agents. Nature reviews. Drug discovery 5, 671-688.

Ferlay, J., Autier, P., Boniol, M., Heanue, M., Colombet, M., Boyle, P., 2007. Estimates of the cancer incidence and mortality in Europe in 2006. Annals of oncology : official journal of the European Society for Medical Oncology / ESMO 18, 581-592.

Filipp, F.V., Scott, D.A., Ronai, Z.A., Osterman, A.L., Smith, J.W., 2012. Reverse TCA cycle flux through isocitrate dehydrogenases 1 and 2 is required for lipogenesis in hypoxic melanoma cells. Pigment cell & melanoma research 25, 375-383.

Fink, B.D., Hong, Y.S., Mathahs, M.M., Scholz, T.D., Dillon, J.S., Sivitz, W.I., 2002. UCP2-dependent proton leak in isolated mammalian mitochondria. The Journal of biological chemistry 277, 3918-3925.

Finley, D.S., Pantuck, A.J., Belldegrun, A.S., 2011. Tumor biology and prognostic factors in renal cell carcinoma. The oncologist 16 Suppl 2, 4-13.

Fleury, C., Neverova, M., Collins, S., Raimbault, S., Champigny, O., Levi-Meyrueis, C., Bouillaud, F., Seldin, M.F., Surwit, R.S., Ricquier, D., Warden, C.H., 1997. Uncoupling protein-2: a novel gene linked to obesity and hyperinsulinemia. Nature genetics 15, 269-272.

Fuchs, B.C., Bode, B.P., 2005. Amino acid transporters ASCT2 and LAT1 in cancer: partners in crime? Seminars in cancer biology 15, 254-266.

George, S.M., Park, Y., Leitzmann, M.F., Freedman, N.D., Dowling, E.C., Reedy, J., Schatzkin, A., Hollenbeck, A., Subar, A.F., 2009. Fruit and vegetable intake and risk of cancer: a prospective cohort study. The American journal of clinical nutrition 89, 347-353.

Gimeno, R.E., Dembski, M., Weng, X., Deng, N., Shyjan, A.W., Gimeno, C.J., Iris, F., Ellis, S.J., Woolf, E.A., Tartaglia, L.A., 1997. Cloning and characterization of an uncoupling protein homolog: a potential molecular mediator of human thermogenesis. Diabetes 46, 900-906.

Gnaiger, E., Mendez, G., Hand, S.C., 2000. High phosphorylation efficiency and depression of uncoupled respiration in mitochondria under hypoxia. Proceedings of the National Academy of Sciences of the United States of America 97, 11080-11085.

Golozoubova, V., Hohtola, E., Matthias, A., Jacobsson, A., Cannon, B., Nedergaard, J., 2001. Only UCP1 can mediate adaptive nonshivering thermogenesis in the cold. FASEB journal : official publication of the Federation of American Societies for Experimental Biology 15, 2048-2050.

Griguer, C.E., Oliva, C.R., Gillespie, G.Y., 2005. Glucose metabolism heterogeneity in human and mouse malignant glioma cell lines. Journal of neuro-oncology 74, 123-133.

Gross, M.I., Demo, S.D., Dennison, J.B., Chen, L., Chernov-Rogan, T., Goyal, B., Janes, J.R., Laidig, G.J., Lewis, E.R., Li, J., Mackinnon, A.L., Parlati, F., Rodriguez, M.L., Shwonek, P.J., Sjogren, E.B., Stanton, T.F., Wang, T., Yang, J., Zhao, F., Bennett, M.K., 2014. Antitumor activity of the glutaminase inhibitor CB-839 in triple-negative breast cancer. Molecular cancer therapeutics 13, 890-901.

Han, D., Antunes, F., Canali, R., Rettori, D., Cadenas, E., 2003. Voltage-dependent anion channels control the release of the superoxide anion from mitochondria to cytosol. The Journal of biological chemistry 278, 5557-5563.

Hartman, T.R., Nicolas, E., Klein-Szanto, A., Al-Saleem, T., Cash, T.P., Simon, M.C., Henske, E.P., 2009. The role of the Birt-Hogg-Dube protein in mTOR activation and renal tumorigenesis. Oncogene 28, 1594-1604.

Hensley, C.T., Wasti, A.T., DeBerardinis, R.J., 2013. Glutamine and cancer: cell biology, physiology, and clinical opportunities. The Journal of clinical investigation 123, 3678-3684.

Herrero, A., Barja, G., 1998. H2O2 production of heart mitochondria and aging rate are slower in canaries and parakeets than in mice: sites of free radical generation and mechanisms involved. Mechanisms of ageing and development 103, 133-146.

Hervouet, E., Demont, J., Pecina, P., Vojtiskova, A., Houstek, J., Simonnet, H., Godinot, C., 2005. A new role for the von Hippel-Lindau tumor suppressor protein: stimulation of mitochondrial oxidative phosphorylation complex biogenesis. Carcinogenesis 26, 531-539.

Heyde, E., Ainsworth, S., 1968. Kinetic studies on the mechanism of the malate dehydrogenase reaction. The Journal of biological chemistry 243, 2413-2423.

Hinz, W., Faller, B., Gruninger, S., Gazzotti, P., Chiesi, M., 1999a. Recombinant human uncoupling protein-3 increases thermogenesis in yeast cells. FEBS letters 448, 57-61.

Hinz, W., Gruninger, S., De Pover, A., Chiesi, M., 1999b. Properties of the human long and short isoforms of the uncoupling protein-3 expressed in yeast cells. FEBS letters 462, 411-415.

Hoberman, H.D., 1975. Is there a role for mitochondrial genes in carcinogenesis? Cancer research 35, 3332-3335.

Holloszy, J.O., Oscai, L.B., Don, I.J., Mole, P.A., 1970. Mitochondrial citric acid cycle and related enzymes: adaptive response to exercise. Biochemical and biophysical research communications 40, 1368-1373.

Holness, M.J., Sugden, M.C., 2003. Regulation of pyruvate dehydrogenase complex activity by reversible phosphorylation. Biochemical Society transactions 31, 1143-1151.

Hong, Y., Fink, B.D., Dillon, J.S., Sivitz, W.I., 2001. Effects of adenoviral overexpression of uncoupling protein-2 and -3 on mitochondrial respiration in insulinoma cells. Endocrinology 142, 249-256.

Hood, D.A., Zak, R., Pette, D., 1989. Chronic stimulation of rat skeletal muscle induces coordinate increases in mitochondrial and nuclear mRNAs of cytochrome-c-oxidase subunits. European journal of biochemistry / FEBS 179, 275-280.

Horimoto, M., Resnick, M.B., Konkin, T.A., Routhier, J., Wands, J.R., Baffy, G., 2004. Expression of uncoupling protein-2 in human colon cancer. Clinical cancer research : an official journal of the American Association for Cancer Research 10, 6203-6207.

Horowitz, B., Madras, B.K., Meister, A., Old, L.J., Boyes, E.A., Stockert, E., 1968. Asparagine synthetase activity of mouse leukemias. Science 160, 533-535.

Horwich, A.L., Kalousek, F., Fenton, W.A., Furtak, K., Pollock, R.A., Rosenberg, L.E., 1987. The ornithine transcarbamylase leader peptide directs mitochondrial import

through both its midportion structure and net positive charge. The Journal of cell biology 105, 669-677.

Hsu, P.P., Sabatini, D.M., 2008. Cancer cell metabolism: Warburg and beyond. Cell 134, 703-707.

Hu, C.J., Wang, L.Y., Chodosh, L.A., Keith, B., Simon, M.C., 2003. Differential roles of hypoxia-inducible factor 1alpha (HIF-1alpha) and HIF-2alpha in hypoxic gene regulation. Molecular and cellular biology 23, 9361-9374.

Huang, Y.Z., Knox, W.E., 1976. A comparative study of glytaminase isozymes in rat tissues. Enzyme 21, 408-426.

Iliopoulos, O., Levy, A.P., Jiang, C., Kaelin, W.G., Jr., Goldberg, M.A., 1996. Negative regulation of hypoxia-inducible genes by the von Hippel-Lindau protein. Proceedings of the National Academy of Sciences of the United States of America 93, 10595-10599.

Isaacs, J.S., Jung, Y.J., Mole, D.R., Lee, S., Torres-Cabala, C., Chung, Y.L., Merino, M., Trepel, J., Zbar, B., Toro, J., Ratcliffe, P.J., Linehan, W.M., Neckers, L., 2005. HIF overexpression correlates with biallelic loss of fumarate hydratase in renal cancer: novel role of fumarate in regulation of HIF stability. Cancer cell 8, 143-153.

James, T.W., Bohman, R., 1981. Proliferation of mitochondria during the cell cycle of the human cell line (HL-60). The Journal of cell biology 89, 256-260.

Jemal, A., Siegel, R., Xu, J., Ward, E., 2010. Cancer statistics, 2010. CA: a cancer journal for clinicians 60, 277-300.

Johnson, L.V., Walsh, M.L., Bockus, B.J., Chen, L.B., 1981. Monitoring of relative mitochondrial membrane potential in living cells by fluorescence microscopy. The Journal of cell biology 88, 526-535.

Karami, S., Boffetta, P., Rothman, N., Hung, R.J., Stewart, T., Zaridze, D., Navritalova, M., Mates, D., Janout, V., Kollarova, H., Bencko, V., Szeszenia-Dabrowska, N., Holcatova, I., Mukeria, A., Gromiec, J., Chanock, S.J., Brennan, P., Chow, W.H., Moore, L.E., 2008. Renal cell carcinoma, occupational pesticide exposure and modification by glutathione S-transferase polymorphisms. Carcinogenesis 29, 1567-1571.

Katunuma, N., Huzino, A., Tomino, I., 1967. Organ specific control of glutamine metabolism. Advances in enzyme regulation 5, 55-69.

Katunuma, N., Katsunuma, T., Towatari, T., Tomino, I., 1973. Regulatory mechanisms of glutamine catabolism, in: Prusiner, S., Stadtman, E.R. (Eds.), The Enzymes of Glutamine Metabolism Academic Press, New York, pp. 227-258.

Katunuma, N., Kominami, E., Kominami, S., Kito, K., 1972. Mode of action of specific inactivating enzymes for pyridoxal enzymes and NAD-dependent enzymes and their biological significance. Advances in enzyme regulation 10, 289-306.

Katunuma, N., Okada, M., 1963. Respiratory inhibition of TCA cycle and control of glutamic acid synthesis by ammonia in rat liver mitochondria. Biochemical and biophysical research communications 12, 252-256.

Kibel, A., Iliopoulos, O., DeCaprio, J.A., Kaelin, W.G., Jr., 1995. Binding of the von Hippel-Lindau tumor suppressor protein to Elongin B and C. Science 269, 1444-1446.

Kim, J.W., Tchernyshyov, I., Semenza, G.L., Dang, C.V., 2006. HIF-1-mediated expression of pyruvate dehydrogenase kinase: a metabolic switch required for cellular adaptation to hypoxia. Cell metabolism 3, 177-185.

Knox, W.E., 1976. Enzyme Patterns in Fetal, Adult and Neoplastic Rat Tissues, 2nd ed. Kargar, Basel.

Knox, W.E., Horowitz, M.L., Friedell, G.H., 1969. The proportionality of glutaminase content to growth rate and morphology of rat neoplasms. Cancer research 29, 669-680.

Knox, W.E., Tremblay, G.C., Spanier, B.B., Friedell, G.H., 1967. Glutaminase activities in normal and neoplastic tissues of the rat. Cancer research 27, 1456-1458.

Kondo, K., Kim, W.Y., Lechpammer, M., Kaelin, W.G., Jr., 2003. Inhibition of HIF2alpha is sufficient to suppress pVHL-defective tumor growth. PLoS biology 1, E83.

Kondo, K., Klco, J., Nakamura, E., Lechpammer, M., Kaelin, W.G., Jr., 2002. Inhibition of HIF is necessary for tumor suppression by the von Hippel-Lindau protein. Cancer cell 1, 237-246.

Koppenol, W.H., Bounds, P.L., Dang, C.V., 2011. Otto Warburg's contributions to current concepts of cancer metabolism. Nature reviews. Cancer 11, 325-337.

Koukourakis, M.I., Giatromanolaki, A., Simopoulos, C., Polychronidis, A., Sivridis, E., 2005. Lactate dehydrogenase 5 (LDH5) relates to up-regulated hypoxia inducible factor pathway and metastasis in colorectal cancer. Clinical & experimental metastasis 22, 25-30.

Kovacevic, Z., McGivan, J.D., Chappell, J.B., 1970. Conditions for activity of glutaminase in kidney mitochondria. The Biochemical journal 118, 265-274.

Kovacs, G., Akhtar, M., Beckwith, B.J., Bugert, P., Cooper, C.S., Delahunt, B., Eble, J.N., Fleming, S., Ljungberg, B., Medeiros, L.J., Moch, H., Reuter, V.E., Ritz, E., Roos, G., Schmidt, D., Srigley, J.R., Storkel, S., van den Berg, E., Zbar, B., 1997. The Heidelberg classification of renal cell tumours. The Journal of pathology 183, 131-133.

Kuai, X.Y., Ji, Z.Y., Zhang, H.J., 2010. Mitochondrial uncoupling protein 2 expression in colon cancer and its clinical significance. World journal of gastroenterology : WJG 16, 5773-5778.

Kushnareva, Y., Murphy, A.N., Andreyev, A., 2002. Complex I-mediated reactive oxygen species generation: modulation by cytochrome c and NAD(P)+ oxidation-reduction state. The Biochemical journal 368, 545-553.

Lampidis, T.J., Bernal, S.D., Summerhayes, I.C., Chen, L.B., 1983. Selective toxicity of rhodamine 123 in carcinoma cells in vitro. Cancer research 43, 716-720.

Landis, S.H., Murray, T., Bolden, S., Wingo, P.A., 1999. Cancer statistics, 1999. CA: a cancer journal for clinicians 49, 8-31, 31.

LaNoue, K.F., Schoolwerth, A.C., 1979. Metabolite transport in mitochondria. Annual review of biochemistry 48, 871-922.

Lardner, A., 2001. The effects of extracellular pH on immune function. Journal of leukocyte biology 69, 522-530.

Latif, F., Tory, K., Gnarra, J., Yao, M., Duh, F.M., Orcutt, M.L., Stackhouse, T., Kuzmin, I., Modi, W., Geil, L., et al., 1993. Identification of the von Hippel-Lindau disease tumor suppressor gene. Science 260, 1317-1320.

Lee, J.E., Giovannucci, E., Smith-Warner, S.A., Spiegelman, D., Willett, W.C., Curhan, G.C., 2006. Total fluid intake and use of individual beverages and risk of renal cell cancer in two large cohorts. Cancer epidemiology, biomarkers & prevention : a publication of the American Association for Cancer Research, cosponsored by the American Society of Preventive Oncology 15, 1204-1211.

Lichtor, T., Dohrmann, G.J., 1987. Oxidative metabolism and glycolysis in benign brain tumors. Journal of neurosurgery 67, 336-340.

Lim, H.Y., Ho, Q.S., Low, J., Choolani, M., Wong, K.P., 2011. Respiratory competent mitochondria in human ovarian and peritoneal cancer. Mitochondrion 11, 437-443.

Linder-Horowitz, M., Knox, W.E., Morris, H.P., 1969. Glutaminase activities and growth rates of rat hepatomas. Cancer research 29, 1195-1199.

Linehan, W.M., Srinivasan, R., Schmidt, L.S., 2010. The genetic basis of kidney cancer: a metabolic disease. Nature reviews. Urology 7, 277-285.

Loboda, A., Jozkowicz, A., Dulak, J., 2010. HIF-1 and HIF-2 transcription factors--similar but not identical. Molecules and cells 29, 435-442.

Lungberg BC, C.S., Choi HY, et al., 2011. Etiology and epidemiology. , in: Kirkali Z, M.P. (Ed.), Kidney cancer. International Consultation on Urological Diseases–European Association of Urology, Paris, France.

Ly, J.D., Grubb, D.R., Lawen, A., 2003. The mitochondrial membrane potential (deltapsi(m)) in apoptosis; an update. Apoptosis : an international journal on programmed cell death 8, 115-128.

MacLellan, J.D., Gerrits, M.F., Gowing, A., Smith, P.J., Wheeler, M.B., Harper, M.E., 2005. Physiological increases in uncoupling protein 3 augment fatty acid oxidation and decrease reactive oxygen species production without uncoupling respiration in muscle cells. Diabetes 54, 2343-2350.

MacMillan-Crow, L.A., Crow, J.P., 2011. Does more MnSOD mean more hydrogen peroxide? Anti-cancer agents in medicinal chemistry 11, 178-180.

Mailloux, R.J., Adjeitey, C.N., Harper, M.E., 2010. Genipin-induced inhibition of uncoupling protein-2 sensitizes drug-resistant cancer cells to cytotoxic agents. PloS one 5, e13289.

Mandel, J.S., McLaughlin, J.K., Schlehofer, B., Mellemgaard, A., Helmert, U., Lindblad, P., McCredie, M., Adami, H.O., 1995. International renal-cell cancer study. IV. Occupation. International journal of cancer. Journal international du cancer 61, 601-605.

Mandella, R.D., Sauer, L.A., 1975. The mitochondrial malic enzymes. I. Submitochondrial localization and purification and properties of the NAD(P)+-dependent enzyme from adrenal cortex. The Journal of biological chemistry 250, 5877-5884.

Mates, J.M., Segura, J.A., Campos-Sandoval, J.A., Lobo, C., Alonso, L., Alonso, F.J., Marquez, J., 2009. Glutamine homeostasis and mitochondrial dynamics. The international journal of biochemistry & cell biology 41, 2051-2061.

Mathupala, S.P., Rempel, A., Pedersen, P.L., 2001. Glucose catabolism in cancer cells: identification and characterization of a marked activation response of the type II hexokinase gene to hypoxic conditions. The Journal of biological chemistry 276, 43407-43412.

Matsuno, T., Goto, I., 1992. Glutaminase and glutamine synthetase activities in human cirrhotic liver and hepatocellular carcinoma. Cancer research 52, 1192-1194.

Maxwell, P.H., Wiesener, M.S., Chang, G.W., Clifford, S.C., Vaux, E.C., Cockman, M.E., Wykoff, C.C., Pugh, C.W., Maher, E.R., Ratcliffe, P.J., 1999. The tumour suppressor protein VHL targets hypoxia-inducible factors for oxygen-dependent proteolysis. Nature 399, 271-275.

McGivan, J.D., Bungard, C.I., 2007. The transport of glutamine into mammalian cells. Frontiers in bioscience : a journal and virtual library 12, 874-882.

McLaughlin, J.K., Lipworth, L., Tarone, R.E., 2006. Epidemiologic aspects of renal cell carcinoma. Seminars in oncology 33, 527-533.

Medina, M.A., 2001. Glutamine and cancer. The Journal of nutrition 131, 2539S-2542S; discussion 2550S-2531S.

Meierhofer, D., Mayr, J.A., Fink, K., Schmeller, N., Kofler, B., Sperl, W., 2006. Mitochondrial DNA mutations in renal cell carcinomas revealed no general impact on energy metabolism. British journal of cancer 94, 268-274.

Meierhofer, D., Mayr, J.A., Foetschl, U., Berger, A., Fink, K., Schmeller, N., Hacker, G.W., Hauser-Kronberger, C., Kofler, B., Sperl, W., 2004. Decrease of mitochondrial DNA content and energy metabolism in renal cell carcinoma. Carcinogenesis 25, 1005-1010.

Melo, R.F., Stevan, F.R., Campello, A.P., Carnieri, E.G., de Oliveira, M.B., 1998. Occurrence of the Crabtree effect in HeLa cells. Cell biochemistry and function 16, 99-105.

Metallo, C.M., Gameiro, P.A., Bell, E.L., Mattaini, K.R., Yang, J., Hiller, K., Jewell, C.M., Johnson, Z.R., Irvine, D.J., Guarente, L., Kelleher, J.K., Vander Heiden, M.G., Iliopoulos, O., Stephanopoulos, G., 2012. Reductive glutamine metabolism by IDH1 mediates lipogenesis under hypoxia. Nature 481, 380-384.

Millet, L., Vidal, H., Larrouy, D., Andreelli, F., Laville, M., Langin, D., 1998. mRNA expression of the long and short forms of uncoupling protein-3 in obese and lean humans. Diabetologia 41, 829-832.

Miroux, B., Frossard, V., Raimbault, S., Ricquier, D., Bouillaud, F., 1993. The topology of the brown adipose tissue mitochondrial uncoupling protein determined with antibodies against its antigenic sites revealed by a library of fusion proteins. The EMBO journal 12, 3739-3745.

Mitchell, P., 1966. Chemiosmotic coupling in oxidative and photosynthetic phosphorylation. Biological reviews of the Cambridge Philosophical Society 41, 445-502.

Modica-Napolitano, J.S., Aprille, J.R., 1987. Basis for the selective cytotoxicity of rhodamine 123. Cancer research 47, 4361-4365.

Molina, M., Segura, J.A., Aledo, J.C., Medina, M.A., Nunez de Castro, I., Marquez, J., 1995. Glutamine transport by vesicles isolated from tumour-cell mitochondrial inner membrane. The Biochemical journal 308 (Pt 2), 629-633.

Mulder, A.H., Visser, J.W., 1987. Separation and functional analysis of bone marrow cells separated by rhodamine-123 fluorescence. Experimental hematology 15, 99-104.

Muller, M., Siems, W., Buttgereit, F., Dumdey, R., Rapoport, S.M., 1986. Quantification of ATP-producing and consuming processes of Ehrlich ascites tumour cells. European journal of biochemistry / FEBS 161, 701-705.

Murphy, M.P., Brand, M.D., 1987. Variable stoichiometry of proton pumping by the mitochondrial respiratory chain. Nature 329, 170-172.

Myhre, O., Andersen, J.M., Aarnes, H., Fonnum, F., 2003. Evaluation of the probes 2',7'-dichlorofluorescin diacetate, luminol, and lucigenin as indicators of reactive species formation. Biochemical pharmacology 65, 1575-1582.

Nakashima, R.A., Mangan, P.S., Colombini, M., Pedersen, P.L., 1986. Hexokinase receptor complex in hepatoma mitochondria: evidence from N,N'-dicyclohexylcarbodiimide-labeling studies for the involvement of the pore-forming protein VDAC. Biochemistry 25, 1015-1021.

Ng, L.E., Vincent, A.S., Halliwell, B., Wong, K.P., 2006. Action of diclofenac on kidney mitochondria and cells. Biochemical and biophysical research communications 348, 494-500.

Noma, T., Fujisawa, K., Yamashiro, Y., Shinohara, M., Nakazawa, A., Gondo, T., Ishihara, T., Yoshinobu, K., 2001. Structure and expression of human mitochondrial adenylate kinase targeted to the mitochondrial matrix. The Biochemical journal 358, 225-232.

Nyhan, M.J., El Mashad, S.M., O'Donovan, T.R., Ahmad, S., Collins, C., Sweeney, P., Rogers, E., O'Sullivan, G.C., McKenna, S.L., 2011. VHL genetic alteration in CCRCC does not determine de-regulation of HIF, CAIX, hnRNP A2/B1 and osteopontin. Cellular oncology 34, 225-234.

Papandreou, I., Cairns, R.A., Fontana, L., Lim, A.L., Denko, N.C., 2006. HIF-1 mediates adaptation to hypoxia by actively downregulating mitochondrial oxygen consumption. Cell metabolism 3, 187-197.

Park, H.J., Lyons, J.C., Ohtsubo, T., Song, C.W., 1999. Acidic environment causes apoptosis by increasing caspase activity. British journal of cancer 80, 1892-1897.

Parlo, R.A., Coleman, P.S., 1984. Enhanced rate of citrate export from cholesterol-rich hepatoma mitochondria. The truncated Krebs cycle and other metabolic ramifications of mitochondrial membrane cholesterol. The Journal of biological chemistry 259, 9997-10003.

Parton, L.E., Ye, C.P., Coppari, R., Enriori, P.J., Choi, B., Zhang, C.Y., Xu, C., Vianna, C.R., Balthasar, N., Lee, C.E., Elmquist, J.K., Cowley, M.A., Lowell, B.B., 2007. Glucose sensing by POMC neurons regulates glucose homeostasis and is impaired in obesity. Nature 449, 228-232.

Pascual, D., Borque, A., 2008. Epidemiology of kidney cancer. Advances in urology, 782381.

Pavlovich, C.P., Grubb, R.L., 3rd, Hurley, K., Glenn, G.M., Toro, J., Schmidt, L.S., Torres-Cabala, C., Merino, M.J., Zbar, B., Choyke, P., Walther, M.M., Linehan, W.M., 2005. Evaluation and management of renal tumors in the Birt-Hogg-Dube syndrome. The Journal of urology 173, 1482-1486.

Payne, R.M., Strauss, A.W., 1994. Expression of the mitochondrial creatine kinase genes. Molecular and cellular biochemistry 133-134, 235-243.

Pedersen, P.L., 1978. Tumor mitochondria and the bioenergetics of cancer cells. Progress in experimental tumor research 22, 190-274.

Penta, J.S., Johnson, F.M., Wachsman, J.T., Copeland, W.C., 2001. Mitochondrial DNA in human malignancy. Mutation research 488, 119-133.

Peruzzi, B., Bottaro, D.P., 2006. Targeting the c-Met signaling pathway in cancer. Clinical cancer research : an official journal of the American Association for Cancer Research 12, 3657-3660.

Pfaffenroth, E.C., Linehan, W.M., 2008. Genetic basis for kidney cancer: opportunity for disease-specific approaches to therapy. Expert opinion on biological therapy 8, 779-790.

Pinkus, L.M., Windmueller, H.G., 1977. Phosphate-dependent glutaminase of small intestine: localization and role in intestinal glutamine metabolism. Archives of biochemistry and biophysics 182, 506-517.

Puigserver, P., Wu, Z., Park, C.W., Graves, R., Wright, M., Spiegelman, B.M., 1998. A cold-inducible coactivator of nuclear receptors linked to adaptive thermogenesis. Cell 92, 829-839.

Rabinovitz, Y.M., Pinus, H.A., Kotelnikova, A.V., 1977. A study of dependence of protein synthesis in mitochondria on the transmembrane potential. Molecular and cellular biochemistry 14, 109-113.

Radi, R., Cassina, A., Hodara, R., Quijano, C., Castro, L., 2002. Peroxynitrite reactions and formation in mitochondria. Free radical biology & medicine 33, 1451-1464.

Reed, L.J., Hackert, M.L., 1990. Structure-function relationships in dihydrolipoamide acyltransferases. The Journal of biological chemistry 265, 8971-8974.

Robey, I.F., Lien, A.D., Welsh, S.J., Baggett, B.K., Gillies, R.J., 2005. Hypoxia-inducible factor-1alpha and the glycolytic phenotype in tumors. Neoplasia 7, 324-330.

Robson, C.J., Churchill, B.M., Anderson, W., 1969. The results of radical nephrectomy for renal cell carcinoma. The Journal of urology 101, 297-301.

Roche, T.E., Baker, J.C., Yan, X., Hiromasa, Y., Gong, X., Peng, T., Dong, J., Turkan, A., Kasten, S.A., 2001. Distinct regulatory properties of pyruvate dehydrogenase kinase and phosphatase isoforms. Progress in nucleic acid research and molecular biology 70, 33-75.

Rodriguez-Enriquez, S., Juarez, O., Rodriguez-Zavala, J.S., Moreno-Sanchez, R., 2001. Multisite control of the Crabtree effect in ascites hepatoma cells. European journal of biochemistry / FEBS 268, 2512-2519.

Rose, I.A., Warms, J.V., 1982. Stability of hexokinase II in vitro and in ascites tumor cells. Archives of biochemistry and biophysics 213, 625-634.

Rossignol, R., Gilkerson, R., Aggeler, R., Yamagata, K., Remington, S.J., Capaldi, R.A., 2004. Energy substrate modulates mitochondrial structure and oxidative capacity in cancer cells. Cancer research 64, 985-993.

Rozhin, J., Sameni, M., Ziegler, G., Sloane, B.F., 1994. Pericellular pH affects distribution and secretion of cathepsin B in malignant cells. Cancer research 54, 6517-6525.

Sauer, L.A., 1977. On the mechanism of the Crabtree effect in mouse ascites tumor cells. Journal of cellular physiology 93, 313-316.

Schleyer, M., Schmidt, B., Neupert, W., 1982. Requirement of a membrane potential for the posttranslational transfer of proteins into mitochondria. European journal of biochemistry / FEBS 125, 109-116.

Schmidt, L., Duh, F.M., Chen, F., Kishida, T., Glenn, G., Choyke, P., Scherer, S.W., Zhuang, Z., Lubensky, I., Dean, M., Allikmets, R., Chidambaram, A., Bergerheim, U.R., Feltis, J.T., Casadevall, C., Zamarron, A., Bernues, M., Richard, S., Lips, C.J., Walther, M.M., Tsui, L.C., Geil, L., Orcutt, M.L., Stackhouse, T., Lipan, J., Slife, L., Brauch, H., Decker, J., Niehans, G., Hughson, M.D., Moch, H., Storkel, S., Lerman, M.I., Linehan, W.M., Zbar, B., 1997. Germline and somatic mutations in the tyrosine kinase domain of the MET proto-oncogene in papillary renal carcinomas. Nature genetics 16, 68-73.

Schmidt, L., Junker, K., Nakaigawa, N., Kinjerski, T., Weirich, G., Miller, M., Lubensky, I., Neumann, H.P., Brauch, H., Decker, J., Vocke, C., Brown, J.A., Jenkins, R., Richard, S., Bergerheim, U., Gerrard, B., Dean, M., Linehan, W.M., Zbar, B., 1999. Novel mutations of the MET proto-oncogene in papillary renal carcinomas. Oncogene 18, 2343-2350.

Schmidt, L.S., Warren, M.B., Nickerson, M.L., Weirich, G., Matrosova, V., Toro, J.R., Turner, M.L., Duray, P., Merino, M., Hewitt, S., Pavlovich, C.P., Glenn, G., Greenberg, C.R., Linehan, W.M., Zbar, B., 2001. Birt-Hogg-Dube syndrome, a genodermatosis associated with spontaneous pneumothorax and kidney neoplasia, maps to chromosome 17p11.2. American journal of human genetics 69, 876-882.

Seltzer, M.J., Bennett, B.D., Joshi, A.D., Gao, P., Thomas, A.G., Ferraris, D.V., Tsukamoto, T., Rojas, C.J., Slusher, B.S., Rabinowitz, J.D., Dang, C.V., Riggins, G.J., 2010. Inhibition of glutaminase preferentially slows growth of glioma cells with mutant IDH1. Cancer research 70, 8981-8987.

Semenza, G.L., Roth, P.H., Fang, H.M., Wang, G.L., 1994. Transcriptional regulation of genes encoding glycolytic enzymes by hypoxia-inducible factor 1. The Journal of biological chemistry 269, 23757-23763.

Setiawan, V.W., Stram, D.O., Nomura, A.M., Kolonel, L.N., Henderson, B.E., 2007. Risk factors for renal cell cancer: the multiethnic cohort. American journal of epidemiology 166, 932-940.

Siegel, R., Ma, J., Zou, Z., Jemal, A., 2014. Cancer statistics, 2014. CA: a cancer journal for clinicians 64, 9-29.

Simonnet, H., Alazard, N., Pfeiffer, K., Gallou, C., Beroud, C., Demont, J., Bouvier, R., Schagger, H., Godinot, C., 2002. Low mitochondrial respiratory chain content correlates with tumor aggressiveness in renal cell carcinoma. Carcinogenesis 23, 759-768.

Solaini, G., Harris, D.A., 2005. Biochemical dysfunction in heart mitochondria exposed to ischaemia and reperfusion. The Biochemical journal 390, 377-394.

Springer, E.L., 1980. Comparative study of the cytoplasmic organelles of epithelial cell lines derived from human carcinomas and nonmalignant tissues. Cancer research 40, 803-817.

Stuart, J.A., Harper, J.A., Brindle, K.M., Jekabsons, M.B., Brand, M.D., 2001. Physiological levels of mammalian uncoupling protein 2 do not uncouple yeast mitochondria. The Journal of biological chemistry 276, 18633-18639.

Stubbs, M., Bashford, C.L., Griffiths, J.R., 2003. Understanding the tumor metabolic phenotype in the genomic era. Current molecular medicine 3, 49-59.

Sudarshan, S., Sourbier, C., Kong, H.S., Block, K., Valera Romero, V.A., Yang, Y., Galindo, C., Mollapour, M., Scroggins, B., Goode, N., Lee, M.J., Gourlay, C.W., Trepel, J., Linehan, W.M., Neckers, L., 2009. Fumarate hydratase deficiency in renal cancer induces glycolytic addiction and hypoxia-inducible transcription factor 1alpha stabilization by glucose-dependent generation of reactive oxygen species. Molecular and cellular biology 29, 4080-4090.

Sugden, M.C., Holness, M.J., 2003. Recent advances in mechanisms regulating glucose oxidation at the level of the pyruvate dehydrogenase complex by PDKs. American journal of physiology. Endocrinology and metabolism 284, E855-862.

Summerhayes, I.C., Lampidis, T.J., Bernal, S.D., Nadakavukaren, J.J., Nadakavukaren, K.K., Shepherd, E.L., Chen, L.B., 1982. Unusual retention of rhodamine 123 by mitochondria in muscle and carcinoma cells. Proceedings of the National Academy of Sciences of the United States of America 79, 5292-5296.

Sussman, I., Erecinska, M., Wilson, D.F., 1980. Regulation of cellular energy metabolism: the Crabtree effect. Biochimica et biophysica acta 591, 209-223.

Taccoen, X., Valeri, A., Descotes, J.L., Morin, V., Stindel, E., Doucet, L., Joulin, V., Bocqueraz, F., Coulange, C., Rambeaud, J.J., Fournier, G., Mejean, A., Oncology Committee of the Association Francaise, d.U., 2007. Renal cell carcinoma in adults 40 years old or less: young age is an independent prognostic factor for cancer-specific survival. European urology 51, 980-987.

Talbot, D.A., Hanuise, N., Rey, B., Rouanet, J.L., Duchamp, C., Brand, M.D., 2003. Superoxide activates a GDP-sensitive proton conductance in skeletal muscle mitochondria from king penguin (Aptenodytes patagonicus). Biochemical and biophysical research communications 312, 983-988.

Ter-Pogossian, M.M., Phelps, M.E., Hoffman, E.J., Mullani, N.A., 1975. A positron-emission transaxial tomograph for nuclear imaging (PETT). Radiology 114, 89-98.

Tomlinson, I.P., Alam, N.A., Rowan, A.J., Barclay, E., Jaeger, E.E., Kelsell, D., Leigh, I., Gorman, P., Lamlum, H., Rahman, S., Roylance, R.R., Olpin, S., Bevan, S., Barker, K., Hearle, N., Houlston, R.S., Kiuru, M., Lehtonen, R., Karhu, A., Vilkki, S., Laiho, P., Eklund, C., Vierimaa, O., Aittomaki, K., Hietala, M., Sistonen, P., Paetau, A., Salovaara, R., Herva, R., Launonen, V., Aaltonen, L.A., Multiple Leiomyoma, C., 2002. Germline mutations in FH predispose to dominantly inherited uterine fibroids, skin leiomyomata and papillary renal cell cancer. Nature genetics 30, 406-410.

Tong, X., Zhao, F., Thompson, C.B., 2009. The molecular determinants of de novo nucleotide biosynthesis in cancer cells. Current opinion in genetics & development 19, 32-37.

Trojanowski, J.Q., 2003. Rotenone neurotoxicity: a new window on environmental causes of Parkinson's disease and related brain amyloidoses. Experimental neurology 179, 6-8.

Trounce, I.A., Kim, Y.L., Jun, A.S., Wallace, D.C., 1996. Assessment of mitochondrial oxidative phosphorylation in patient muscle biopsies, lymphoblasts, and transmitochondrial cell lines. Methods in enzymology 264, 484-509.

Turcotte, S., Chan, D.A., Sutphin, P.D., Hay, M.P., Denny, W.A., Giaccia, A.J., 2008. A molecule targeting VHL-deficient renal cell carcinoma that induces autophagy. Cancer cell 14, 90-102.

Turrens, J.F., Boveris, A., 1980. Generation of superoxide anion by the NADH dehydrogenase of bovine heart mitochondria. The Biochemical journal 191, 421-427.

Turrens, J.F., Freeman, B.A., Levitt, J.G., Crapo, J.D., 1982. The effect of hyperoxia on superoxide production by lung submitochondrial particles. Archives of biochemistry and biophysics 217, 401-410.

Tzagoloff, A., 1982. The mitochondrion. Academic, New York.

Van Slyke, D.D., Phillips, R.A., Hamilton, P.B., Archibald, R.M., Futcher, P.H., Hiller, A., 1973. Glutamine as source material of urinary ammonia. Journal of Biological Chemistry 150, 481-482.

Vanharanta, S., Buchta, M., McWhinney, S.R., Virta, S.K., Peczkowska, M., Morrison, C.D., Lehtonen, R., Januszewicz, A., Jarvinen, H., Juhola, M., Mecklin, J.P., Pukkala, E., Herva, R., Kiuru, M., Nupponen, N.N., Aaltonen, L.A., Neumann, H.P., Eng, C., 2004. Early-onset renal cell carcinoma as a novel extraparaganglial component of SDHB-associated heritable paraganglioma. American journal of human genetics 74, 153-159.

Ventura-Clapier, R., Garnier, A., Veksler, V., 2008. Transcriptional control of mitochondrial biogenesis: the central role of PGC-1alpha. Cardiovascular research 79, 208-217.

Verner, K., Schatz, G., 1987. Import of an incompletely folded precursor protein into isolated mitochondria requires an energized inner membrane, but no added ATP. The EMBO journal 6, 2449-2456.

Vincent, A.S., Phan, T.T., Mukhopadhyay, A., Lim, H.Y., Halliwell, B., Wong, K.P., 2008. Human skin keloid fibroblasts display bioenergetics of cancer cells. The Journal of investigative dermatology 128, 702-709.

Virbasius, J.V., Scarpulla, R.C., 1994. Activation of the human mitochondrial transcription factor A gene by nuclear respiratory factors: a potential regulatory link between nuclear and mitochondrial gene expression in organelle biogenesis. Proceedings of the National Academy of Sciences of the United States of America 91, 1309-1313.

Vozza, A., Parisi, G., De Leonardis, F., Lasorsa, F.M., Castegna, A., Amorese, D., Marmo, R., Calcagnile, V.M., Palmieri, L., Ricquier, D., Paradies, E., Scarcia, P., Palmieri, F., Bouillaud, F., Fiermonte, G., 2014. UCP2 transports C4 metabolites out of mitochondria, regulating glucose and glutamine oxidation. Proceedings of the National Academy of Sciences of the United States of America 111, 960-965.

Walenta, S., Salameh, A., Lyng, H., Evensen, J.F., Mitze, M., Rofstad, E.K., Mueller-Klieser, W., 1997. Correlation of high lactate levels in head and neck tumors with incidence of metastasis. The American journal of pathology 150, 409-415.

Walenta, S., Wetterling, M., Lehrke, M., Schwickert, G., Sundfor, K., Rofstad, E.K., Mueller-Klieser, W., 2000. High lactate levels predict likelihood of metastases, tumor recurrence, and restricted patient survival in human cervical cancers. Cancer research 60, 916-921.

Wang, J.B., Erickson, J.W., Fuji, R., Ramachandran, S., Gao, P., Dinavahi, R., Wilson, K.F., Ambrosio, A.L., Dias, S.M., Dang, C.V., Cerione, R.A., 2010. Targeting mitochondrial glutaminase activity inhibits oncogenic transformation. Cancer cell 18, 207-219.

Warburg, O., 1956a. On respiratory impairment in cancer cells. Science 124, 269-270.

Warburg, O., 1956b. On the origin of cancer cells. Science 123, 309-314.

Weikert, S., Boeing, H., Pischon, T., Olsen, A., Tjonneland, A., Overvad, K., Becker, N., Linseisen, J., Lahmann, P.H., Arvaniti, A., Kassapa, C., Trichoupoulou, A., Sieri, S., Palli, D., Tumino, R., Vineis, P., Panico, S., van Gils, C.H., Peeters, P.H., Bueno-de-Mesquita, H.B., Buchner, F.L., Ljungberg, B., Hallmans, G., Berglund, G., Wirfalt, E., Pera, G., Dorronsoro, M., Gurrea, A.B., Navarro, C., Martinez, C., Quiros, J.R., Allen, N., Roddam, A., Bingham, S., Jenab, M., Slimani, N., Norat, T., Riboli, E., 2006. Fruits and vegetables and renal cell carcinoma: findings from the European prospective investigation into cancer and nutrition (EPIC). International journal of cancer. Journal international du cancer 118, 3133-3139.

Weinhouse, S., 1956. On respiratory impairment in cancer cells. Science 124, 267-269.

White, M.T., Nandi, S., 1976. Biochemical studies on mitochondria isolated from Normal and Neoplastic Tissues of the Mouse Mammary Gland. Journal of the National Cancer Institute 56, 65-73.

Williams, R.S., Salmons, S., Newsholme, E.A., Kaufman, R.E., Mellor, J., 1986. Regulation of nuclear and mitochondrial gene expression by contractile activity in skeletal muscle. The Journal of biological chemistry 261, 376-380.

Wise, D.R., DeBerardinis, R.J., Mancuso, A., Sayed, N., Zhang, X.Y., Pfeiffer, H.K., Nissim, I., Daikhin, E., Yudkoff, M., McMahon, S.B., Thompson, C.B., 2008. Myc regulates a transcriptional program that stimulates mitochondrial glutaminolysis and leads to glutamine addiction. Proceedings of the National Academy of Sciences of the United States of America 105, 18782-18787.

Wiseman, A., Fields, T.K., Chen, L.B., 1985. Human cell variants resistant to rhodamine 6G. Somatic cell and molecular genetics 11, 541-556.

Wojtczak, L., Wojtczak, A.B., Ernster, L., 1969. The inhibition of succinate dehydrogenase by oxalacetate. Biochimica et biophysica acta 191, 10-21.

Xie, H., Valera, V.A., Merino, M.J., Amato, A.M., Signoretti, S., Linehan, W.M., Sukhatme, V.P., Seth, P., 2009. LDH-A inhibition, a therapeutic strategy for treatment of hereditary leiomyomatosis and renal cell cancer. Molecular cancer therapeutics 8, 626-635.

Yang, Y., Valera, V.A., Padilla-Nash, H.M., Sourbier, C., Vocke, C.D., Vira, M.A., Abu-Asab, M.S., Bratslavsky, G., Tsokos, M., Merino, M.J., Pinto, P.A., Srinivasan, R., Ried, T., Neckers, L., Linehan, W.M., 2010. UOK 262 cell line, fumarate hydratase deficient (FH-/FH-) hereditary leiomyomatosis renal cell carcinoma: in vitro and in vivo model of an aberrant energy metabolic pathway in human cancer. Cancer genetics and cytogenetics 196, 45-55.

Yeaman, S.J., Hutcheson, E.T., Roche, T.E., Pettit, F.H., Brown, J.R., Reed, L.J., Watson, D.C., Dixon, G.H., 1978. Sites of phosphorylation on pyruvate dehydrogenase from bovine kidney and heart. Biochemistry 17, 2364-2370.

Zhang, C.Y., Hagen, T., Mootha, V.K., Slieker, L.J., Lowell, B.B., 1999. Assessment of uncoupling activity of uncoupling protein 3 using a yeast heterologous expression system. FEBS letters 449, 129-134.

Zhang, C.Y., Parton, L.E., Ye, C.P., Krauss, S., Shen, R., Lin, C.T., Porco, J.A., Jr., Lowell, B.B., 2006. Genipin inhibits UCP2-mediated proton leak and acutely reverses obesity- and high glucose-induced beta cell dysfunction in isolated pancreatic islets. Cell metabolism 3, 417-427.

Zhang, H., Gao, P., Fukuda, R., Kumar, G., Krishnamachary, B., Zeller, K.I., Dang, C.V., Semenza, G.L., 2007. HIF-1 inhibits mitochondrial biogenesis and cellular respiration in VHL-deficient renal cell carcinoma by repression of C-MYC activity. Cancer cell 11, 407-420.

Zhang, X., Vincent, A.S., Halliwell, B., Wong, K.P., 2004. A mechanism of sulfite neurotoxicity: direct inhibition of glutamate dehydrogenase. The Journal of biological chemistry 279, 43035-43045.